CENTRO DE INVESTIGACIÓN Y DE ESTUDIOS AVANZADOS DEL INSTITUTO POLITÉCNICO NACIONAL

UNIDAD ZACATENCO

DEPARTAMENTO DE BIOMEDICINA MOLECULAR

Efecto de claudina-6 y claudina-9 sobre la actividad citotóxica de células NK contra la línea celular AGS

T E S I S

Que presenta

SANYOG DWIVEDI

Para obtener el grado de

DOCTOR EN CIENCIAS

EN LA ESPECIALIDAD DE

BIOMEDICINA MOLECULAR

Directores de Tesis:

Tutor- Dr. Vianney Francisco Ortiz Navarrete

Cotutor- Dr. Luis Felipe Montaño Estrada

México, Distrito Federal **Agosto, 2021**

CENTRO DE INVESTIGACIÓN Y DE ESTUDIOS AVANZADOS DEL INSTITUTO POLITÉCNICO NACIONAL

UNIDAD ZACATENCO

DEPARTAMENTO DE BIOMEDICINA MOLECULAR

Effect of claudin-6 and claudin-9 on NK cell cytotoxic activity against AGS cell line

T H E S I S

Presented by

SANYOG DWIVEDI

To obtain the degree

DOCTOR IN SCIENCE

IN THE SPECIALTY OF

MOLECULAR BIOMEDICINE

Thesis Directors:

Tutor- Dr. Vianney Francisco Ortiz Navarrete

Cotutor- Dr. Luis Felipe Montaño Estrada

México, Distrito Federal **August 2021**

Dedication

Every journey is a story that became possible not because one could make it to the end but how one could make it. My journey of being an Indian guy studying Ph.D., in Mexico could never be possible without the support of my family. This thesis is dedicated to my father Mr. ***Brijendra Dwivedi****, my mother Mrs.* ***Neelam Dwivedi,*** *who put the foundation of this man I have become, and to my brother* ***Shagun Dwivedi*** *who is the navigator of my life and taught me to walk and to fight till you win. Special gratitude to my sisters Mrs.* ***Sapna Shukla*** *and Mrs.* ***Shikha Tripathi*** *for their continuous motivation and encouragement to keep moving ahead. Love and gratitude to* ***Nidhi*** *who stood by my side from oceans apart and supported me in the hardest of my days.*

Acknowledgement

I want to convey my special thanks to **Dr. Vianney Francisco Ortiz Navarrete** tutor of my thesis, my mentor, and a father figure who supported me in every step and encouraged me to do my best in the hardest of my days.

Special thanks to **Dr. Luis Felipe Montaño Estrada** and **Dra. Erika Patricia Rendón Huerta** for providing me guidance and allowing me to be a part of their lab team.

My gratitude and thanks to my assesors, **Dr. Leopoldo Santos Argumedo, Dr. Michael Schnoor, Dr. Nicolás Villegas Sepúlveda** for their guidance, commentaries, and support.

Thanks to my friends and colleagues in the lab **Jesús Guzmán, Maria, Juan Carlos, Julio Angel, Dana, Luis, Benjamin, Gaby, Anita, Priscila and Priscila, Carlos, Alex, George, Osmar, and Franklin** for accepting me in the lab, for guidance and support to survive my early days in the lab and providing me company to all my fun days.

Thanks to my friends from the Indian community **Nishu**, **Shiv, Manmohan, Satyam, Goban, Joice, and Sandeep** for making me feel safe and for all those fun get together and adventures we did together.

Special thanks to my friends **Mariana, Eda, Lilliana, Ingrid, Jazmin, Sandra, Marcos, Jocelyn, Laura, Nathanial, Remberto, and Ivan** for their love and support, all those fun talks and adventures that we did together.

Last but not the least I am grateful to the National Council of Science and Technology (CONACYT), for providing me the scholarship during the period 2017-2021 to carry out this doctorate.

Thanks

CONTENTS

LIST OF TABLES

LIST OF FIGURES

ABBRIVIATIONS

1: ABSTRACT

Tight junctions (TJ) are intercellular adhesion complexes of epithelial and endothelial cells that form a virtually impermeable barrier to fluids. As integral part of TJs, claudins (CLDN) provide tissue, size and charge selective paracellular sealing. Normally *CLDN6* and *CLDN9* expression is restricted to embryonic and fetal gastric development, but their expression is deregulated, enhanced and associated to Epithelial Mesenchymal Transition (EMT) in Gastric Cancer (GC). Gastric Adenocarcinoma (AGS) cells transfected with *CLDN6* or *CLDN9* overexpress these claudins in the cytoplasm and the membrane compared to non-transfected (wild type) AGS cells. To further investigate how overexpression of *CLDN6* in AGS cells might affect pathways that support cancer growth and survival, microarray-based gene expression analysis was done. Several differentially expressed genes in AGS-CLDN6 cells were identified over wild type AGS cells. Gene Set Enrichment Analysis (GSEA) revealed that these genes are involved in several cancer hallmark processes like unfolded protein response, MTORC1 signaling, cholesterol homeostasis, hypoxia, and TNFα signaling. Collectively, the results indicated that *CLDN6* transfection induces Endoplasmic Reticulum (ER) stress and deregulation of metabolism. Considering these results, we decided to analyze gastric cancer patient's database, defined by the Cancer Genome Atlas Stomach Adenocarcinoma (TCGA-STAD), to consolidate the observation of *CLDN6* alterations (mutation and differential expression) in GC.

We used the TCGA-STAD pan cancer atlas data of 440 patients using the cBioPortal to analyse large cancer datasets as well as other bioinformatic tools such as GSEA and Gene Ontology (GO) to determine functional enrichment of genes, GeneMANIA to generate genetic networks, Cytoscape to visualize networks, and MCODE to find gene clusters in the network. Our analysis determined that *CLDN6* is modified in 34% of GC patients; the main alterations comprise differential mRNA expression with shallow deletions, diploid and gain. The analysis also demonstrated that 68.79% of samples with *CLDN6* alterations had Tumor Protein *p53* (*TP53*) mutations. Furthermore, *TP53* mutations were also associated to *CLDN3* and *CLDN9* expression in GC tumor samples. Both, *TP53* and *CLDN6* alteration samples principally accumulate in the chromosomally unstable (CIN, according to the TCGA classification) subtype of gastric cancer with very similar copy number alterations and overall mutation in genes used to classify CIN-GC. *CLDN6* alterations were linked to poor overall and progression-free survival. Additionally, we identified in the *CLDN6* and *TP53* altered samples, a group of 137 common differentially expressed genes mainly involved in epithelium

development and differentiation. Gene interaction network analysis of these common differentially expressed genes identified Orosomucoid 2 (*ORM2*) and *MAGEA2* (Melanoma-Associated Antigen2) as most important genes. These results advocate CLDN6 and TP53 as critical players in GC development and suggest that jointly with ORM2 and MAGEA2 might serve as prognostic markers for individuals with CIN GC.

Resumen

Las uniones estrechas (TJ) son complejos de adhesión intercelular de células epiteliales y endoteliales que forman una barrera prácticamente impermeable a los fluidos. Como parte integral de los TJ, las claudinas (CLDN) proporcionan un sellado paracelular selectivo de tejido, tamaño y carga. Normalmente, la expresión de *CLDN6* y *CLDN9* está restringida al desarrollo gastroembrionario y fetal, pero en el Cáncer Gástrico (GC), su expresión está desregulada o incrementada y se asociada a la Transición Epitelial Mesenquimal (EMT). Las células de adenocarcinoma gástrico (AGS) transfectadas con *CLDN6* o *CLDN9* sobreexpresan estas claudinas en el citoplasma y la membrana en comparación con las células AGS no transfectadas. Para investigar más a fondo cómo la sobreexpresión de *CLDN6* en las células AGS podría afectar las vías que participan en el crecimiento y la supervivencia del cáncer, se realizó un análisis de expresión génica basado en microarreglos. Se identificaron varios genes expresados diferencialmente en células AGS-CLDN6 en comparación con células AGS. El análisis de enriquecimiento del conjunto de genes (GSEA) reveló que los genes sobrexpresados, están involucrados en varios procesos característicos del cáncer, como la respuesta de proteínas mal plegadas, la señalización de MTORC1, la homeostasis del colesterol, la hipoxia y la señalización de TNFα. En conjunto, los resultados indicaron que la transfección de *CLDN6* induce estrés en el retículo endoplásmico (ER) y desregulación del metabolismo.

Teniendo en cuenta los resultados anteriores, decidimos analizar la base de datos de pacientes con cáncer gástrico, definida por el Cancer Genome Atlas Stomach Adenocarcinoma (TCGA-STAD). Utilizamos los datos de TCGA-STAD pan-cáncer atlas de 440 pacientes; utilizamos el cBioPortal para analizar grandes conjuntos de datos de cáncer, así como las herramientas bioinformáticas, Gene Set Enrichment Analysis (GSEA) y Gene Ontology (GO) para determinar el enriquecimiento funcional de genes; GeneMANIA para generar redes genéticas, Cytoscape para visualizar redes y MCODE para encontrar grupos de genes en la red. Nuestro análisis determinó que *CLDN6* se modifica en el 34% de los pacientes con GC; las principales alteraciones comprenden expresión diferencial de ARNm con deleciones de un alelo, diploidia o ganancia de función. El análisis también demostró que el 68,79% de las muestras con alteraciones de *CLDN6* tenían mutaciones en la proteína *p53* (*TP53*). Además, la alteración de TP53 también se asoció con la expresión de *CLDN3* y *CLDN9* en muestras de tumores de GC. Las muestras con alteración de *TP53* y *CLDN6* se acumulan principalmente en el subtipo

cromosómicamente inestable (CIN, según la clasificación TCGA) de cáncer gástrico con alteraciones en el número de copias y mutación en los genes utilizados para clasificar CIN-GC. Las alteraciones de *CLDN6* se relacionaron con una baja supervivencia y baja supervivencia libre de progresión. Además, identificamos en las muestras alteradas *CLDN6* y *TP53*, un grupo de 137 genes comunes expresados e involucrados principalmente en el desarrollo y diferenciación del epitelio. El análisis de la red de interacción de genes identificó al Orosomucoide 2 (*ORM2*) y al *MAGEA2* (Antígeno asociado al melanoma 2) como los genes más importantes. Estos resultados sugieren que CLDN6 y TP53 como actores críticos en el desarrollo de GC e indican que junto con ORM2 y MAGEA2 podrían servir como marcadores de pronóstico para individuos con CIN GC.

1: Introduction

Gastric cancer (GC) is one of the most important cancer of the gastrointestinal tract that contributed, 5.6% of total cases worldwide and 7.7% mortality of a total number of deaths due to cancer in the year 2020 (GLOBOCAN 2020)(1). Eastern Asia followed by central and eastern Europe tops in the number of cases and mortality of stomach cancer cases while other countries also follow with a significant number of cases worldwide in both sexes (The Global Cancer Observatory -December 2020).

1.1: Gastric cancer classification

GC can be classified on behalf of different parameters- Anatomical, Histological, or molecular. Based on anatomy it is important to differentiate cancer in non-cardia (true GC) from the cancer of gastro-esophageal cancer which develops in the cardia, as they differ in incidence, geographical distribution, cause, and treatment. Tumors can be best categorized by Siewert classification (as type I/II/III) (2) in assistance with TNM classification, depending upon the epicenter location and tumor mass extension regions (3).

The majority (95%) of the cancers of the stomach are adenocarcinomas which can be further classified into three different histological forms- Intestinal, Diffuse, and mixed type as per Lauren classification (4). The intestinal subtype of GC is linked with atrophic gastritis and is associated with infectious agents including *H. pylori* and *Epstein-Barr virus* (EBV), while the diffuse subtype is unrelated with *H. pylori* and typically develops from normal gastric mucosa without atrophic gastritis (5). Intestinal carcinomas are well differentiated with well to moderate gland formation while the diffuse type is composed of solitary or feebly cohesive cells that develop poorly differentiated carcinomas. With a broad perspective WHO classifies GC in 5 different histopathological classes based on histological patterns of carcinoma (tubular, papillary, mucinous, poorly cohesive, and rare variants). WHO classification provides improved harmonization with other cancers of the gut. However, histologically poorly cohesive GC belong to diffuse-type GC and papillary and tubular carcinomas resemble to the intestinal type (6).

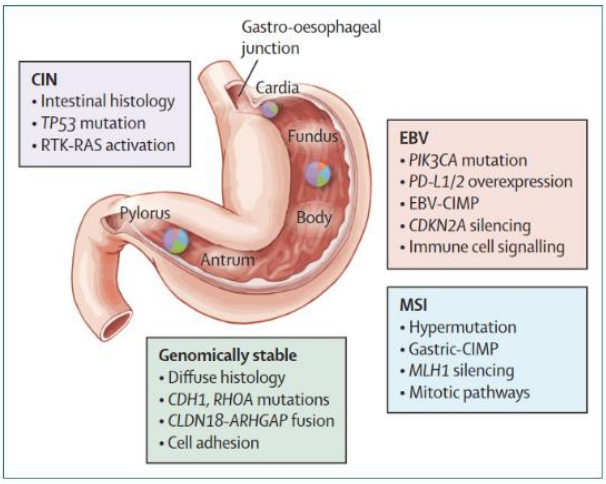

Figure 1 Molecular characterization of subtypes of Gastric carcinomas. CIN=chromosomally instable tumors, EBV=Epstein-Barr virus-infected tumors. CIMP=CpG island methylation phenotype. MSI=microsatellite unstable tumors (7).

The Cancer Genome Atlas (TCGA) research network extended GC classification to the molecular level with help of complex statistical analysis of complete genetic profiling of 295 primary gastric adenocarcinomas. TCGA classifies GC into 4 subgroups- Epstein-Barr virus (EBV), microsatellite unstable tumors, genomically stable tumors, and chromosomally unstable tumors (CIN) (8). Relatively newer in the classification system, it has advanced rapidly in the past few years and is expected to assist in prognosis determination and customize treatment options in the future (Figure 1).

1.2: Symptoms and diagnostics

Patients are usually diagnosed for GC in the advanced stages and according to the Cancer Staging Manual, 8th edition, of the American Joint Committee on Cancer, only 30% of the cases are diagnosed before metastasis. The symptoms generally include anorexia, dyspepsia, weight loss, and abdominal pain. Endoscopy and biopsy are principal diagnosis methods and ultrasonography, and CT of the chest/abdomen are primary means for the staging of locally advanced gastric adenocarcinoma (9).

1.3: Tight junctions, claudins, and Gastric adenocarcinoma

Epithelial and endothelial cells make a protective barrier over organs and allow the establishment of homeostasis. Cells adhere to other cells and to the extracellular matrix through transmembrane proteins like Integrins, cadherins, selectins, and immunoglobulins. Several such proteins usually attach to each other and form large macromolecular adhesion complexes-

known as cell junctions. According to morphology, adhesion molecules and their interaction with the cytoskeleton, cell junctions are classified into 4 different categories- Tight junctions, Adherent junctions, desmosomes, and gap junctions.

Tight junctions (TJs) also known as zonula occludens are intercellular adhesion complexes of epithelial and endothelial cells that form close membrane-membrane contacts among cells lining corporeal compartments (10). TJs deliver several functions like- selective barrier functions on epithelial and endothelial cell layers over organs to facilitate specialized organ functions such as regulation of air-fluid balance in the lungs and appropriately concentrated urine in the kidney (11).

1.4: TJ structure

TJs were firstly identified as physical barriers at the apical surface of epithelial cells. They are composed of more than 40 proteins that mechanically link adjacent cells and regulate tension, solute transport, selectivity along with cell signaling and gene expression (13). Among several components, three transmembrane proteins are common to all TJs (Figure 2): claudins, MARVEL domain proteins, and junctional adhesion molecules (JAMs) (10). The claudin family has 27 different members and is known to regulate the perm selectivity of TJs (discussed below in detail). MARVEL domain proteins include tetra-membrane spanning proteins like occludin and tricellulin, which regulate the recruitment of signaling complex proteins to TJs (14). JAMs (typically JAM-A, -B, -C) are members of the immunoglobulin superfamily (IgSF) and belong to the CTX subfamily which is characterized by two extracellular Ig-like domains, a single transmembrane domain and a small cytoplasmic tail (15). JAMs interact with their extracellular domains to other IgSF members, other JAM members, and with Integrins- notably, leukocyte-specific β integrin family such as-αLβ2 and αMβ2 integrins. The cytoplasmic domain of JAMs has a PDZ binding domain motif that in turn interacts with proteins like- ZO-1, ZO-2, Afadin, Par3, and MUPP1 (15). JAMs regulate a multitude of molecular interactions, and so regulate cell-cell contact formation, cell migration, and mitotic spindle orientation contributing to several biological processes like- epithelial and endothelial barrier formation, homeostasis, angiogenesis, hematopoiesis, germ cell development, and the development of the central and peripheral nervous system (15).

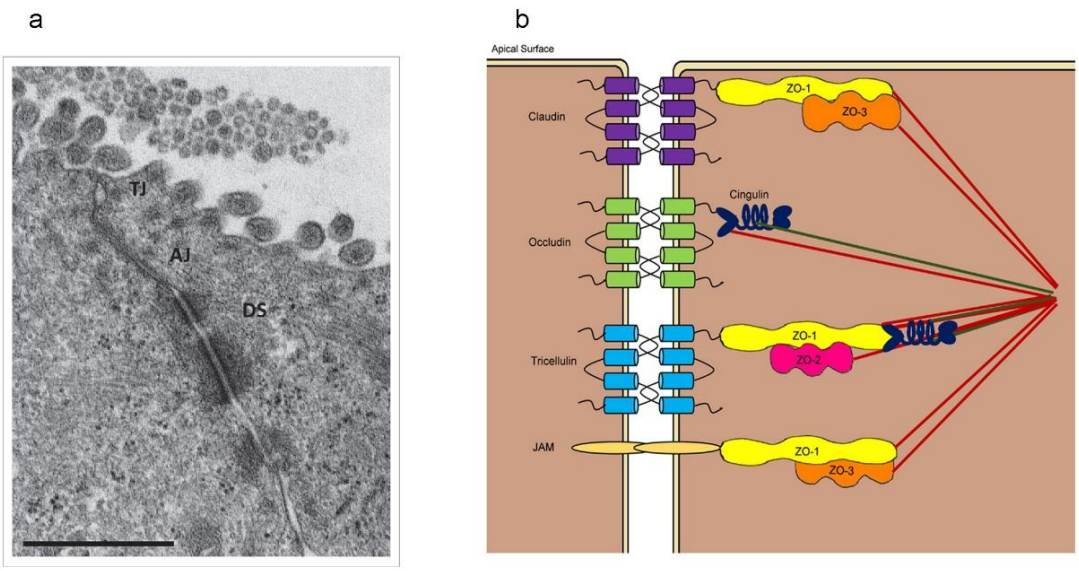

Figure 2 Structure of TJs.1 a) Transmission electron microscopy (TEM) image of an 'apical junctional complex' (polarized T84 human colorectal carcinoma epithelial cells) (16). b) Schematic drawing of TJ structure at the apicolateral membranes of the paracellular space. TJ's transmembrane proteins such as claudins, occludin, junctional adhesion molecules (JAM), and tricellulin establish intercellular interactions at paracellular spaces. Cytoplasmic plaque proteins such as three zonula occludens (ZO) proteins and cingulin facilitate interaction between transmembrane proteins and cytoskeleton (17).

1.5: Claudins and their role in GC

1.5.1: Claudin structure

Claudins form the backbone of tight junctions. It's a multigene family, comprised of 27 different members which express in a tissue-specific manner (18). Most of the claudins are 20–34 kDa size range and though they differ genetically, all claudin members share a structural topology of 4 transmembrane segments, a large extracellular loop, and a short secondary extracellular loop (19). CLDN1-10, 14, 15, 17, and 19 share great sequence homology and so are grouped as classical claudins while others are named as non-classic claudins (20). Intracellularly mammalian claudins are composed of N-terminal (7 amino acid), loop (12 amino acid), and C- terminal (25-55 amino acid), while CLDN12, 16, and 23 are exceptions to this general distribution of amino acid with 25- loop, 73- N-terminal, 111- C-terminal, amino acids sequentially (21).

Recently Hiroshi et.al. expressed various claudin subtypes in Sf9 insect cells and assessed their capability to form TJ-like strands (22). X-ray crystallographic studies of modified mouse *Cldn15* construct (22) revealed insights of claudin structure (Figure 3), with 4 transmembrane

segments (TM1-TM4), typical left-handed four-helix bundles, two large extracellular loops that form β-sheet structure (Figure 3).

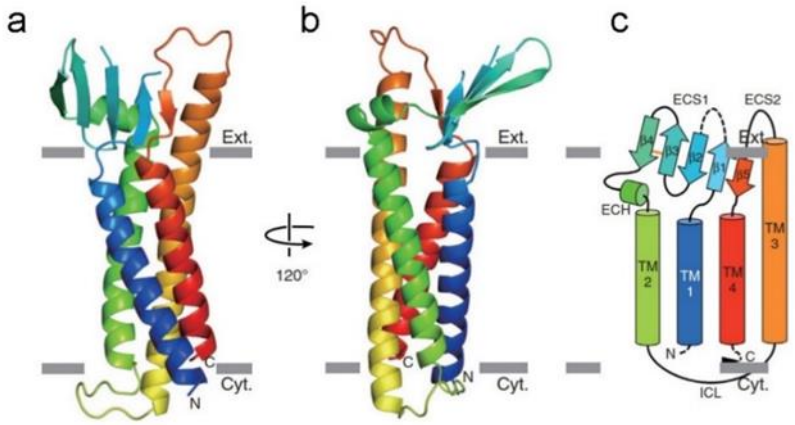

Figure 3 Structure of mouse CLDN15. (a, b) Ribbon presentation of monomeric mouse CLDN15 views parallel to the membrane. (c) Secondary structure diagram of mouse CLDN15.

Length of TM1/2/4 helices is consistent with lipid bilayer except for T3, which is longer. Two extracellular segments (ESC) contribute 5 β- sheets, 4 from ESC1 and 1 from ESC2 (Figure 3c). Homology modeling studies have revealed that the four-helix bundles and ECH regions are well conserved among claudins with slight variation in β sheets (22).

TJs can form paracellular ion channels with distinct charge selectivity or a strict barrier against paracellular diffusion of solutes. These functions depends largely on the type of claudins TJs constitute (23). The charge selectivity for ion permeation through TJs is determined by specific residues in the C-terminal half of the first extracellular domain of claudins (7,11,24). C-terminal of claudins has a PDZ binding motif which provides interaction with PDZ domain proteins like, PDZ1 of ZO-1, ZO-2, and ZO-3 bind with CLDN1-8, MUPP1 bind with CLDN1 and CLDN8 and Pals1- associated TJ protein- PATJ binds with CLDN1(20). Among the classic claudins, the –Y–V motif in the C-terminal positions -1 and 0 exhibit 100% conservation, while non-classic claudins demonstrate a greater variety of motives (H/S/Y/D/E/R–V/L).

Claudins have a short half-life in comparison to other transmembrane proteins for e.g. CLDN4 has a half-life of about 4 hours, which also indicates their tightness and pore functions are highly dynamic (25,26). Short term regulation of claudins is also pointed by many fold phosphorylation, which is primarily catalyzed by mitogen-activated protein kinase (MAPK) (Thr203, rat) (27) and protein kinase C (PKC) (28) in CLDN1, or by protein kinase A (PKA)

in CLDN3 (Thr192, human) (29) and CLDN5 (Thr207, rat) (30). Threonine/serine kinase WNK4 also phosphorylates CLDN1-4 (31) while receptor tyrosine kinase EPHA2 phosphorylates the PDZ binding C-terminus of CLDN4 (Tyr-208, human) and results in its dislocation from cell-cell junction (32). Moreover, phosphorylation of claudins may also decrease TJ strength as seen in the case of CLDN3 and -5 in ovarian cancer cells and endothelial cells, sequentially (29,30). Besides phosphorylation claudins also undergo s-acylation (reported in CLDN14) and palmitoylation at conserved cysteine residues proximal to membrane following TM1&2 in epithelial and fibroblast cells. Palmitoylation is essential for efficient localization and trafficking of TJ but not for stability and strand assembly (33). So besides slight differences in claudin structures post-translational modifications like phosphorylation and palmitoylation contribute to diverse functions of claudins in different tissues. Though the studies had put forth deep ideas about the claudin structure and their assembly and contribution to TJ formation, yet studies are in need to unveil further complexities about claudin assembly, and dysregulations in transformed cells.

1.5.2: Claudin functions

As part of the TJ, claudins contributes to the formation of tissue, size, and charge selective paracellular sealing. CLDN1, -5, -11, and -14 found to be involved in tightening functions as in blood-brain barrier (34), myelin sheaths, Sertoli cell layers (35), and epithelium in the inner ear (36) respectively. A tightening potential for CLDN3 has been observed in ovarian cancer cell lines, where a mutation mimicking phosphorylation of CLDN3 decreases TJ strength and indicate its role in tightening (29). Several claudins in TJs form paracellular channels selective to anion, cation or to neutral molecules. For example, CLDN15 forms a paracellular channel permeable to mono/divalent ions and to small uncharged molecules like water. In-vivo and in-vitro experiments confirmed that CLDN2, 10b,15, 16 and 21 form cation-selective channels, while CLDN10a, and 17 form anion-selective paracellular channels (37,38). On the other side some claudins contribute to barrier functions of TJs. So far CLDN1 (37), 4 (39), 5 (40), 8 (41), 11 (42), 14 (36), 18 (37) and 19 (43) has shown barrier functions in different experiments. Functions of CLDN6, 9, 12, 13, 17, 18, and 20–24 is relatively unexplored and is under study. In MDCKII cells CLDN6 and 9 regulates chloride and sodium permeability and increases transepithelial electrical resistance (44). They also have a Ca^{++} independent cell adhesion activity. CLDN6 is a global marker of definitive endoderm development and the development of organs like pancreas, lung, and liver (45). CLDN6 plays a major role in epithelial differentiation and epidermal permeability barrier assembly/maintenance during embryonic

development (45–47). Role of CLDN6 as an important regulator of adipogenesis and fat deposition has also been discussed. Mice fed on fat diet differentially expressed *Cldn*6 mRNA in different adipose tissues (48). Levels of *Cldn*6 transcripts were increased during differentiation of 3T3-L1 cells (fibroblast cell line, chemically induced to differentiate into adipocyte-like cells) in vitro which was reverted by small interfering RNA-mediated reduction of *Cldn*6 mRNA (48), further confirms the role of CLDN6 in adipogenesis. CLDN6 and CLDN9 expression in the neonatal proximal tubule results in an increased transepithelial resistance, decreased chloride permeability, and decreased relative sodium-to-chloride permeability (P(Na)/P(Cl)) and P(HCO3)/P(Cl) (44). Epigenetic regulators such as TSA, 5-aza, and DMSO significantly enhance the expression of CLDN9, trans endothelial electrical resistance and thus enhancing the corneal barrier function, in murine experimental corneal trauma (49). Barrier functions of CLDN9 are also essential for hearing. A nonsense mutation in CLDN9 eliminated its localization in cochlear tight junction and resulted reduced paracellular permeability to Na^+ and K^+ and loss of sensory hairs (50). Hence, different claudins impart different functions in different tissues. Moreover, they contribute to biological functions which get affected by deregulation of claudins and cause tissue specific disease including tumors and cancers of different organs (Table 1) as discussed in the next section.

1.5.3: Claudins and Cancers

Most of the cancer incidence and associated deaths (~95% cases) represent cancers originating from the epithelium for example cancers of oral cavity, esophagus, stomach, colon, rectum, prostate, ovary, bladder, kidney, lung, pancreas, breast, and liver (51–55). Irrespective of variable morphology and specialized functions of differentiated epithelium in different tissues and organs, few traits like polarized architecture, are shared among all. When an epithelial cell transformed to cancer cell it undergoes Epithelial Mesenchymal Transition (EMT) that includes disruption of cell-cell adhesion structures, altered polarity, and reorganized cytoskeleton.

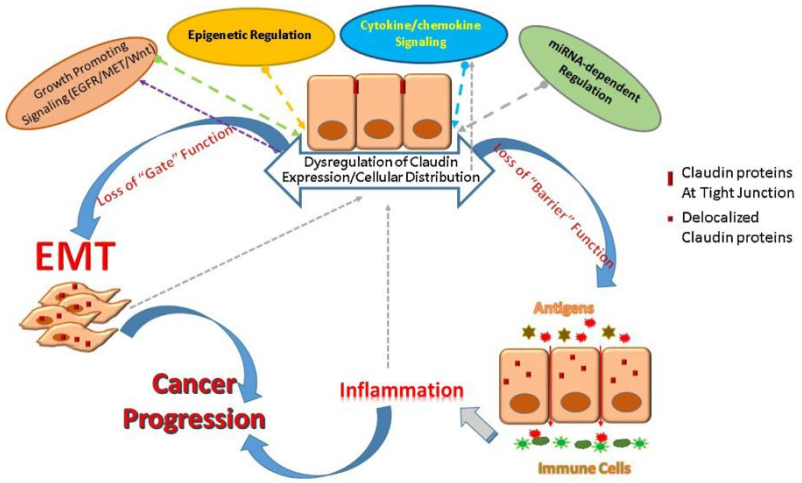

Figure 4 Roles and regulations of claudins in cancer progression. Claudin expression and localization is regulated by epigenetic factors, growth factors, and cytokines and their dysregulation leads to loss of the gate and barrier function which contributes in inflammation, EMT, and cancer progression.

As a result, cells become isolated and motile and do Metastasis i.e. move from the primary tumor site to distant vital organs and initiate secondary tumors (56,57). As integral part of TJs, claudins play a major role in EMT and metastasis and their deregulation has been documented in several cancers, for example upregulation of CLDN3 and -4 in multiple cancer types including prostate, pancreatic and ovarian cancer (58–60), increased however mislocalized (cytosolic/nuclear) expression of CLDN1 in colorectal cancer (61) and downregulation of CLDN1 in lung adenocarcinomas, prostate and breast cancer (Table 1). Recent studies have further suggested that claudin expression may even be distinct within specific subtypes of the cancers. This highlight claudins may partner with different proteins and involvement of diverse molecular mechanisms for regulation of claudin expression in different tissue microenvironments.

Table 1 Claudin expression and association with different cancers.

Cancer type	**Family member**	**Expression**	**Clinical association**
Lung (adenocarcinoma	Claudin-1	Downregulation	Poor survival
Lung (squamous cell lung carcinoma)	Claudin-1	Downregulation	LN metastasis, TMN stage, disease progression, Poor survival
Lung	Claudin-3	Upregulation	Poor survival

Lung (NSCLC)	Claudin-6 Claudin-7	Downregulation	LN metastasis, Higher TMN stage, Poor survival
Prostate	Claudin-1 Claudin-2 Claudin-3 Claudin-4 Claudin-5 Claudin-7 Claudin-8	Downregulation Downregulation Upregulation Upregulation Downregulation Downregulation Downregulation	High tumor grade, disease recurrence Advanced disease Advanced stage, disease recurrence Advanced stage disease, Lower-grade Advanced disease High tumor grade Advanced disease
Ovarian	Claudin-3 Claudin-4 Claudin-7	Upregulation Upregulation Upregulation	Disease progression, poor survival Disease progression Disease progression, poor survival, poor progression-free survival, poor sensitivity to platinum-based chemotherapy
Gastric	Claudin-1 Claudin-4 Claudin-6 Claudin-9	Downregulation Upregulation Upregulation Upregulation	Poor survival, advance disease, LN metastasis Histological differentiation, LN metastasis, higher TNM stage, poor survival Poor survival, advance disease Poor survival, advance disease
Colorectal	Claudin-1 Claudin-7 Claudin-23	Downregulation Upregulation Upregulation Downregulation Downregulation	LN metastasis, higher TNM stage, lymphatic invasion, poor survival, poor progression-free survival, poor survival recurrence Disease progression Tumor invasiveness, poor progression-free survival Liver metastasis recurrence, disease progression, Poor survival Poor survival
Breast	Claudin-1 Claudin-2 Claudin-3 Claudin-4	Upregulation Downregulation Upregulation Downregulation Downregulation Downregulation	Basal sub-type poor survival Poor progression-free survival, poor survival LN metastasis, ILC, liver metastasis LN metastasis and liver metastasis LN metastasis

	Claudin-7	Upregulation	LN metastasis
		Downregulation	Poor progression-free survival, poor survival, Basal sub-type poor survival, Basal sub-type cellular differentiation
		Upregulation	Poor progression-free survival, higher tumor grade, cellular decohesion, disease progression

1.5.4: CLDN6 and -9 in GC

CLDN6 and -9 are closely related with gastric cancer pathogenesis and their overexpression (mRNA and protein) is documented in GC tumors and in several cell lines (62–64). Overexpressed CLDN6 and -9 mis localized from TJ to cytoplasmic fractions over weaker expression in cytoskeleton and membrane (Figure 5) (63).

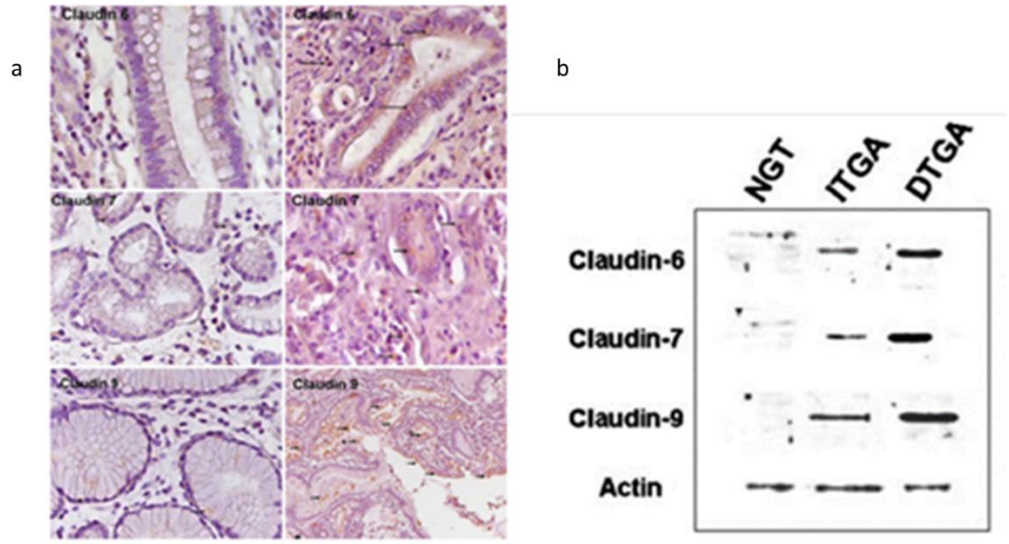

Figure 5 Overexpression of CLDN6/7/9 in gastric cancer patients. a) Normal gastric tissue (left panels) and gastric adenocarcinoma (right panels). b) Western blot analysis of whole cells protein lysate isolated from normal gastric tissue (NGT), diffuse-type gastric adenocarcinoma (DTGA), and intestinal-type gastric adenocarcinoma (ITGA) biopsies. (63)

CLDN6 interferes with the Hippo signaling pathway by reducing the phosphorylation of LATS1/2 and enhance the entry of YAP1 (Yes1 Associated Transcriptional Regulator) into the nucleus, which consequently effect the transcription of downstream target genes like *CYR61,*

CTGF, AREG, and AMOTL2 (64). YAP1 interacts with snail1 to affect the process of EMT and enhance the invasive ability of GC cells (64). Knockdown of *CLDN6* significantly affect snail1 but not zeb1 and twist1 (also seen in our lab's unpublished data) that further confirms, *CLDN6* promoted EMT in GC depends on YAP1 and YAP1-snail1 axis (64). In our experimental model, *CLDN6* and *-9* transfected AGS cells (individually) demonstrate increased proliferation, cell migration, and invasiveness (65). AGS-CLDN6 cells overexpress CLDN1 which was found to be colocalized with MMP-2 and MMP-14 with a significant increase in the membrane and cytosolic concentrations of MMP-14. Moreover, an increased amount of pro-MMP-2 was noticed in transfected cells which later secrete and provide a strong MMP-2 activity in culture supernatants (66). *CLDN6* and *-9* transfection seem to induce stem cell-like properties in AGS cells evident from increased CD44 expression on membrane and cytoplasm, and a significant increase in expression of transcription factors SOX-2 and SNAIL (unpublished results) in the nucleus. These studies indicate overexpressed CLDN6 and -9 in GC tumors mis localize in cytoplasm, promote EMT via YAP1-snail1 axis and help in acquire of an intermediate stem cell state to help cancer progression.

2: Natural killer cells

Natural killer (NK) cells belong to innate immune cells that respond with spontaneous cytolytic activity against cells under stress such as transformed cancer cells and virus-infected cells. They constitute 2–7% of lymphocytes in mouse peripheral blood and 5–15% of human peripheral blood mononuclear cells (PBMCs). Under physiological conditions NK cells are present in the skin, gut, liver, lung, uterus, kidney, joints, and breast. NK cells develop from common lymphoid progenitor cells (67) in bone marrow however, they can also develop in the liver and thymus (68,69). The development of NK cells happens through various stages of maturation, expansion, and acquisition of specific receptors and depends on several intrinsic factors (like transcription factors) and external signals (like cytokine and growth factors). NK cell receptors are independent of RAG-mediated recombination (70).

NK cells express a diverse receptor pool on their surface and fate of NK cell activation depends on engagement of these receptors with cognate ligands on target cell. These receptors can be group into two categories- activation receptors and inhibitory receptors (Figure 6). Normal healthy cells express MHC class I (MHCI) molecules which interact with inhibitory receptors of NK cells and refrain NK cells from activation and cytotoxic activity. However, viral infection or tumor transformation of cells results in loss of MHCI expression and

simultaneously increases expression of ligands linked with DNA damage response, stress, senescence, etc. These cumulatively interact with activating receptors and triggers the cytotoxic activity of NK cells (71).

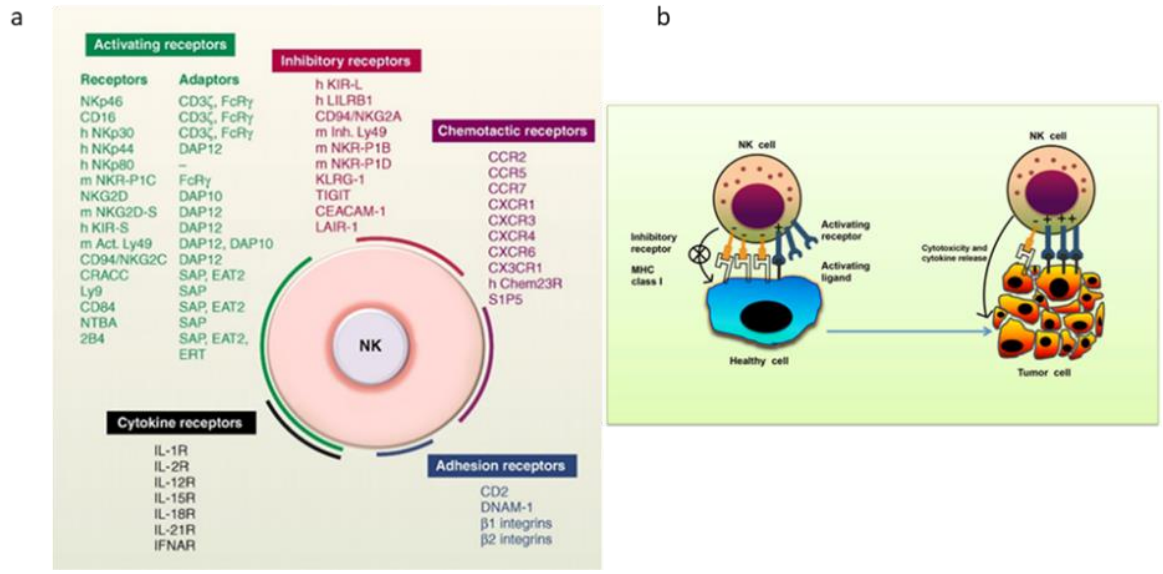

Figure 6 a) Important activation and inhibitory receptors on NK cell membrane and respective adaptors. b) Model of NK-Target contact and receptor ligand interaction following the killing of the target cell.

2.1: Inhibitory and activating receptors on NK cells

NK Inhibitory receptors have immunoreceptor tyrosine-based inhibitory motifs (ITIM), present in cytoplasmic tail, which upon ligand engagement undergo phosphorylation and recruitment of phosphatases- Src homology-containing tyrosine phosphatase 1 (SHP-1), SHP-2, and lipid phosphatase SH2 domain-containing inositol-5-phosphatase (SHIP). These phosphatases dephosphorylate the immunoreceptor tyrosine-based activation motif (ITAM) bearing Vav-1 molecules under inhibitory signal and prevent following downstream signaling (72,73). Humans express the killer cell immunoglobulin-like receptor (KIR) family of proteins (74) which are functional homolog of Ly49 (type II glycoprotein of C-type lectin-like superfamily) of mice. KIRs are type-I transmembrane proteins with two or three IgG-like domains and a short or long cytoplasmic tail. KIRs bind to HLA -A, -B, and -C molecules at their peptide-binding region. Individual NK cells express different KIRs, and their heterogeneity enhances further due to allelic variation in KIR genes in different individuals. Inhibitory KIRs include KIR2DL1–3, KIR2DL5, and KIR3DL1–3 (75). Another C-type lectin family of the inhibitory receptor-CD94-natural-killer group 2, member A (NKG2A) also contains the ITIM motif. NKG2A is expressed as a heterodimer with CD94 and it identifies non-classical MHC

molecules such as HLA-E (76,77) on target cells. CD94/NKG2A engagement protects host cells from inappropriate NK cell activation (78,79).

Lack of MHCI is not sufficient to trigger NK cell activation and it needs recognition of stress-induced molecules by activation receptors. Most activating receptors signal through ITAMs and engagement of receptor-ligand complexes leads to phosphorylation of ITAM by the Src family of tyrosine kinases such as Lck, Fyn, Src, Yes, Fgr, and Lyn. Phosphorylation of the ITAM subunit leads to recruitment and activation of the tyrosine kinase Syk and Zap70. The downstream signaling pathway of Zap70 phosphorylation involves phosphorylation of different proteins such as SLP-76, Shc, and phosphatidylinositol-3-OH kinase [PI3K], assembly of Grb2, linker for the activation of T cells (LAT), Vav-1, and Vav-2, activation of MAPKs and extracellular signal-regulated kinases (ERKs). These signals result in the elevation of calcium levels and reorganization of actin cytoskeleton which triggers transcription of cytokine and chemokine genes and release of perforin and granzymes containing cytolytic granules (80).

First in the most important activation receptors- Natural-killer group 2, member D (NKG2D) is a C-type lectin-like type II transmembrane protein. NKG2D is expressed as a homodimer on the surface of all murine and human NK cells, NKT cells, and activated $CD8^+$ T cells in mice, and all $CD8^+$ T cells and a subset of γδ T cells in humans(81). A single NKG2D homodimer along with two DAP10 homodimers forms a hexameric complete receptor of NKG2D (81). DAP10 adaptors contain YINM motif which get phosphorylated by Jak3 or Src family of kinases following recruitment of p85 subunit of PI3K or Grb2 adaptor protein. Phosphorylation of Grb2 induces phosphorylation of Vav1, PLC-γ2, and SLP-76. Such activation PI3K and Grb-Vav1 signaling induces phosphorylation of Jak2, STAT5, Akt, MEK1/2, and Erk (82–84). Effector functions of DAP10 and DAP12 differ from each other in both mice and humans. Deficiency studies have revealed that NKG2D-DAP10 signaling induces cytotoxicity while DAP12 can induce both cytotoxicity and cytokine secretion (85–87). NKG2D expression on NK and $CD8^+$ T cells is affected by several cytokines, for example- IL-7, IL-12, and IL-15 can upregulate the NKG2D expression, whereas interferon gamma (IFN-γ) and transforming growth factor-β (TGF-β) can reduce it (88–90). The NKG2D molecule in humans binds with several structural homologs of MHC class I molecules, which are organized into two families- MHC class I chain-related protein A (MICA) and B (MICB) and UL16-binding proteins (ULBP1-6) (91). Healthy adults express very low levels of NKG2D ligands (91,92) however,

they are highly upregulated in tumor cells such as leukemia, glioma, neuroblastoma, melanoma, breast, lung, colon, kidney, and prostate tumors (93–96). NKG2C and NKG2E, two other members of the NKG2 family, express as a heterodimer with CD94 and act as an activation receptor (97,98) and recognize class Ib molecule Qa-1b and interact with DAP12 and activate downstream signaling (98,99).

Natural cytotoxicity receptors (NCRs) are another important activating receptor of NK cells. They contain an extracellular immunoglobulin-like domain for ligand binding. Mouse NK cells express only NKP46 while human NK cells express three distinct types of NCRs- NKp46 (CD335), NKp44 (CD336), and NKp30 (CD337) (100). NKp44 expression is limited to activated NK cells, whereas NKp46 and NKp30 are expressed by both resting and activated NK cells. NCRs can bind to adaptor proteins FcεRI-γ and CD3-ζ which then transduce the signal through ITAM. NCRs recognize a wide variety of ligands on target cells ranging from viral, bacterial, and parasite proteins to molecules from tumor cells and other host cells (100).

CD38 is another molecule expressed by NK cells and other lymphocytes. CD38 is an ectoenzyme that catalyzes the conversion of beta-Nicotinamide adenine dinucleotide (beta-NAD+) and Beta-Nicotinamide Adenine Dinucleotide 2'-Phosphate (beta-NADP+) into cyclic adenosine diphosphate-ribose (cADPR), adenosine diphosphate-ribose (ADPR), and nicotinic acid adenine dinucleotide phosphate (NAADP). CD38 and ADPR get localized in cytolytic granules, promotes granule polarization and degranulation in tumor-activated NK cells (101). (CD38 is discussed in detail in the later sections.)

NK cell-mediated cytotoxicity and cytokine-chemokine secretion involve a synergistic combination of several receptors. Intriguing, only CD16 alone could trigger degranulation of resting human NK cells while most activating receptors such as NKG2D and NCRs can perform activation of NK cells only with synergistic activation of several other receptors that lead to convergence to achieve activation of central signaling molecule beyond the threshold (102,103).

2.2: Cytotoxicity of NK cells

The NK cell cytotoxic response is divided into four major steps-

(1) Formation of immunological synapse between the target cell and NK cell and reorganization of the actin cytoskeleton.

(2) Polarization of microtubule organizing center (MTOC) and secretory lysosome toward lytic synapse.
(3) Docking of secretory lysosome with the plasma membrane of NK cells.
(4) Fusion of secretory lysosome with the plasma membrane of target cells.

The entire process that results to the release of cytotoxic molecules such as perforin and granzyme is known as degranulation and is often used for indirect measurement of NK cell's cytotoxic activity (104). During degranulation, lysosomal-associated membrane protein-1(LAMP-1 or CD107a) and -2 (LAMP-2 or CD107b) transiently appear on the surface of NK cells and for the same reason, LAMP-1 expression on NK cell surface is used as an indirect measurement of NK cells cytolytic function (105).

Perforin- a pore-forming cytolytic protein, once released it polymerizes, and forms the pores on the target cell membrane to facilitate the entry of granzymes (serine proteases). Granzymes activate caspases that induce apoptosis in target cells. Perforin-dependent cytotoxicity is crucial for NK cell-mediated control of several tumors but is also supplemented with death receptor-induced target cell apoptosis. NK cells express TNF receptor ligand—Fas ligand (FasL), Tumor necrosis factor (TNF), and Tumor necrosis factor-related apoptosis-inducing ligand (TRAIL) and their engagement to cognate receptors induces conformational changes in the receptors and recruitment of adaptor proteins leading to apoptosis of target cells.

3: CD38

3.1: Structure

CD38 is a 45 Kd type II transmembrane glycoprotein with a single transmembrane segment near its N-terminus. It shares a 20-30% sequence identity with Aplysia ADP-ribosyl cyclase, BST-1 also termed CD157, and a GPI-anchored protein found in *Schistosoma mansoni* (106–108). It is formed by two identical monomers that favor a physiologically stable structure with a pocket at the middle of the cleft that is the enzyme active site(109). The crystal structure of the extra-membrane domain, which is fully active enzymatically and is crystallized as head-to-tail dimers, has been well determined (110–115).

3.2: CD 38 function

CD38 functions as a lymphocyte receptor and transducer of signals(116) and an ectoenzyme that generates cADPR involved in intracellular calcium mobilization(112). First, thought to be expressed only on thymocytes and activated T cells, CD38 was later found to be widely expressed on B cells, circulating monocytes, dendritic cells, granulocytes, plasma cells, both resting and circulating NK cells, neutrophils, and granulocytes (117–120). CD38 is also found on the surface of erythrocytes and platelets (121,122) where it plays an essential role, together with platelet/endothelial cell adhesion molecule 1 (CD31), in microenvironment retention of cancer cells(123). CD38 is also expressed in the cytoplasm and nucleus of non-lymphoid cells such as normal prostatic epithelial cells, pancreatic islet cells, smooth and striated muscle cells, renal tubules, retinal gangliar cells, and cornea(112,113).

As a surface receptor, CD38 is necessary for the activation and proliferation of immune cells. It establishes a weak and dynamic interaction with the non-substrate ligand CD31(113,124), in an interaction necessary for leukocyte adhesion and migration(125). CD38 has a very small cytoplasmic tail(126) suggesting it is unable to initiate a signaling cascade and so it associates with other signaling receptors such as TCR/CD3 in T cells(127,128), BCR (CD19/CD21 in B cells(129) and CD16/CD61 in NK cells(130). In addition, CD38 ligation with a counter ligand induces the expression and secretion of IL-1β, IL-6, IL-10, and IFN-γ from monocytes and T cells(131,132). NAADP, produced through the enzymatic activity of CD38(133) regulates T cell activation(134,135), proliferation(136,137) and chemotaxis(138). CD38 is found in recycling endosomes that contain perforin and granzymes(139) in the immunological synapse

when the TCR of cytotoxic T cells is engaged(140). CD38 is expressed on membrane rafts where it promotes cell signaling via Akt and Erk activation and it is exported out of the cells through the exocytic pathway(141). CD38 association to the signaling complex CD16/CD61 in NK cells membrane has a critical role in transducing activating signals(112). $CD38^{high}CD8^{+}$ T cells suppress the proliferation of $CD38^{-}CD4^{+}$ T cells(142), thus indicating its capacity to modulate T cell subsets with regulatory properties(143).

3.3: CD38 and cancer

Tumor microenvironment (TME), a coordinated network of immune, non-immune, and cancer cells with other noncellular components are vital for the development, progression, immune suppression, and persistence of cancer(144) as biological processes such as hypoxia, angiogenesis, autophagy, apoptosis resistance, and metabolic reprogramming are triggered.

High CD38 expression in immune cells such as T regs, B regs, MDSCs, and CD16-$CD56^{+}$NK cells contribute to a change in their immune function(145–148). A typical example of the latter is represented by the $CD4^{+}CD25^{high}FOX3^{+}$ Treg cells with high CD38 expression that define a suppressive subset of Tregs in multiple myeloma(145) and non-Hodgkin lymphoma(146) via cytokine-dependent mechanisms. However, CD31- T regs depict reduced immune suppressive activity that indicates the importance of CD38/CD31 interaction in Treg mediated immunosuppression(149). $CD38^{high}$ B reg cells produce Il-10(148), which inhibits T naïve cell differentiation to Th1 and Th17 cells while supporting the proliferation of T regs(150,151). The immunosuppressive role of myeloid-derived suppressor cells (MDSCs) strongly expanded in the cancer microenvironment(147), is well documented. CD38 expression is considered as a marker of MDSCs activity and $CD38^{high}$MDSCs have more prominent immune suppressive effects(151–153). At the same time, MDSCs promote neovascularization and tumor invasion(153).

The enhanced concentration of adenosine in the TME lead to increase or decrease of Adenylate cyclase or intracellular cyclic adenosine monophosphate in immune cells expressing adenosine receptor (T cells, Nk cells, dendritic cells, neutrophils, macrophages)(154,155) thus interfering with the activation of immune cells and favoring tumor progression(154–156).

TME is also characterized by the presence of hypoxia due to poor blood supply and increased oxygen consumption(157,158). NAD^{+} is produced by salvage pathway in hypoxic TME, which

is further converted to adenosine by CD38 expressing cells, thus further suppressing the immune response by recruitment of MDSCs, Tregs, tumor associated macrophages (TAMs)(159,160). Besides adenosine arbitrated immune suppression, CD38 bestowed NAADP is also involved in VEGF mediated angiogenesis through its involvement in Ca^{++} signaling. VEGF interacts with receptors VEGFR1 and VEGFR2. VEGF binding with VEGFR2 leads to the release of Ca^{++} in a process where CD38 contributes(161–164). Therefore, cells overexpressing CD38 in the TME direct the generation of an immune suppressive environment that reduces effector T cell functions but also promotes angiogenesis, provides immune escape, and helps in cancer progression.

4: CD38 and cytotoxic activity of NK cells

Target cell adhesion, granule polarization, and the degranulation processes of NK cells broadly depend on Ca^{++} mobilization achieved either by the influx of extracellular Ca^{++} or mobilization of Ca^{++} from intracellular stores like endoplasmic reticulum (ER) or lysosomes (165,166). Intracellular mobilization of Ca^{++} is based on three major intracellular Ca^{++} mobilizing second messengers- inositol 1,4,5-trisphosphate (IP3), cADPR and NAADP (167–169). Recently ADPR, a new Ca^{++} secondary messenger has been added to this list (170). NAADP, cADPR, and ADPR are pyridine nucleotide metabolites and are formed under multiple enzymatic activities of CD38- NAD glycohydrolase , ADP-ribosyl cyclase, and cADPR hydrolase activity (171). CD38 is frequently present in the cell surface and on membranes of several intracellular organelles including cytolytic granules on lymphocytes like NK and T cells. Activation of cytotoxic cells leads to activation of IP3 that triggers Ca^{++} release from ER and results in the influx of Ca^{++} through store-operated Ca^{++} entry (SOCE), moreover drives internalization of CD38 from cell membranes in early endosomes. CD38 in endosomes and on acidic granules further helps in Ca^{++} mobilization and SOCE via synthesis of cADPR and NAADP (170). It is rather interesting that tumor cell engagement and subsequent activation of NK cells and their cytotoxic activity, if not solely, highly depends on CD38. Interaction of NK cell with tumor cell activates CD38 to produce ADPR but not cADPR/NAADP, for the exocytosis of cytolytic granules (101). ADPR targets TRPM2 channels on cytolytic granules, and TRPM2-mediated Ca^{++} signaling induces cytolytic granule polarization and degranulation, resulting antitumor activity(101). NK cells treated with 8-Br-ADPR, an ADPR antagonist, as well as NK cells from $Cd38^{-/-}$ mice showed reduced tumor-induced granule polarization, degranulation, granzyme B secretion, and cytotoxicity of NK cells (101,170). Such observations clearly state role of CD38

in NK cell's cytotoxic activity after stimulation with cancer cells is principally lead by ADPR-TRPM2- Ca^{++} axis.

5: Background

CLDN6 and CLDN9 impart significantly in the progression of GC. In our experimental model AGS-CLDN6 and AGS-CLDN9 transfected cells exhibited a significant increase in proliferation, migration, and invasiveness over wt AGS cells. Additionally, these transfected cells overexpress CD44, snail, and SOX-2 which also indicate intermediate EMT stage and stem cell-like properties in these cells. Considering their metastatic and invasive potential, it is intriguing if they have immune-suppressive properties as well. When transfected cells co-cultured with human peripheral blood NK cells for 4 hours, NK cells co-cultured with AGS-CLDN6 and AGS-CLDN9 showed reduced expression of FasL and LAMP1 on their surface in comparison to NK cells co-cultured with wild type (wt) AGS cells (Figure 7a).

FasL and LAMP1 are transported to the membrane through lytic granules in NK cells, which once get activated by the contact of cancer cells, shoot these granules at immune synapse targeting cancer cells. LAMP1 is considered as an indirect measurement of cytolytic activity of cytotoxic cells like NK and T cells, a reduction of same indicated a reduction in the cytolytic activity of NK cells. Similarly, engagement of FasL and TRAIL to their cognate receptors on target cells triggers apoptosis in target cells. A reduction in FasL on the membrane of NK cells may indicate a defect in cytotoxic activity or cytolytic granule trafficking in our model. However immature but the second observation that supports these facts that there was no change in TNF secretion but in IL-6 and IL-8 (Figure 7 b, c, d) which differ in vesicular trafficking and secretion mechanisms. To our assumptions that may link with Ca^{++} mobilizations from acidic stores and annexed SOCE that regulate several functions including vesicular and cytolytic granule trafficking in NK cells.

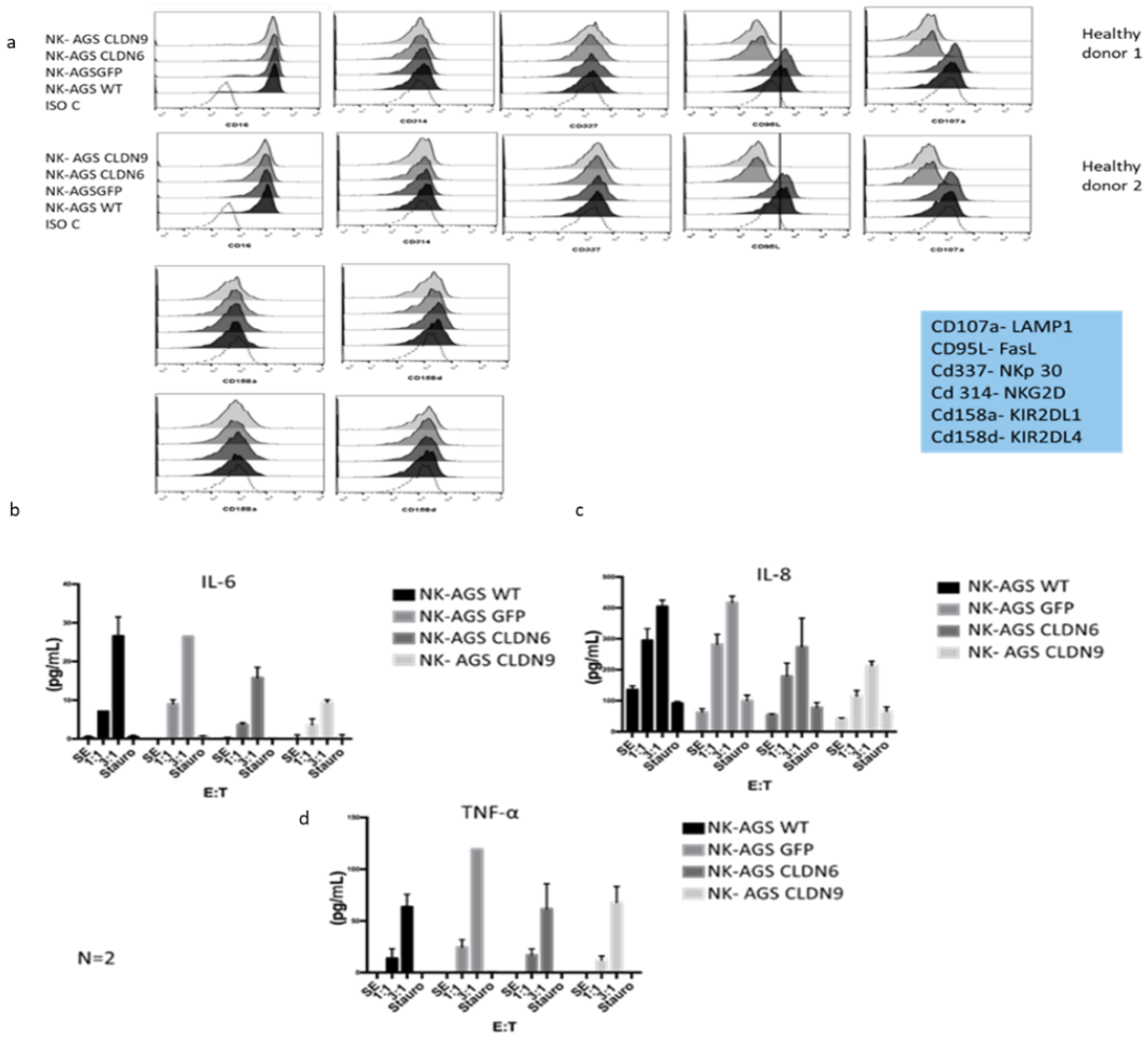

Figure 7 a) Expression of major receptors on NK cells after stimulation for 4 hours with AGS-CLDN6/9 cells. b), c), d) Secretion of IL-6, IL8, and TNFα from NK cells after stimulation with AGS-CLDN6/9 cells for 4 hours.

6: Justification

CLDN6 and CLDN9 impart significantly in the progression of GC and in our experimental model AGS-CLDN6 and AGS-CLDN9 transfected cells showed metastatic and invasive potential. When transfected cells were co-cultured with human peripheral blood NK cells for 4 hours, NK cells co-cultured with AGS-CLDN6 and AGS-CLDN9 showed reduced expression of FasL and LAMP1on their surface in comparison to NK cells co-cultured with wt AGS cells- evidently reduced cytolytic activity of NK cells. However, important receptors like- NKp30, NKG2D, KIR2DL1, KIR2DL4, etc. found to be unaffected which indicates the involvement of alternate mechanisms that affect granular polarity and reduction in NK cell's cytotoxic activity. Recent studies clarified the role of CD38-ADPR-TRPM2 axis mediated Ca^{++} movement from acidic granules, an alternative that deeply affects cytolytic granule polarity and cytotoxic activity of NK cells.

7: Hypothesis

- Stimulation/contact with AGS-CLDN6 and CLDN9 cells affect CD38-ADPR-TRPM2 axis in NK cells and interfere with cytolytic granule polarization.
- GC tumor with *TP53* and *CLDN6* alterations make a subgroup of CIN GC with distinctive prognostic signature.

8: General objective

- To analyze the effect on CD38 mediated cytolytic granule polarization in NK cells after stimulation/contact with CLDN6/9 transfected AGS cells.
- Analysis of *CLDN6* and *TP53* alterations (mutations and differential expression) in GC.

8.1: Specific objectives

A. To Investigate the changes in CD38 expression/activity is due to direct contact or by some secreted component of AGS transfected cells.

B. To check expression and activity in NK cells +/- stimulation with AGS-CLDN6/9 cells

   a. Check expression of CD38 on the surface and in the cytoplasm of NK cells.

   b. Intracellular localization of- FasL, LAMP1, and CD38 in NK cells.

   c. Localization of perforin and granzyme in cytolytic granules.

   d. Monitor Ca^{++} mobilization and cytolytic granule targeting.

C. Analysis of *CLDN6* and *TP53* alterations in GC.

   a. Analysis of the differentially expressed genes in AGS-CLDN6 transfected cells over wt AGS cells.

   b. Analysis of *CLDN6* alterations in TCGA-STAD data.

   c. Analysis of *TP53* alterations in TCGA-STAD data.

   d. Analyse correlation between *CLDN6* and *TP53* alterations in terms of altered genes and pathways to find common prognostic targets.

9: Material and methods

9.1: AGS cell culture and transfection

AGS cells ($1x10^6$, ATTC, CRL-1739), were cultured to >90% confluence in DMEM, supplemented with 5% FBS, 0.1 U/ml insulin, 2 mM sodium pyruvate, 2 mM L-Glutamine and 1% penicillin/streptomycin (Gibco; Biolegend Inc; Sigma-Aldrich and ThermoFisher Scientific), at 37°C and 5% CO2. AGS cells were transfected with *GFP-CLDN6* (Pmax GFP-*CLDN6* vector). *GFP-CLDN6* was linearized with AflII (New England Biolabs) and added into AGS cells with lipofectamine 2000 according to the manufacturer's protocol. Stable GFP positive cells were selected in supplemented DMEM with 500 μg/ml of G-418, sorted with a BD FACSAria™ III sorter (BD Biosciences) and plated (1 cell/well/96-well plate) for the selection of a stable clone. Expression of *GFP-CLDN6* was confirmed by immunofluorescence and flow cytometry.

9.2: NK and NK92mi cell culture

NK cells were purified from peripheral blood mononuclear cells of two healthy volunteers using Ficoll-Paque™ and Miltenyi Biotec NK cell isolation reagents. NK cells were cultured with 1,000 U/mL human rIL2 and its purity (>95%) was assessed by flow cytometry using fluorochrome-labeled anti-CD16, anti-CD56, and anti-CD3 antibodies. The IL-2-independent human NK-92MI (ATTC, CLR-2408) cells were cultured in α-MEM without nucleosides supplemented with 12.5% FBS, 12.5% horse serum, 1% penicillin/streptomycin, 2 mM L-glutamine, 0.2 mM inositol, 20 mM folic acid, and 100 μM 2-mercaptoethanol at 37°C and 5% CO2 until reaching >90% confluence.

9.3: NK/AGS cells co-cultures

AGS wt, AGS-CLDN6, and AGS-CLDN9 ($1x10^5$ cells/well) were seeded in 96-well plates, incubated for 12 h at 37°C and 5% CO2, and challenged with NK or NK92mi cells at 1:1 and 3:1 NK-AGS (E:T) cell ratios. After 4h of co-culture, cells were collected, centrifuged, the supernatant was discarded, and cells were resuspended in 100 μL of PBS buffer for further studies.

9.4: Flow cytometry

AGS and AGS-CLDN6 cells were fixed and permeabilized with Fix Buffer I and Perm Buffer III (BD Phosflow), according to manufacturer instructions. Cells were suspended in FACS buffer (PBS, 0.09% sodium azide, and 1% FBS) and incubated 30 min at 4°C with primary mouse antibodies against activating (anti-NKG2D, anti-NKp30, anti-FasL, anti-LAMP1) or inhibitory (anti-KIR2DL1, anti-KIR2DL4) receptors. Afterward, cells were washed with FACS buffer and incubated with the secondary fluorochrome-conjugated antibody for 1 h. Flow cytometry analysis was performed using the Flow Cytometer. For CD38 expression NK92mi cells were co-culture with AGS wt/CLDN6/CLDN9 cells and collected as mentioned above. Later NK92mi cells were fixed with Fix Buffer I washed with FACS buffer and subsequent incubation with fluorochrome-conjugated anti-CD38 antibody (Biolegend) at 4°C in dark for 30 minutes. Cells were washed with FACS buffer and studied with the flow-cytometer.

9.5: Stimulation of NK92mi cells with AGS conditioned media

AGS wt/CLDN6/CLDN9 cells were seeded ($1x10^6$) in fresh P-100 Petri plates and allowed to adhere overnight. The next morning cells were washed twice with PBS and cultured with fresh DMEM (supplemented as before) for 24 hours. The next day the culture media was carefully collected and used for stimulation of NK92mi cells. NK92mi cells were cultured in a T75 culture flask in α-MEM (supplemented) after 3 passages cells were counted and $2x10^5$ cells were transferred in each well of 6 well culture plates. Following stimulation of cells with culture media (50% conditioned with fresh serum-free α-MEM) from AGS transfected cells for 4 hours. Following the collection, NK92mi cells were washed twice with FACS buffer and subsequent incubation with fluorochrome-conjugated anti-CD38 antibody (Biolegend) at 4°C in dark for 30 minutes. Cells were washed with FACS buffer and studied with the flow cytometer.

9.6: Databases and expression data-based analysis

Affymetrix Hugene2.0 microarray was used to analyse mRNA expression in AGS-CLDN6 cells taking wt AGS cells as control. Expression data files were normalized and further processed for identification of differentially expressed genes (DEGs) using R version 4.0. CBioPortal was used to extract and analyze data from TCGA Stomach Adenocarcinoma Pan-

Cancer Atlas Data (STAD) (172,173). *CLDN6* was used in the query gene-based search of STAD 440 patient's data following selection of 139 patients/samples with *CLDN6* alterations in cldn-6 group while 268 patients/samples were assigned to the non-cldn-6 group. Group comparison tool was used to analyze aneuploidy score, mutation count, MSIsensor score, fractional genome altered, survival of patients, GC grade distribution, histological subtype classification, TCGA-STAD classification subtype, and sex ratio distribution between groups. Direct genome interactions were analyzed with default settings for overlap among patients/samples, with log-ratio calculated from Log2 based ratio of (pct in (A) cldn-6 group/pct in (B) non cldn-6 group, the p-value was derived from one-sided Fisher Exact test and q value was based on Benjamini-Hochberg procedure. Changes in gene expression were compared through mRNA expression levels of altered genes in both groups in terms of μ score (mean log2 expression of genes), σ score (standard deviation of log2 expression of genes), log-ratio (Log2 of the ratio of (unlogged) mean in the cldn-6 group to (unlogged) mean in the non-cldn-6 group), with p-value (Derived from Student's t-test) and q-value (Derived from Benjamini-Hochberg procedure). Volcano plots, heatmaps, and clustering were done using the CBioPortal query gene-based search result with default settings. Query gene-based search and Oncoprint features of CBioPortal were used to find total alterations and z scores of genes among samples in groups and data were plotted in GraphPad Prism (version 8). Similarly, TCGA STAD data was divided in to TP53 and non TP53 mutations groups according to *TP53* mutation in GC patients/samples and compared to generate results as mentioned above using CBioPortal and GraphPad Prism.

9.7: Gene set enrichment analysis (GSEA) and Gene ontology (GO) enrichment

Data were collected from previously done microarray expression analysis of AGS-CLDN6 cells. All DEGs with logFc≥0.5 and with p-value ≤0.05 were used for GSEA molecular signature database (MSigDB) investigations with a False Discovery Rate (FDR) q value≤0.05. mRNA log-ratio data of DEGs between cldn-6 /non- cldn-6 groups and TP53/nonTP53 groups were downloaded from CBioPortal. GO biological process (BP) functional enrichment of genes was done using the FunRich tool (174) for all DEGs. Common up-regulated DEGs between cldn-6 and TP53 groups were enriched in GO MSigDB of GSEA with FDR q value≤0.05 and p-value ≤0.05.

9.8: Venn diagram and identification of commonly upregulated genes

FunRich was used to generate Venn diagram from a list of DEGs to identify commonly upregulated genes between cldn-6 and TP53 groups. Log-ratio cutoff ≥ 1 and p-value ≤0.05 were used to select upregulated genes in cldn-6 and TP53 groups and further comparison of common genes using FunRich and Venn diagram was done.

9.9: Gene interaction network, gene expression comparison, and survival curves

Common DEGs between cldn-6 and TP53 group samples with log ration cutoff ≥1 were analyzed for gene interaction through GeneMANIA with default settings. Networks were further analyzed using Cytoscape (175) software. Molecular Complex Detection (MCODE) app in Cytoscape (176) was used for identification of important clusters in each group with a degree cutoff-2.0, node cutoff- 0.2, K-score-2, and max depth-100. Batch normalized from illumine HiSeq_RNASeqV2 mRNA expression of top 10 DEGs in cldn-6 and TP53 groups were obtained from the CBioPortal group comparison tool. Kaplan-Meier Plotter (Kaplan-Meier plotter [Gastric] (kmplot.com)) was used to assess the effect of genes on the survival of patients (n=631).

10: Results

10.1: Effect on CD38 mediated cytolytic granule polarization in NK cells after stimulation/contact with *CLDN6/9* transfected AGS cells

Previous results that demonstrate the reduction in peripheral blood NK cells' cytotoxic activity after co-culture/stimulation with AGS-CLDN6/CLDN9 cells need a mechanistic explanation of such stimulation. Two basic probabilities are AGS-CLDN6/CLDN9 cells induce such immunosuppressive effects either by a secreted component or by direct contact.

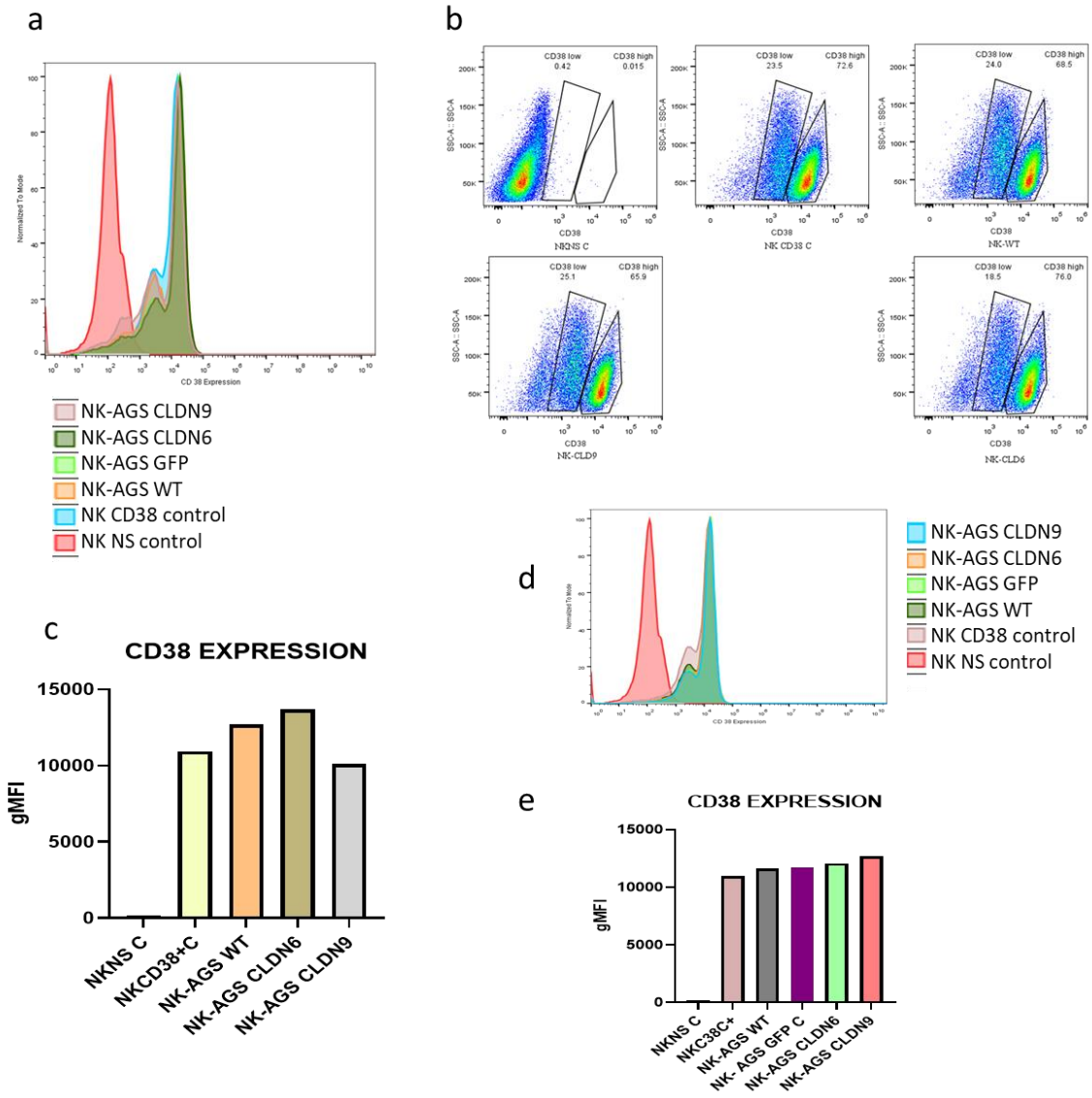

Figure 8 (a-c) surface expression of CD38 on NK92mi cells after co-culture with AGS-CLDN6/CLDN9 cells for 4 hours. d, e) CD38 expression on the cell membrane of NK92mi cells after stimulation for 4 hours with 50% conditioned media from AGS-CLDN6/CLDN9.

The other important question is to understand the underlying mechanism induced in NK cells that results in reduction of surface expression of FasL and LAMP1 after stimulation with AGS-CLDN6/CLDN9 which we hypothesize is, CD38 mediated cytolytic granule polarity.

10.2: Expression of CD38 in NK92mi cells after co-culture with *CLDN6/CLDN9* transfected AGS cells

In stable cultures, NK92mi cells express high amounts of CD38 on the surface, however, overall populations were divided into three different groups, high expression (majority), low expression, and minimal expression (minority) (Figure 8a, b). When these cells were co-cultured with AGS-CLDN6/CLDN9 cells for 4 hours we saw the same pattern, NK92mi populations were divided into high, low, and no expression. However, NK92mi cells co-cultured with AGS-CLDN9 demonstrate an overall reduction in gMFI (geometric mean fluorescence intensity) of surface CD38 (Figure 8c). To check if this change was induced by a secreted component from transfected cells, NK92mi cells were stimulated with 50% conditioned media from AGS-CLDN6/CLDN9 for 4 hours and checked for CD38 surface expression. Interestingly there was no significant change in CD38 surface expression which indicates the reduction in CD38 expression in NK cells co-cultured with AGS-CLDN9 was induced by direct AGS-NK contact (Figure 8d, e).

In future experiments, NK cells from the peripheral blood will be purified through a MACS magnetic separator kit to be used for co-culture experiments. After a 4-hour stimulation with AGS-CLDN6/CLDN9, NK cells will be analyzed for intracellular expression of CD38 by immunofluorescence. Similarly, post-stimulation localization of FasL and LAMP1 along with perforin and granzyme will be investigated within NK cells. To confirm the role of CD38 mediated Ca^{++} in cytolytic granule polarity NK cells will be loaded with 5 mM Fluo-4 AM (Invitrogen) in HBSS at 37°C for 40 min and changes in $[Ca^{++}]_i$ will be determined at 488 nm excitation/530 nm emission wavelengths using a confocal microscope. As already mentioned, any changes in CD38 activity post-stimulation will affect the mobility of cytolytic granules and/or localization of FasL and LAMP1. We will also use CD38 inhibitors like Cibacron Blue-3GA to further confirm the role of CD38.

10.3: Analysis of *CLDN6* and *TP53* alterations in GC

In recent years, generation of high throughput expression data from Microarrays and RNA sequencing has immensely expanded cancer research horizon. Availability of this data in large public databases curated under national and international alliances like Gene Expression Omnibus and TCGA and parallel development of bioinformatics tools like Gene ontology, GSEA, and CBioPortal, further facilitate interplay with insights of this data for good. The GO knowledgebase is the world's largest source of information on the functions of genes which is easily accessible and is human and machine-readable. GSEA is a powerful analytical method for interpreting gene expression data. The method focusses on gene sets, that is, groups of genes that share common biological function, chromosomal location, or regulation that helps identify smallest of contributions made by genes in a pathway. Moreover, GSEA allows to explore and investigate independent Molecular Signatures Database which are collection of annotated gene sets for use with GSEA software. CBioPortal is an interactive web application platform that allows data exploration and analysis. CBioPortal currently hosts more than 40 datasets from TCGA and other large-scale genomic studies, which can be interrogated across genes, samples, and data types. Such mRNA expression data intricated with clinical information allows identification of DEGs and tools like GO, and GSEA aligns their functional role leading to identification of driver pathways, key genes, biomarkers, and prognostic targets in several cancers.

In a similar attempt, we used Microarray based mRNA expression data from AGS cells transfected with *CLDN6* (L. F. Montaño's lab) and expression data from TCGA-STAD to explore further entanglements of *CLDN6* in GC. *CLDN6* expression in GC is discussed in several researches and presents a controversial image. In current study we seek, how overexpression of *CLDN6* affects several pathways and promotes cancer survival and progression? How alterations in *CLDN6* affect GC patients and distribution of such GC tumors in Lauren and TCGA GC classification subtypes and lastly to identify DEGs linked with *CLDN6* alterations to be used as prognostic targets.

10.3.1: AGS-CLDN6 transfected cells have altered metabolism and persistent ER stress

AGS-CLDN6 transfected cells were checked for DEGs over wt AGS cells using Affymetrix Hugene2.0 microarray. Genes with LogFC≥0.5 were considered significant and used for GSEA

analysis. A total of 530 genes were investigated in the MSigDB- Hallmark gene set enrichment. Top 10 overlap (Table 3) includes 29 genes in unfolded protein response group, 34 genes in MTORC1 signaling, following 17,19, and 17 genes in cholesterol homeostasis, hypoxia, and TNFα signaling via NFkB gene sets. In GO MSigDB enrichment most of the genes accumulated in organelles, ER, and nuclear compartments (Table 4). Moreover, in the biological process genes were enriched in response to ER stress, topologically incorrect proteins, and small molecule metabolic processes categories (Table 4). Collectively, AGS-CLDN6 transfected cells have complex deregulation of metabolism, disruption in ER homeostasis and may have persistent ER stress.

10.3.2: *CLDN6* alterations are associated with poor survival and higher aneuploidy in GC tumors

STAD data of TCGA with 440 patients were divided into two groups with CBioPortal interface for patients with or without *CLDN6* alterations. Cldn-6 group with *CLDN6* alterations have139 GC patients/samples (34%) while the non-cldn-6 group gathered data of 268 GC patients/samples. Major alterations in *CLDN6* include shallow deletion, diploid, gain, and overexpressed mRNA (Figure 9 a, b). The samples in the cldn-6 group demonstrate higher aneuploidy, with higher fraction genome altered and lower MSI score than non-cldn-6 group samples. However, there is no significant difference in mutation load among groups (Figure 9 c-f). *CLDN6* alterations were indeed linked with worst overall and progression free survival (Figure 9 g, h). The distribution of samples for different GC Grade, histological types, and sex revealed, cldn-6 group samples frequently distributed in Intestinal-type GC over Diffuse type besides the non-cldn-6 group have more samples in general (Figure 10 a, b). Interestingly, cldn-6 group samples primarily accumulated in CIN subtype of STAD classification of GC over a broader distribution of samples in different subtypes in the non-cldn-6 group. As expected CIN is the major subtype in both groups (Figure 10 c). These observations conclude that *CLDN6* alterations in GC belongs to a subgroup of Intestinal type which is more justified as a subgroup of CIN GC subtype.

Table 2 List of top overexpressed genes in AGS-CLDN6 transfected cells.

PROBEID	ENTREZID	SYMBOL	GENENAME	logFC	AveExpr	t	P.Value	adj.P.Val
17112656	27035	NOX1	NADPH oxidase 1	2.467	4.997	6.533	0.000	0.028
16979917	23657	SLC7A11	solute carrier family 7 member 11	2.183	9.046	7.351	0.000	0.017
16823251	9074	CLDN6	claudin 6	2.170021	3.934294	10.13342	3.56E-07	0.003
16819325	9709	HERPUD1	homocysteine inducible ER protein with ubiquitin like domain 1	2.162	9.425	9.091	0.000	0.006
16666055	1491	CTH	cystathionine gamma-lyase	1.901	6.474	9.222	0.000	0.006
16705961	54541	DDIT4	DNA damage inducible transcript 4	1.840	6.842	4.902	0.000	0.111
16794318	317760	ADAM20P1	ADAM metallopeptidase domain 20 pseudogene 1	1.741	6.400	8.778	0.000	0.007
16700911	56605	ERO1B	endoplasmic reticulum oxidoreductase 1 beta	1.684	5.340	7.468	0.000	0.017
17124338	80350	LPAL2	lipoprotein(a) like 2, pseudogene	1.654	4.553	4.211	0.001	0.165
16756310	255394	TCP11L2	t-complex 11 like 2	1.644	5.616	6.269	0.000	0.032
17083614	286343	LURAP1L	leucine rich adaptor protein 1 like	1.630	8.250	8.655	0.000	0.007
16848079	55062	WIPI1	WD repeat domain, phosphoinositide interacting 1	1.630	8.415	6.839	0.000	0.021
16962022	27074	LAMP3	lysosomal associated membrane protein 3	1.593	6.795	7.965	0.000	0.015
16796694	7453	WARS	tryptophanyl-tRNA synthetase	1.524	8.298	7.203	0.000	0.018
16962661	9076	CLDN1	claudin 1	1.520	9.019	7.233	0.000	0.018
17121072	400221	FLJ22447	uncharacterized LOC400221	1.469	5.107	2.596	0.024	0.418
16795394	6400	SEL1L	SEL1L, ERAD E3 ligase adaptor subunit	1.461	9.290	6.715	0.000	0.022
16716478	27063	ANKRD1	ankyrin repeat domain 1	1.455	9.375	7.733	0.000	0.017
16686201	6536	SLC6A9	solute carrier family 6 member 9	1.441	7.558	6.121	0.000	0.035
16998810	134429	STARD4	StAR related lipid transfer domain containing 4	1.421	6.084	5.359	0.000	0.072
17125034	440	ASNS	asparagine synthetase (glutamine-hydrolyzing)	1.411	8.701	5.863	0.000	0.047
16782548	5106	PCK2	phosphoenolpyruvate carboxykinase 2, mitochondrial	1.378	7.050	7.425	0.000	0.017
16705551	80201	HKDC1	hexokinase domain containing 1	1.332	4.875	3.195	0.008	0.316
17060061	440	ASNS	asparagine synthetase (glutamine-hydrolyzing)	1.330	7.891	5.987	0.000	0.041
16785048	400221	FLJ22447	uncharacterized LOC400221	1.319	7.687	2.671	0.021	0.404
16795794	9252	RPS6KA5	ribosomal protein S6 kinase A5	1.303	5.908	5.243	0.000	0.075
16992467	153222	CREBRF	CREB3 regulatory factor	1.288	4.860	6.817	0.000	0.021
16799739	79094	CHAC1	ChaC glutathione specific gamma-glutamylcyclotransferase 1	1.287	8.585	4.219	0.001	0.164
16949292	51726	DNAJB11	DnaJ heat shock protein family (Hsp40) member B11	1.283	9.862	7.103	0.000	0.019
16937050	9695	EDEM1	ER degradation enhancing alpha-mannosidase like protein 1	1.268	7.594	6.996	0.000	0.020
17072653	1.01E+08	PCAT1	prostate cancer associated transcript 1	1.260	5.789	4.398	0.001	0.154
16927633	23753	SDF2L1	stromal cell derived factor 2 like 1	1.259	7.933	6.952	0.000	0.020
16925158	757	TMEM50B	transmembrane protein 50B	1.240	7.744	6.313	0.000	0.032
16766588	693201	MIR616	microRNA 616	1.239	3.161	4.209	0.001	0.165
17063507	80853	KDM7A	lysine demethylase 7A	1.239	6.794	6.737	0.000	0.022
16747991	57494	RIMKLB	ribosomal modification protein rimK like family member B	1.219	6.542	5.442	0.000	0.070
16690704	9122	SLC16A4	solute carrier family 16 member 4	1.218	6.832	4.074	0.002	0.182
16766578	1649	DDIT3	DNA damage inducible transcript 3	1.215	5.467	4.173	0.001	0.168
17050328	4189	DNAJB9	DnaJ heat shock protein family (Hsp40) member B9	1.180	5.728	6.289	0.000	0.032
16672489	1.01E+08	LINC01133	long intergenic non-protein coding RNA 1133	1.179	6.650	5.827	0.000	0.048
17125794	5645	PRSS2	serine protease 2	1.176	9.730	2.751	0.018	0.390
16979256	9871	SEC24D	SEC24 homolog D, COPII coat complex component	1.160	8.237	4.702	0.001	0.125
16996684	11174	ADAMTS6	ADAM metallopeptidase with thrombospondin type 1 motif 6	1.154	5.415	4.879	0.000	0.113
16671856	1E+08	MSTO2P	misato family member 2, pseudogene	1.148	6.083	5.397	0.000	0.072
17081401	10397	NDRG1	N-myc downstream regulated 1	1.124	5.985	6.125	0.000	0.035
16941167	7873	MANF	mesencephalic astrocyte derived neurotrophic factor	1.121	7.254	6.272	0.000	0.032
17009093	7422	VEGFA	vascular endothelial growth factor A	1.117	8.036	6.041	0.000	0.039
17064135	9601	PDIA4	protein disulfide isomerase family A member 4	1.112	10.358	5.520	0.000	0.065
16986583	133746	JMY	junction mediating and regulatory protein, p53 cofactor	1.110	7.484	4.468	0.001	0.154
16931569	79174	CRELD2	cysteine rich with EGF like domains 2	1.104	6.760	5.590	0.000	0.062
17125032	440	ASNS	asparagine synthetase (glutamine-hydrolyzing)	1.101	3.120	4.122	0.001	0.178
16776117	5095	PCCA	propionyl-CoA carboxylase subunit alpha	1.089	7.694	5.301	0.000	0.074
16830202	54739	XAF1	XIAP associated factor 1	1.088	6.945	3.261	0.007	0.306
16735639	440026	TMEM41B	transmembrane protein 41B	1.085	7.275	4.824	0.000	0.116
16924207	6782	HSPA13	heat shock protein family A (Hsp70) member 13	1.083	7.694	4.790	0.000	0.120
16982006	1.05E+08	LINC02365	long intergenic non-protein coding RNA 2365	1.078	5.816	3.475	0.005	0.269
16740342	84447	SYVN1	synoviolin 1	1.071	7.375	4.747	0.000	0.124
16794321	8748	ADAM20	ADAM metallopeptidase domain 20	1.069	4.586	5.956	0.000	0.041
17054328	90637	ZFAND2A	zinc finger AN1-type containing 2A	1.063	6.123	5.016	0.000	0.097
16880712	6509	SLC1A4	solute carrier family 1 member 4	1.062	7.441	3.902	0.002	0.206
16806561	1.02E+08	DNM1P50	dynamin 1 pseudogene 50	1.062	5.188	4.360	0.001	0.154
16898578	2673	GFPT1	glutamine--fructose-6-phosphate transaminase 1	1.059	10.073	4.307	0.001	0.158
16833327	162394	SLFN5	schlafen family member 5	1.045	7.809	5.173	0.000	0.082
17098411	3309	HSPA5	heat shock protein family A (Hsp70) member 5	1.036	12.258	5.380	0.000	0.072
16757098	10019	SH2B3	SH2B adaptor protein 3	1.029	6.477	5.547	0.000	0.063
17056310	55033	FKBP14	FK506 binding protein 14	1.028	6.997	4.897	0.000	0.111
16673104	51478	HSD17B7	hydroxysteroid 17-beta dehydrogenase 7	1.026	5.428	4.264	0.001	0.163
16929562	3162	HMOX1	heme oxygenase 1	1.024	7.303	2.304	0.040	0.466
17009117	221416	C6orf223	chromosome 6 open reading frame 223	1.019	5.748	5.271	0.000	0.074
16860644	1054	CEBPG	CCAAT enhancer binding protein gamma	1.014	8.301	5.639	0.000	0.060
17022736	51175	TUBE1	tubulin epsilon 1	1.014	6.444	5.355	0.000	0.072
16745186	10525	HYOU1	hypoxia up-regulated 1	1.007	10.248	4.620	0.001	0.130
16767324	1E+08	SNORA70G	small nucleolar RNA, H/ACA box 70G	1.006	3.643	5.217	0.000	0.077

Table 3 Enrichment of DEGs (LogFC≥0.5, p-value ≤0.05) from AGS-CLDN6 cells in Hallmarks gene sets MSigDB of GSEA.

Gene Set Name [# Genes (K)]	Description	# Genes in Overlap (k)	k/K	p-value	FDR q-value
HALLMARK_UNFOLDED_PROTEIN_RESPONSE [113]	Genes up-regulated during unfolded protein response, a cellular stress response related to the endoplasmic reticulum.	29		$3.72\ e^{-30}$	$1.86\ e^{-28}$
HALLMARK_MTORC1_SIGNALING [200]	Genes up-regulated through activation of mTORC1 complex.	34		$1.13\ e^{-28}$	$2.82\ e^{-27}$
HALLMARK_CHOLESTEROL_HOMEOSTASIS [74]	Genes involved in cholesterol homeostasis.	17		$2.54\ e^{-17}$	$4.24\ e^{-16}$
HALLMARK_HYPOXIA [200]	Genes up-regulated in response to low oxygen levels (hypoxia).	19		$6.8\ e^{-12}$	$8.5\ e^{-11}$
HALLMARK_TNFA_SIGNALING_VIA_NFKB [200]	Genes regulated by NF-kB in response to TNF [GeneID=7124].	17		$4.99\ e^{-10}$	$4.99\ e^{-9}$
HALLMARK_ANDROGEN_RESPONSE [100]	Genes defining response to androgens.	12		$3.63\ e^{-9}$	$3.03\ e^{-8}$
HALLMARK_P53_PATHWAY [200]	Genes involved in p53 pathways and networks.	14		$1.93\ e^{-7}$	$1.38\ e^{-6}$
HALLMARK_INTERFERON_ALPHA_RESPONSE [97]	Genes up-regulated in response to alpha interferon proteins.	9		$2.99\ e^{-6}$	$1.87\ e^{-5}$
HALLMARK_INTERFERON_GAMMA_RESPONSE [200]	Genes up-regulated in response to IFNG [GeneID=3458].	12		$7.08\ e^{-6}$	$3.54\ e^{-5}$
HALLMARK_XENOBIOTIC_METABOLISM [200]	Genes encoding proteins involved in processing of drugs and other xenobiotics.	12		$7.08\ e^{-6}$	$3.54\ e^{-5}$

Table 4 Enrichment of DEGs (LogFC≥0.5, p-value ≤0.05) from AGS-CLDN6 cells in GO MSigDB of GSEA.

Gene Set Name [# Genes (K)]	Description	# Genes in Overlap (k)	p-value	FDR q-value
GOCC_ORGANELLE_SUBCOMPARTMENT [1772]	A compartment that consists of a lumen and an enclosing membrane and is part of an organelle. [GOC:mah, GOC:pz]	89	$2.61\ e^{-30}$	$2.66\ e^{-26}$
GOBP_RESPONSE_TO_ENDOPLASMIC_RETICULUM LUM_STRESS [295]	Any process that results in a change in state or activity of a cell (in terms of movement, secretion, enzyme production, gene expression, etc.) as a result of a stress acting at the endoplasmic reticulum. ER stress usually results from the accumulation of unfolded or misfolded proteins in the ER lumen. [GOC:cjm, GOC:mah]	39	$1.94\ e^{-28}$	$9.87\ e^{-25}$
GOBP_RESPONSE_TO_TOPOLOGICALLY_INCORRE RRECT_PROTEIN [205]	Any process that results in a change in state or activity of a cell or an organism (in terms of movement, secretion, enzyme production, gene expression, etc.) as a result of a protein that is not folded in its correct three-dimensional structure. [GOC:bf]	33	$4.6\ e^{-27}$	$1.56\ e^{-23}$
GOBP_CELLULAR_RESPONSE_TO_TOPOLOGICALL ALLY_INCORRECT_PROTEIN [168]	Any process that results in a change in state or activity of a cell (in terms of movement, secretion, enzyme production, gene expression, etc.) as a result of a protein that is not folded in its correct three-dimensional structure. [GOC:bf]	30	$4.23\ e^{-26}$	$1.08\ e^{-22}$
GOBP_ENDOPLASMIC_RETICULUM_UNFOLDED_PR _PROTEIN_RESPONSE [127]	The series of molecular signals generated as a consequence of the presence of unfolded proteins in the endoplasmic reticulum (ER) or other ER-related stress; results in changes in the regulation of transcription and translation. [GOC:mah, PMID:12042763]	26	$2.11\ e^{-24}$	$4.29\ e^{-21}$
GOCC_NUCLEAR_OUTER_MEMBRANE_ENDOPLASMI SMIC_RETICULUM_MEMBRANE_NETWORK [1141]	The continuous network of membranes encompassing the nuclear outer membrane and the endoplasmic reticulum membrane. [GOC:bf, GOC:jl, GOC:mah, GOC:mcc, GOC:pr, GOC:vw]	62	$7.21\ e^{-23}$	$1.22\ e^{-19}$
GOCC_ENDOPLASMIC_RETICULUM [1960]	The irregular network of unit membranes, visible only by electron microscopy, that occurs in the cytoplasm of many eukaryotic cells. The membranes form a complex meshwork of tubular channels, which are often expanded into slitlike cavities called cisternae. The ER takes two forms, rough (or granular), with ribosomes adhering to the outer surface, and smooth (with no ribosomes attached). [ISBN:0198506732]	81	$4.18\ e^{-22}$	$6.08\ e^{-19}$
GOBP_IRE1_MEDIATED_UNFOLDED_PROTEIN _RE _RESPONSE [67]	A series of molecular signals mediated by the endoplasmic reticulum stress sensor IRE1 (Inositol-requiring transmembrane kinase/endonuclease). Begins with activation of IRE1 in response to endoplasmic reticulum (ER) stress, and ends with regulation of a downstream cellular process, e.g. transcription. One target of activated IRE1 is the transcription factor HAC1 in yeast, or XBP1 in mammals; IRE1 cleaves an intron of a mRNA coding for HAC1/XBP1 to generate an activated HAC1/XBP1 transcription factor, which controls the up regulation of UPR-related genes. At least in mammals, IRE1 can also signal through additional intracellular pathways including JNK and NF-kappaB. [GOC:bf, GOC:PARL, PMID:22013210]	15	$2.93\ e^{-15}$	$3.73\ e^{-12}$
GOBP_SMALL_MOLECULE_METABOLIC_PROCESS [1886]	The chemical reactions and pathways involving small molecules, any low molecular weight, monomeric, non-encoded molecule. [GOC:curators, GOC:pde, GOC:vw]	67	$4.38\ e^{-15}$	$4.96\ e^{-12}$
GOMF_MISFOLDED_PROTEIN_BINDING [29]	Interacting selectively and non-covalently with a misfolded protein. [GOC:ai]	11	$2.17\ e^{-14}$	$2.21\ e^{-11}$

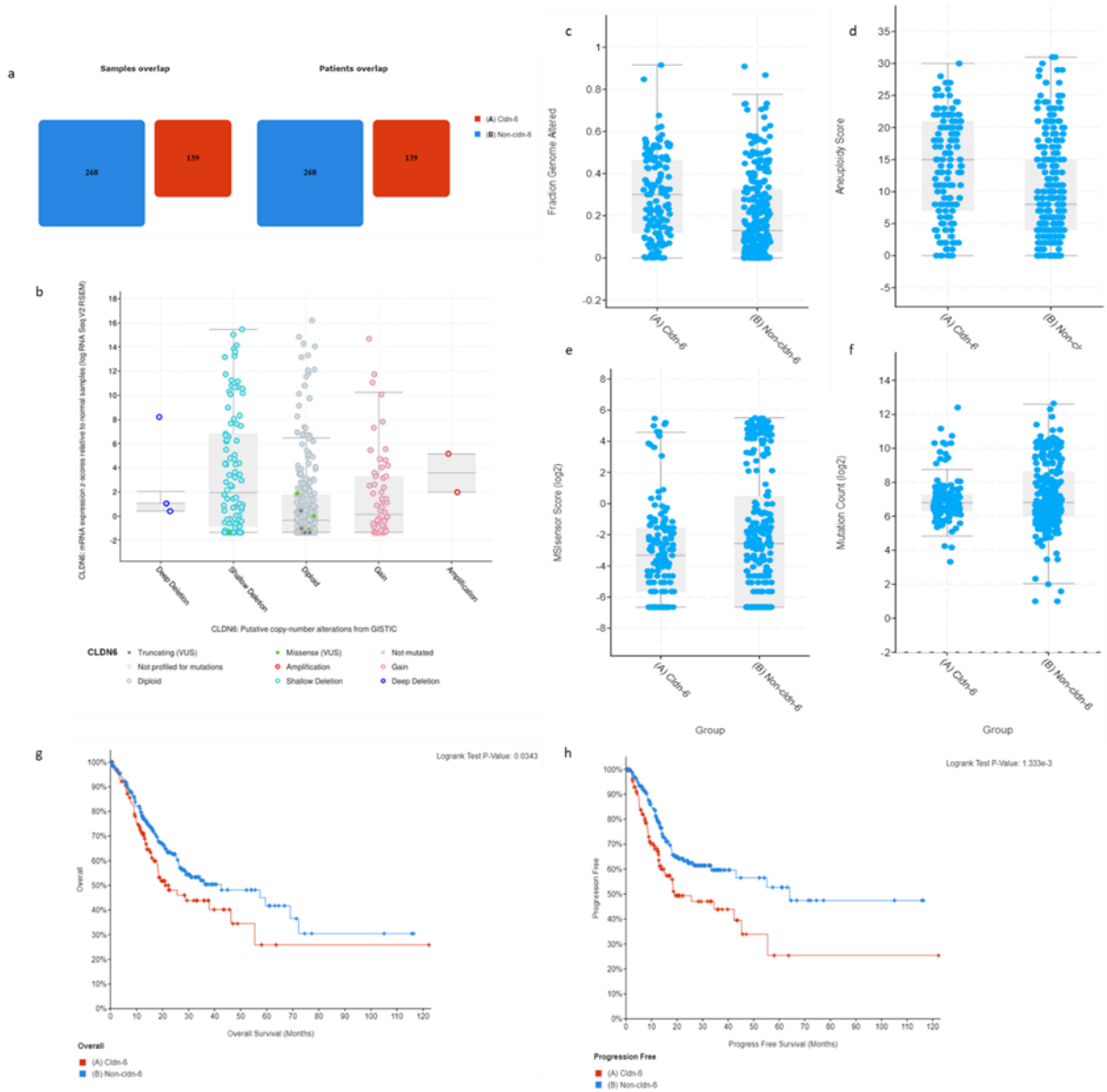

Figure 9 TCGA-STAD data analysis in terms of alterations in *CLDN6*. a) Sample and patients overlap between cldn-6 and non-cldn-6 groups. b) Mutations in *CLDN6* in TCGA-STAD data. c, d, e, f) Fraction genome altered, aneuploidy scores, MSI sensor score, and mutation count between cldn-6 and non-cldn-6 groups. g, h) Difference in overall and progression free survival of patients in both groups.

Table 5 Important genomic alterations linked with *CLDN6*.

Gene	Cytoband	(A) cldn-6 group	(B) Non-cldn-6 group	Log Ratio	p-value	q-Value
TP53	17p13.1	97 (68.79%)	119 (39.80%)	0.79	9.49E-09	2.16E-04
CLDN-6	16p13.3	15 (10.64%)	0 (0.00%)	>10	2.27E-08	2.59E-04
LINC01270	20q13.13	21 (14.89%)	9 (3.01%)	2.31	1.12E-05	0.044
LINC01271	20q13.13	21 (14.89%)	9 (3.01%)	2.31	1.12E-05	0.044
LINC01273	20q13.13	20 (14.18%)	8 (2.68%)	2.41	1.16E-05	0.044

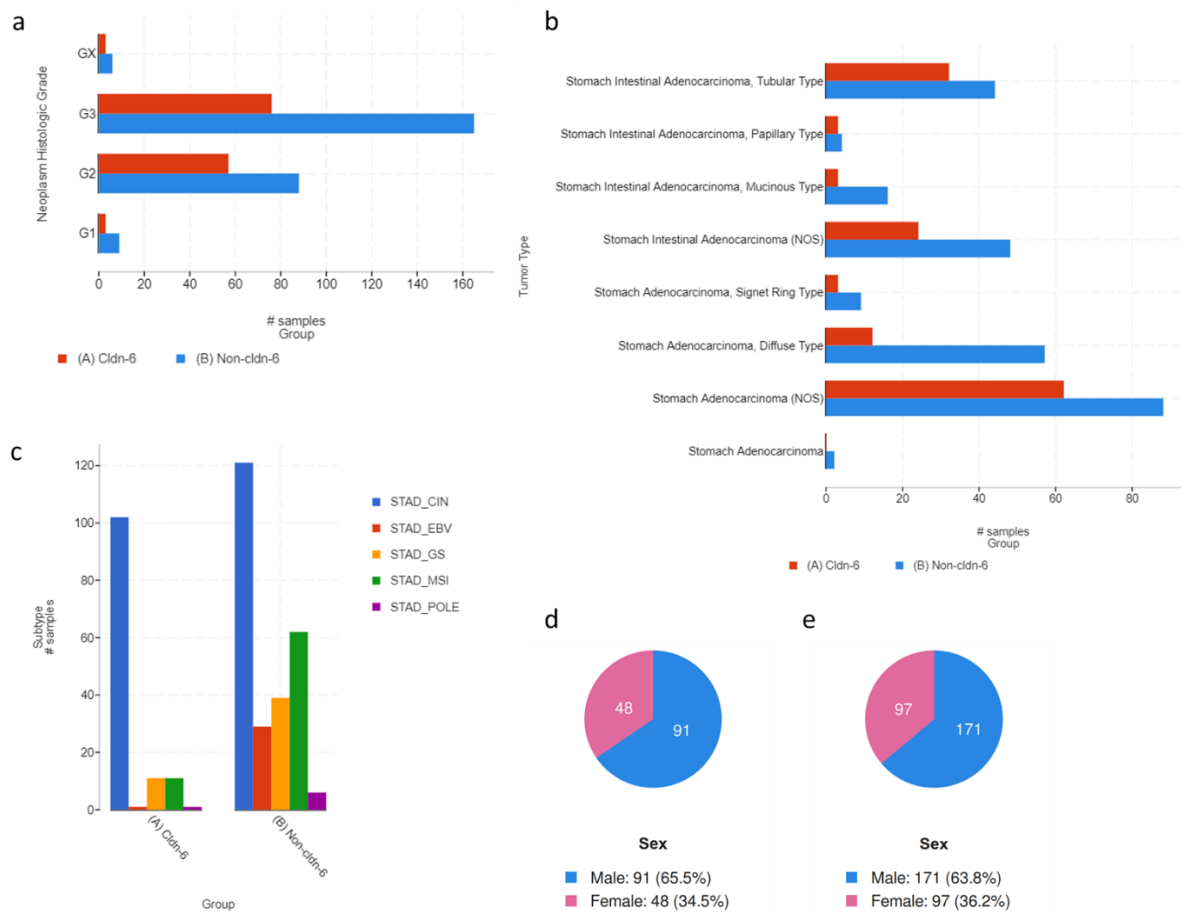

Figure 10 Distribution of samples between cldn-6 and non-cldn-6 groups. a-c) Different GC grades, histological types, and subtypes. Frequency of male and female patients in d) cldn-6 and e) non-cldn-6 group.

10.3.3: *TP53* mutations are closely linked with *CLDN6* alterations in GC

Cldn-6 and non-cldn-6 groups were scanned for associated genomic alterations. *TP53* mutations demonstrate a close association with samples in the cldn-6 group with an overlap of 68.79% in comparison to 39.80% in the non-cldn-6 alterations group (Table 5). Sample overlap of several other important mutations, *TTN*, *MUC16*, *WWOX*, *ARID1A*, *CCSER1*, *LRPB1*, *CSMD3*, *DMD*, and *SYNE1* were analyzed using query gene-based search in both groups. Intriguing that *AIRD1A* in the non-cldn-6 group altered significantly in 32.44% of samples in comparison with 15.6% of the cldn-6 group (Figure 11 a). To analyze the changes in gene expression both groups were compared for mRNA expression levels of altered genes. GO enrichment of BP category of DEGs in both groups unveiled DEGs in the cldn-6 group are related with cell cycle control in comparison with genes involved in different signaling events related with integrin receptor interaction, sphingosine phosphate pathway, TRAIL pathway and VEGF-VEGFR signaling network etc. for the non-cldn-6 group (Figure 11 c, d). In the cldn-6

group, overexpression of several Melanoma-associated antigen A (*MAGEA*) gene family members- *MAGEA6, MAGEA3, MAGEA4, MAGEA9B, MAGEA2, MAGEA12, and MAGEA10*, etc. along with *IGF2BP1, APOA1,* and *CLDN9* found to be intimately associated with *CLDN6* (Table 6, Figure 12). In contrast, the non-cldn-6 group showed association with a broad range of different genes including- *ONECUT3, PIK3C2G, GABRP, FCGBP, HLA-DRB5, PLEKHS1, NPSR1, SLCO4A, CIITA,* and *TLR8,* etc. (Table 7). Gene signatures of several common pathways associated with cancer survival and progression (provided by CBioPortal search tool) were checked for overall mutations in both groups (Figure 13 a). cldn-6 group samples have higher overall mutations in genes associated with the TP53 signaling and cell cycle control pathways (Figure 13 a). There is no significant difference in *TP53* expression, but a significant reduction in Mouse double minute 2 homolog (*MDM2*) expression and overexpression of Cyclin-dependent kinase inhibitor 2A (*CDKN2A*) was observed in cldn-6 group samples (Figure 13 b). Higher *TP53* mutations in cldn-6 group samples are associated with a higher frequency of *CDKN2A* mutations (mostly deep deletions) over non-cldn-6 group samples (Figure 14a). Heatmap based on TP53 pathway genes' mRNA expression z scores relative to normal samples (log RNA Seq V2 RSEM) of both groups revealed an overlap of *CLDN6* with *CDKN2A* and *TP53* in most samples in the cldn-6 group. Interestingly, *TP53* mutations and overexpression depict dispersed overlap with *MDM2* in samples with *CLDN6* alterations (Figure 14 b). However, with reduced expression and mutations of *CLDN6* in the non-cldn-6 group, most of the samples show clustering among *TP53* and *MDM2* which intermittently overlaps with *MDM4* and *TP53BP1*(p53-binding protein 1) throughout the group (Figure 14 b). This indicates that samples with *CLDN6* alterations have higher *TP53* mutations that may affect *TP53* interaction with *MDM2*, a negative regulator of *TP53* functions.

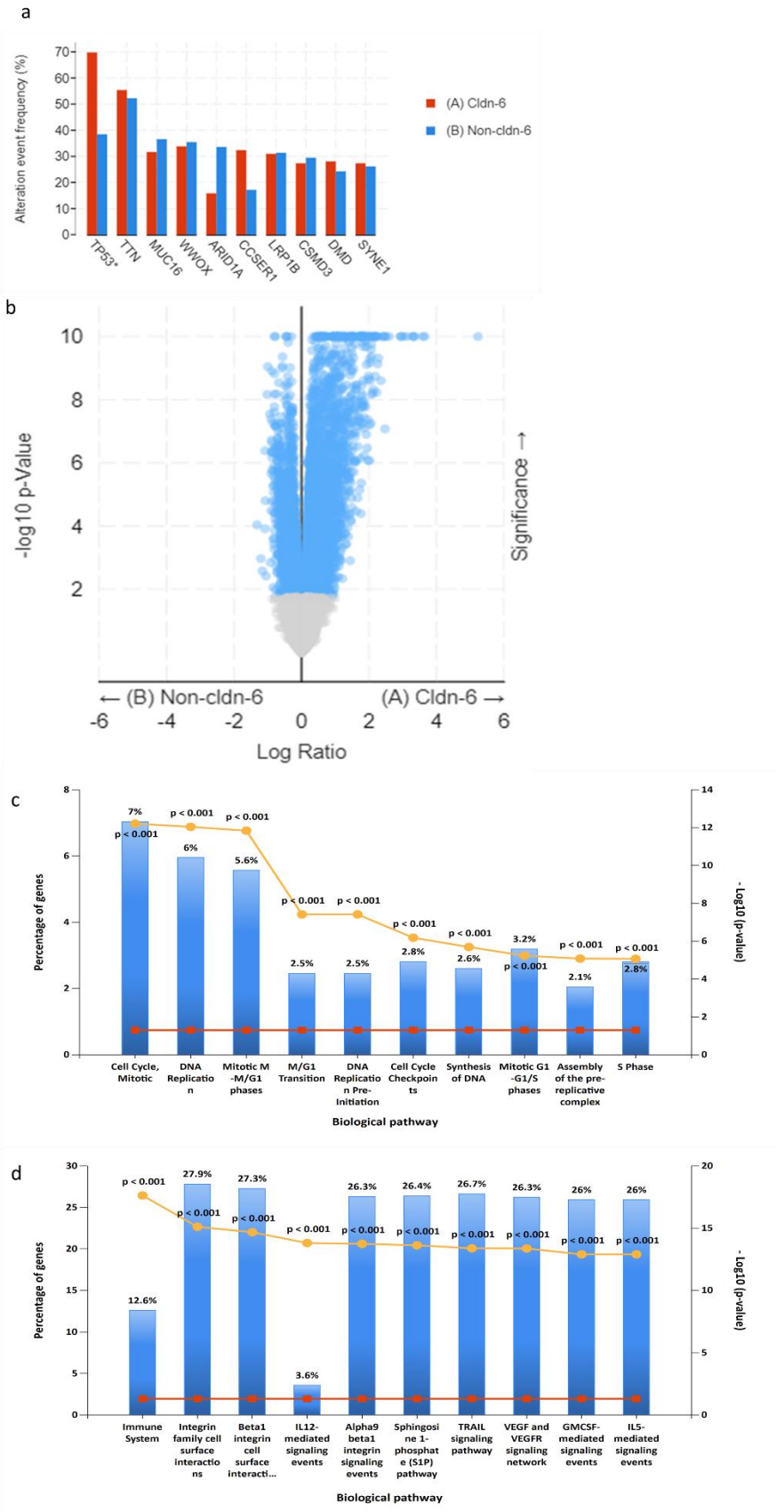

Figure 11 Genomic alterations linked with *CLDN6*. a) Overlap of samples among major mutations between cldn-6 and non-cldn-6 groups. b) Volcano plot of DEGs in both groups. GO enrichment of DEGs in BP category c) cldn-6 d) non-cldn-6.

Table 6 DEGs associated with cldn-6 group.

Gene	Cytoband	μ in cldn group	μ in non CLDN6 group	σ in cldn group	σ in non CLDN6 group	Log Ratio	p-value	q-Value
CLDN6	16p13.3	5.84	0.64	3.34	0.75	5.2	1.08E-39	2.03E-35
MAGEA6	Xq28	6.97	3.34	4.42	3.56	3.63	2.79E-14	2.07E-11
MAGEA3	Xq28	6.76	3.18	4.27	3.47	3.57	1.20E-14	1.19E-11
MAGEA4	Xq28	4.83	1.51	4.62	2.55	3.32	1.04E-12	3.94E-10
IGF2BP1	17q21.32	6.11	2.78	3.87	2.56	3.32	4.10E-16	9.68E-13
MAGEA9B	Xq28	4.61	1.34	3.97	2.24	3.26	1.66E-15	2.84E-12
APOA1	11q23.3	6.76	3.69	3.99	2.59	3.07	1.53E-14	1.44E-11
MAGEA2	Xq28	6.06	3.05	3.96	3.1	3.01	9.56E-13	3.76E-10
MAGEA12	Xq28	5.75	2.84	3.91	2.83	2.91	1.24E-12	4.52E-10
LGALS7B	19q13.2	4.63	1.72	3.13	2.13	2.9	4.83E-18	1.52E-14
CSAG1	Xq28	4.94	2.36	3.63	2.6	2.57	9.70E-12	2.41E-09
FABP1	2p11.2	8.14	5.6	4.14	4.18	2.54	3.67E-08	1.63E-06
SLC15A1	13q32.2-q32.3	6.55	4.05	3.14	2.94	2.5	8.09E-13	3.25E-10
TF	3q22.1	5.22	2.78	3.77	2.01	2.45	1.62E-11	3.65E-09
CLDN9	16p13.3	5.31	2.91	2.07	1.61	2.4	3.79E-26	3.58E-22
MAGEA10	Xq28	3.18	0.79	3.54	1.38	2.39	5.27E-12	1.46E-09
APOA4	11q23.3	4.28	1.95	3.82	2.79	2.33	3.01E-09	2.33E-07
ISX	22q12.3	4.61	2.33	3.45	2.85	2.28	4.74E-10	5.66E-08
DSCR8	21q22.13	3.13	0.89	3.33	1.8	2.24	1.83E-11	4.03E-09
PRAME	22q11.22	6.57	4.34	3.50	3.14	2.23	9.81e-10	9.80e-8

Table 7 DEGs associated with the non-cldn-6 group.

Gene	Cytoband	μ in cldn group	μ in non CLDN6 group	σ in cldn group	σ in non CLDN6 group	Log Ratio	p-value	q-Value
ONECUT3	19p13.3	3.11	4.41	2.95	3.24	-1.3	1.07E-04	8.54E-04
PIK3C2G	12p12.3	4.65	5.84	3.4	3.74	-1.19	2.04E-03	8.92E-03
GABRP	5q35.1	7.31	8.48	3.36	3.37	-1.16	1.56E-03	7.22E-03
FCGBP	19q13.2	9.78	10.89	2.47	2.98	-1.11	6.96E-05	6.13E-04
HLA-DRB5	6p21.32	9.36	10.43	2.01	2	-1.07	5.49E-07	1.39E-05
PLEKHS1	10q25.3	8.92	9.98	2.45	2.04	-1.06	1.54E-05	1.88E-04
NPSR1	7p14.3	3.11	4.16	3.22	3.5	-1.06	3.46E-03	0.0136
SLCO4A1	20q13.33	8.27	9.28	1.76	1.22	-1.01	5.60E-09	3.92E-07
CIITA	16p13.13	8.11	9.11	1.49	1.52	-1	5.50E-10	6.40E-08
TLR8	Xp22.2	5	5.92	1.54	1.66	-0.92	4.58E-08	1.91E-06
ANK1	8p11.21	5.25	6.13	1.37	2.08	-0.89	3.37E-07	9.56E-06
CR1	1q32.2	5.46	6.34	2.03	2.07	-0.88	4.28E-05	4.21E-04
CD84	1q23.3	5.8	6.68	1.53	1.55	-0.88	8.33E-08	3.05E-06
SLC6A14	Xq23	8.11	8.98	2.61	2.69	-0.88	2.33E-03	9.89E-03
AOAH	7p14.2	5.94	6.81	1.72	1.53	-0.87	7.30E-07	1.74E-05
CD274	9p24.1	4.72	5.59	1.2	1.58	-0.87	1.37E-09	1.25E-07
FCRL6	1q23.2	2.89	3.76	1.53	1.73	-0.86	3.38E-07	9.56E-06
PTPRN2	7q36.3	8.07	8.93	1.73	1.85	-0.86	4.18E-06	6.78E-05
NCF1B	7q11.23	4.11	4.97	1.67	1.76	-0.86	1.73E-06	3.39E-05
IFNG	12q15	1.6	2.46	1.45	1.84	-0.86	3.62E-07	1.00E-05

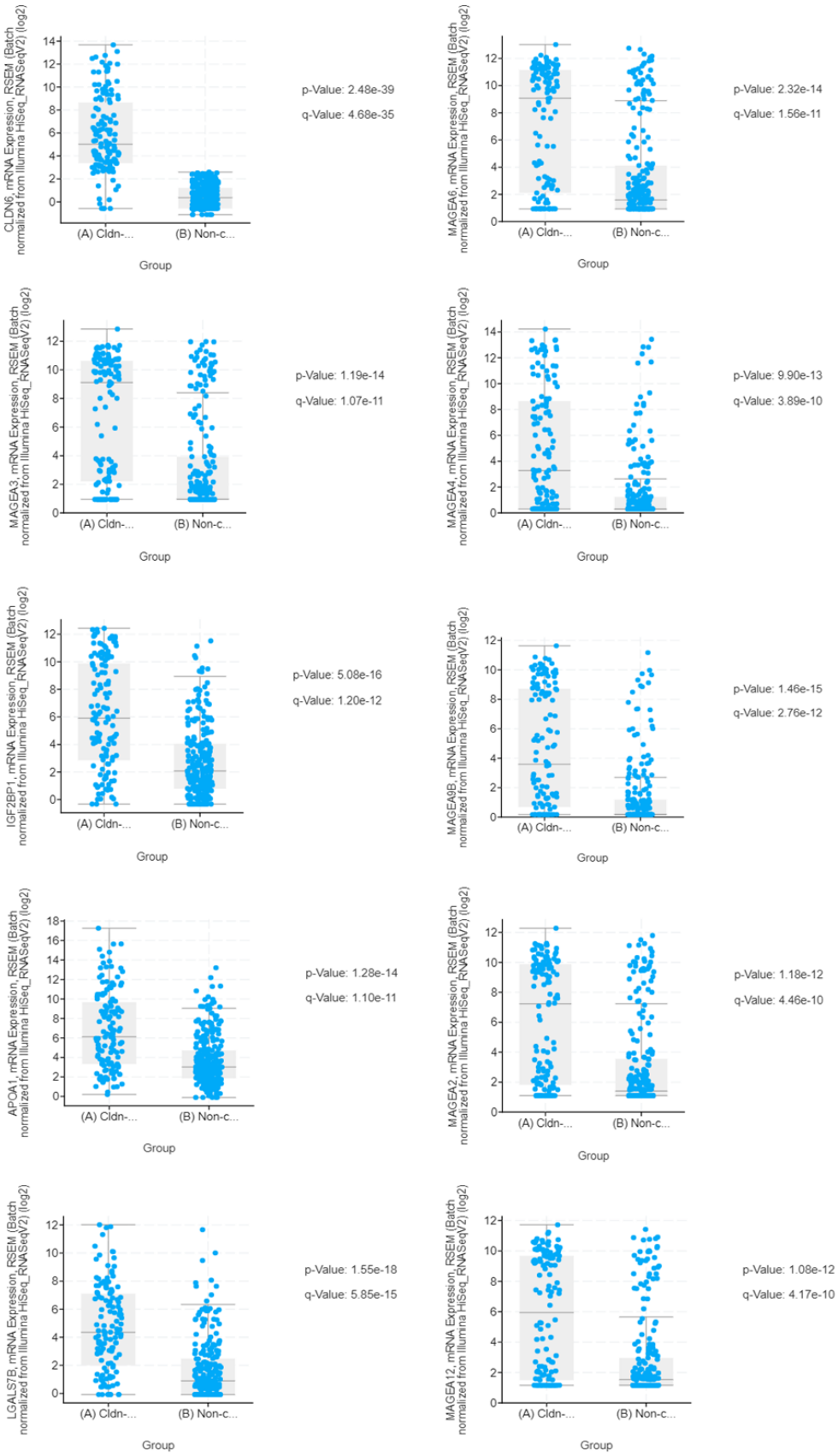

Figure 12 Expression of top 10 DEGs in cldn-6 group samples over non-cldn-6 group samples (mRNA expression, batch normalized from illumine HiSeq_ RNASeqV2).

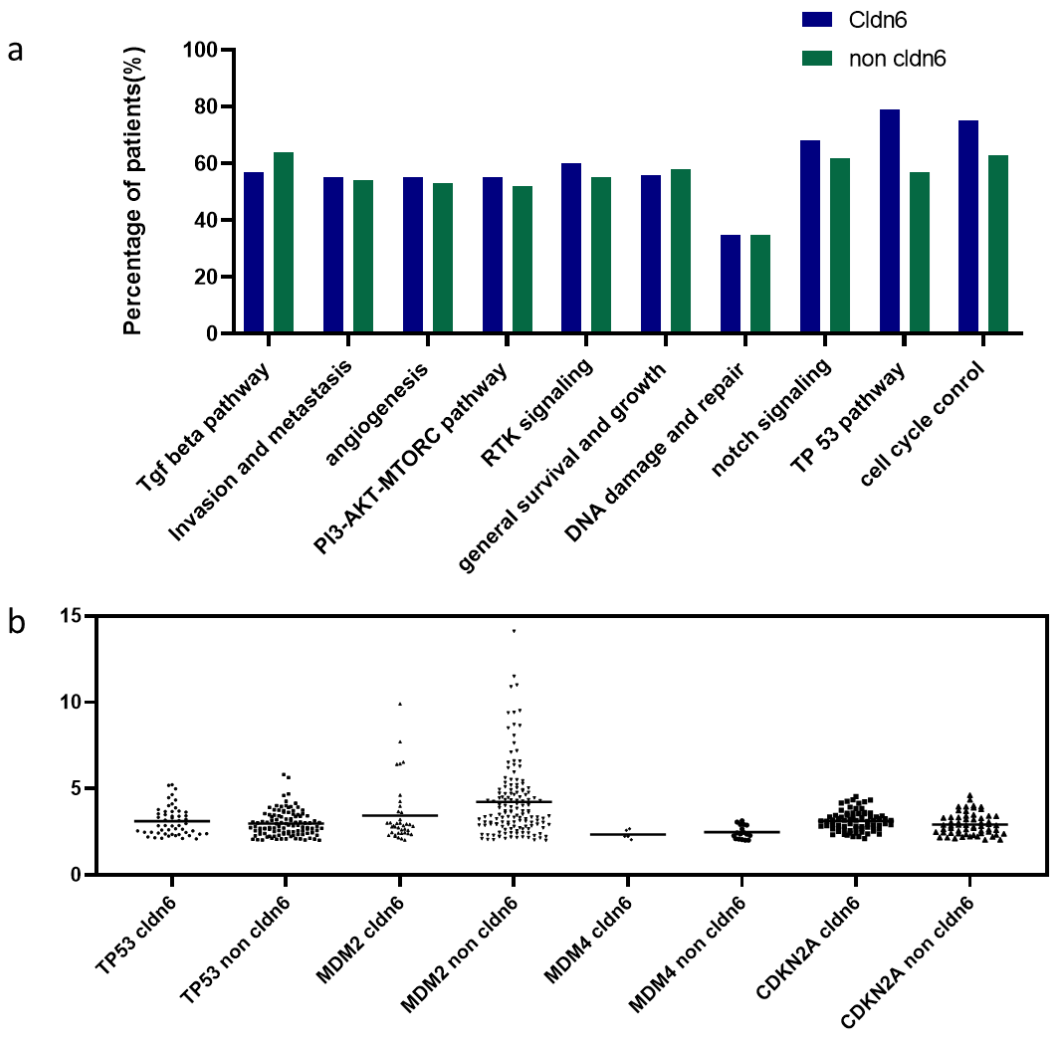

Figure 13 a) Alterations in common gene signatures/pathways among cldn-6 and non-cldn-6 groups. b) Difference in z scores normalized to normal samples of TP53 pathway signature genes in cldn-6 and non-cldn-6 groups.

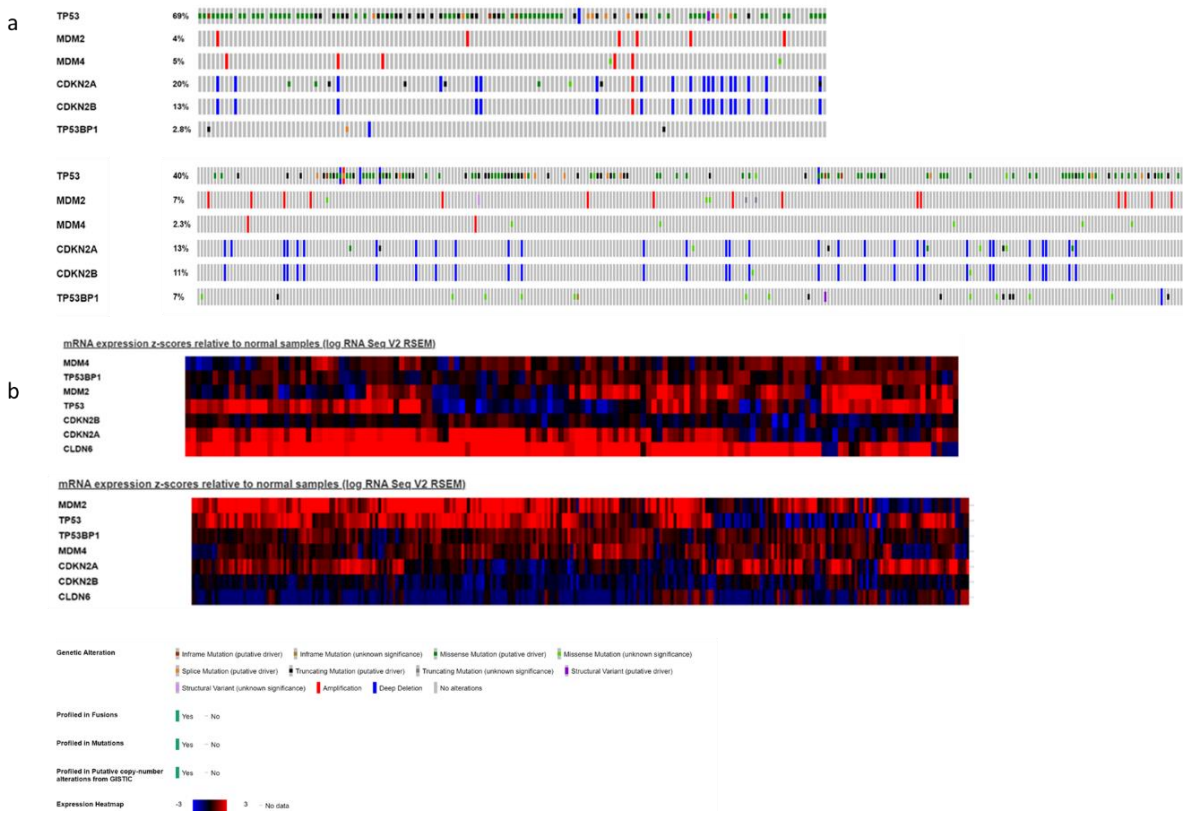

Figure 14 *TP53* gene signature in both groups. a) Overall mutation in genes; cldn-6 (up) and non-cldn-6 (down) groups. b) Heatmap of *TP53* gene signature and clustering between genes, cldn-6 (up) and non-cldn-6 (down) groups.

10.4: Analysis of *TP53* mutations in TCGA-STAD data

TP53 is a tumor suppressor gene which codes a protein that repairs DNA to prevent altered DNA from being passed on to daughter cells, and when the damage in DNA is beyond repair, TP53 protein signals cells to undergo programmed cell death (apoptosis). Most tumors induce mutations in *TP53* which not only inactivate but alter it to gain new functions that help sustain the cancer growth. This "Gain of Functions" includes- Inducing resistance to cancer drugs, reworked metabolism, metastasis, favored growth and inhibition of apoptosis, angiogenesis, and genomic instability. *TP53* mutations are one of the major mutations in several solid tumors including GC. *TP53* mutation-associated GC is classified under CIN tumors which makes the biggest class in TCGA GC classification and covers approximately 50% of total GC cases. However, as *TP53* mutation is not universal to all GC patients, deeper insights of molecular and clinical parameters are desired for more targeted therapy among patients diverged by *TP53* mutations. In the previous section, analysis of the TCGA-STAD for *CLDN6* alterations revealed that *CLDN6* alterations are also linked with *TP53* mutations with a high overlap among samples. Such observation raises further questions, if both mutations group belong to the same category or *CLDN6* mutation patients form a subgroup of CIN GC with *TP53* mutations associated with poorer prognosis.

10.4.1: *TP53* mutations are associated with high aneuploidy and high genome alterations

STAD data (440 patients) were divided into two groups based on *TP53* mutations- TP53 group (213 GC patients/samples with *TP53* mutations) and non TP53 mutations group (227 GC patients/samples) (Figure 15 a). Major mutation in *TP53* include- truncating, shallow deletion, inframe, missense, amplification, deep deletion, and gain. Samples in the TP53 group show higher aneuploidy scores and a higher fraction of genome altered in comparison to the non TP53 group (Figure 15 b, c). However, there is no significant difference in the total mutation count nor in the overall, disease free, progression free survival or sex distribution for the patients in both groups (Figure 15 d-h). The mutation count of most of the samples in non TP53 group stays ≤ 50 mutations and 50-100 mutations group which spreads from 50-200 mutations in the TP53 group. Fraction genome altered in most of the samples lies in ≤0.05 group and spreads till 0.25 with about ≥20 samples in each group, while samples are quite distributed in groups ranges ≤0.05 to 0.55 in TP53 group (Figure 16 a-d). The histological grade distribution

of samples in both groups shows a higher accumulation of samples with *TP53* mutations in G2 grade although non TP53 group samples grouped in G3 grade of GC (Figure 16 e, f).

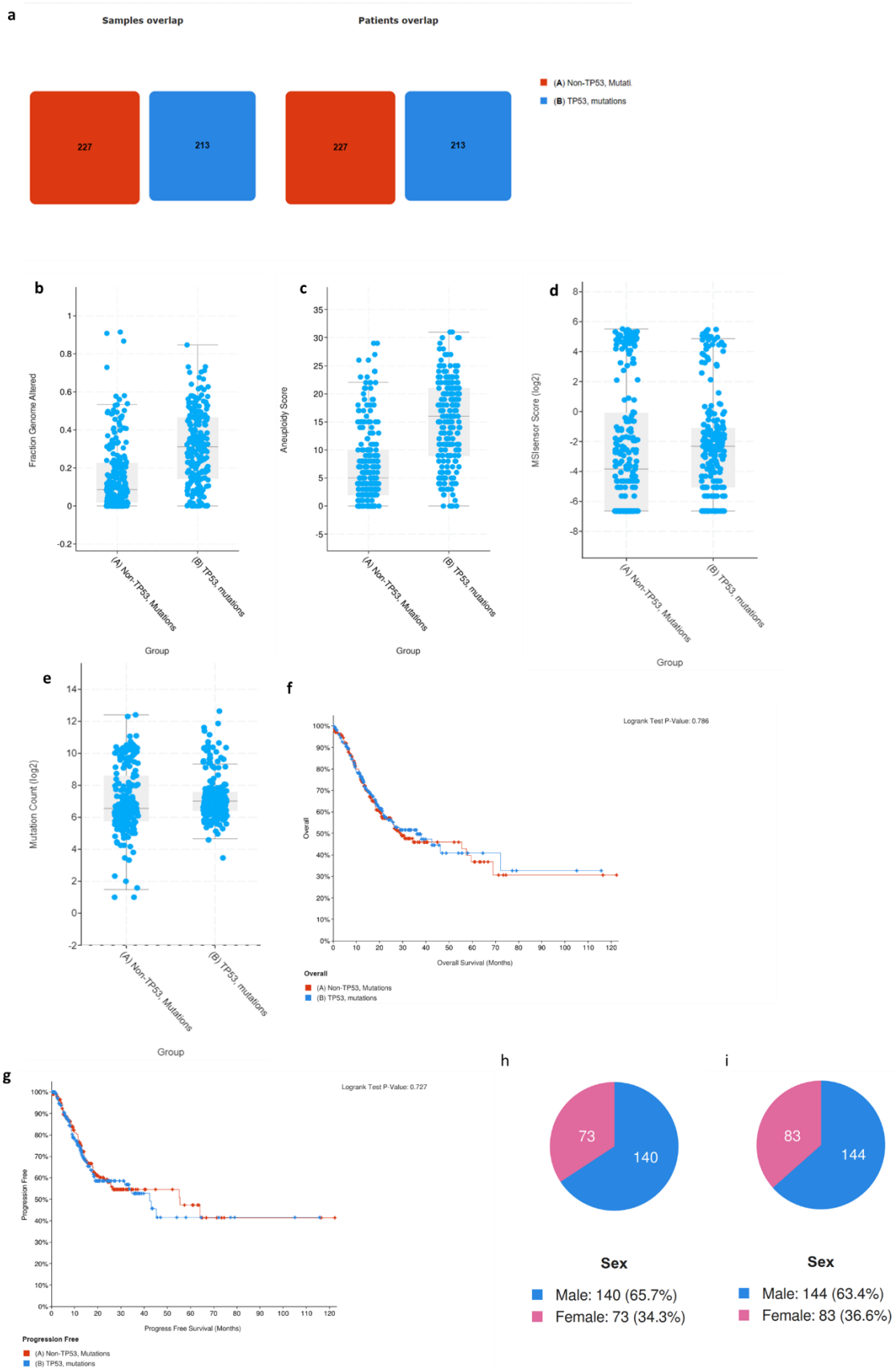

Figure 15 TP53 and nonTP53 group analysis. a) Number of patients/samples in TP53 and Non TP53 groups made from TCGA-STAD data. b, c, d, e) Fraction genome altered, aneuploidy scores, MSI sensor score, and mutation

count between Non TP53 and TP53 groups. f, g) Comparison of overall and progression free survival of patients in both groups. Sex distribution among groups h) TP53 group i) Non TP53 group.

TP53 group samples are more frequently classified into tubular stomach adenocarcinoma vs diffuse type for non TP53 samples. In general, there are more samples with non TP53 which gathers several important mutations beyond *TP53*, or else there is no significant difference in the distribution of samples in other histological classes of GC like intestinal type, papillary, and signet ring cell carcinoma (Figure 16 f). Most of the samples in both groups gathered in non-metastatic GC, yet it seems non TP53 GC has more metastatic GC cases, but any such conclusion suffers from an inadequate number of metastatic GC patient's data (Figure 16 g). TP53 group samples principally gathered in the CIN STAD subtype (80.43%) vs a wider distribution of samples in different subtypes in non TP53 group (Figure 16 h). These facts indicate that *TP53* mutation positive GC include the early and low-grade CIN GC over other mutations that may create high-grade tumors with less differentiation and high tumor growth.

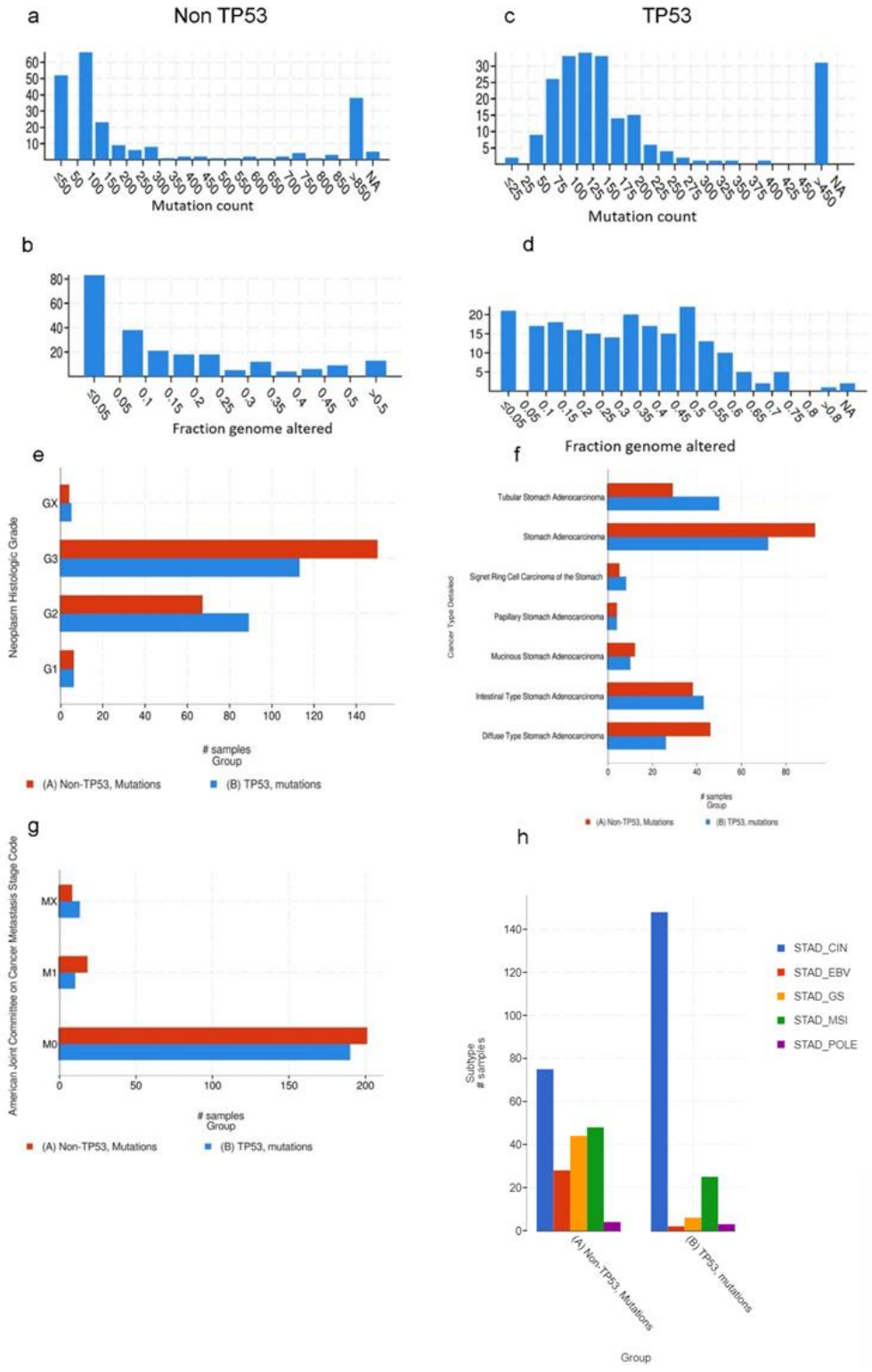

Figure 16 Distribution of samples among non TP53 and TP53 groups. a-d) Mutation count and faction genome altered e) Neoplasm histological grade, f) GC histological subtypes, g) American Joint Committee on Cancer Metastasis Stage Code and h) TCGA-STAD classification subtypes.

10.4.2: *TP53* mutations affect cell cycle control genes

A comparison of both groups for changes in gene expression was done as mentioned in section (10.3.3:). A total of 2609 in non TP53 and 3923 DEGs in TP53 group samples were generated by the CBioPortal comparison tool. GO biological pathway-based enrichment of DEGs uncovered that the genes are involved in cell cycle and regulation categories - 13.4% genes in cell cycle, 11.4% in DNA replication, 10.5% in mitotic M/G1 phases, etc. (Figure 17 a, b) in TP53 group while non TP53 group genes were enriched in- 30.8% genes in integrin family cell surface interactions, 29.7% in β1 integrin cell surface interactions, 29% in TRAIL signaling pathway, 28.4% in α9β1integrin signaling events, 28% in sphingosine1 phosphate pathway, 28% in IL5 mediated signaling events, 28% in GMCSF mediated signaling events, 15% in immune system and 11.9% in epithelial to mesenchymal transition (Figure 17a, c).

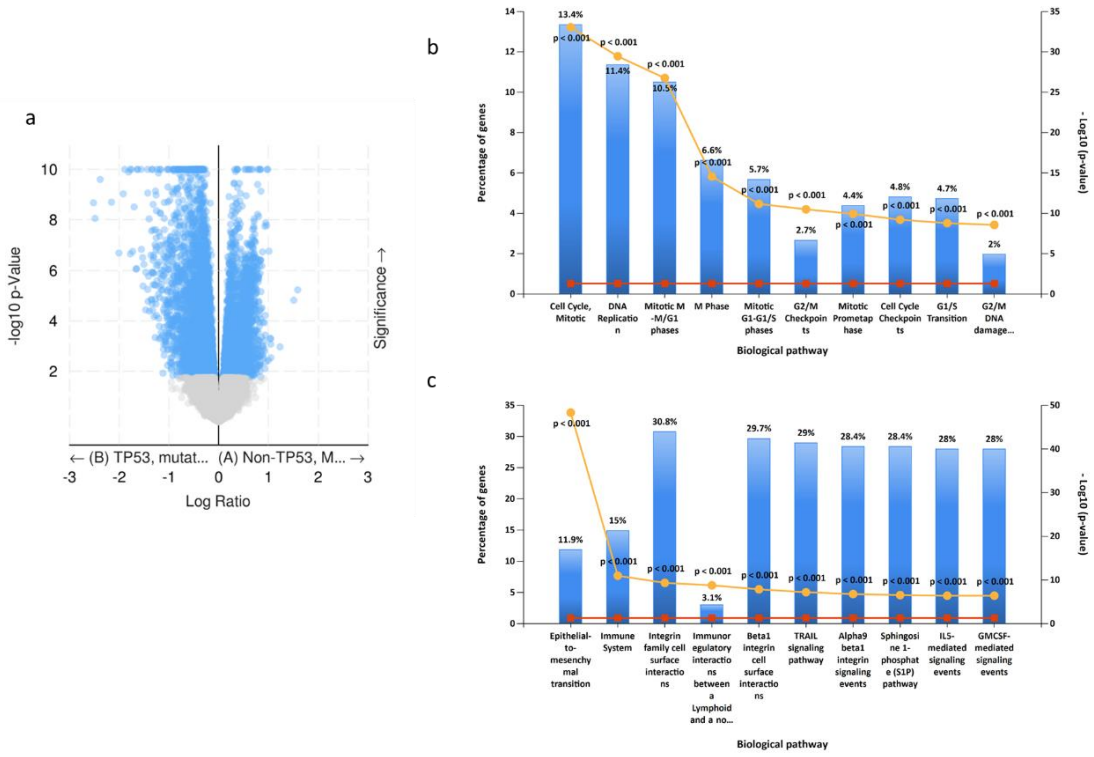

Figure 17 Genomic alterations linked with *TP53*. a) Volcano plot of DEGs between TP53 and non TP53 groups. Enrichment of all DEGs in both categories in GO- BP category- b) TP53 c) non TP53.

10.4.3: *TP53* mutations are associated with *CLDN6, CLDN3,* and *MAGEA* gene family

The top DEGs (Table 8) in each group were further checked for cancer association. *TP53* mutations are correlated with upregulation of the *MAGEA* gene family- *MAGEA3, MAGEA6,*

MAGEA2, *MAGEA12*, *MAGEA4*, *MAGEA9b* along with *CLDN6*, *CLDN3*, *CDKN2A*, and *ACTL8* (Actin like 8). All these genes are highly overexpressed in TP53 group samples over non TP53 group samples (Figure 18) and their overexpression is linked with poor overall survival of GC patients (Figure 19).

Table 8 DEGs associated with the *TP53* mutations.

Gene	Cytoband	μ in (A) Non-TP53, Mutati...	μ in (B) TP53, mutations	σ in (A) Non-TP53, Mutati...	σ in (B) TP53, mutations	Log Ratio	p-Value	q-Value
MAGEA3	Xq28	3.21	5.73	3.49	4.37	-2.52	2.11e-9	**2.00e-7**
MAGEA6	Xq28	3.40	5.89	3.57	4.52	-2.49	8.79e-9	**6.26e-7**
MAGEA2	Xq28	2.94	5.32	3.01	3.99	-2.38	2.50e-10	**3.71e-8**
MAGEA12	Xq28	2.81	4.97	2.81	3.86	-2.16	1.99e-9	**1.93e-7**
MAGEA4	Xq28	1.70	3.70	2.91	4.26	-2.01	2.06e-7	**7.245e-6**
CLDN6	16p13.3	1.49	3.41	2.50	3.57	-1.92	9.28e-10	**1.05e-7**
CDKN2A	9p21.3	5.50	7.39	1.95	2.47	-1.89	2.12e-16	**5.00e-13**
ACTL8	1p36.13	2.10	3.91	2.19	3.22	-1.81	1.27e-10	**2.10e-8**
CLDN3	7q11.23	8.38	10.16	3.19	2.04	-1.78	4.29e-11	**8.81e-9**
MAGEA9B	Xq28	1.63	3.40	2.64	3.75	-1.78	2.24e-7	**7.776e-6**
ESPN	1p36.31	6.39	8.15	2.16	1.62	-1.76	5.10e-19	**2.41e-15**
CSAG1	Xq28	2.42	4.15	2.61	3.59	-1.73	1.79e-7	**6.452e-6**
GABRA3	Xq28	1.34	3.05	2.24	3.09	-1.70	3.08e-9	**2.73e-7**
APOA1	11q23.3	3.94	5.60	3.01	3.69	-1.67	8.94e-7	**2.202e-5**
PRAME	22q11.22	4.31	5.96	3.19	3.49	-1.65	8.63e-7	**2.142e-5**
C12ORF56	12q14.2	1.64	3.27	1.95	2.60	-1.64	3.11e-11	**7.07e-9**
SLC5A12	11p14.2	2.59	4.22	1.82	2.35	-1.63	4.79e-13	**2.38e-10**
FBXO2	1p36.22	6.20	7.77	2.17	2.15	-1.56	1.28e-12	**5.48e-10**
FAR2P1	2q21.1	3.70	5.26	2.74	2.88	-1.56	1.48e-7	**5.523e-6**
HOXC13	12q13.13	2.36	3.89	2.59	3.06	-1.53	3.13e-7	**9.929e-6**

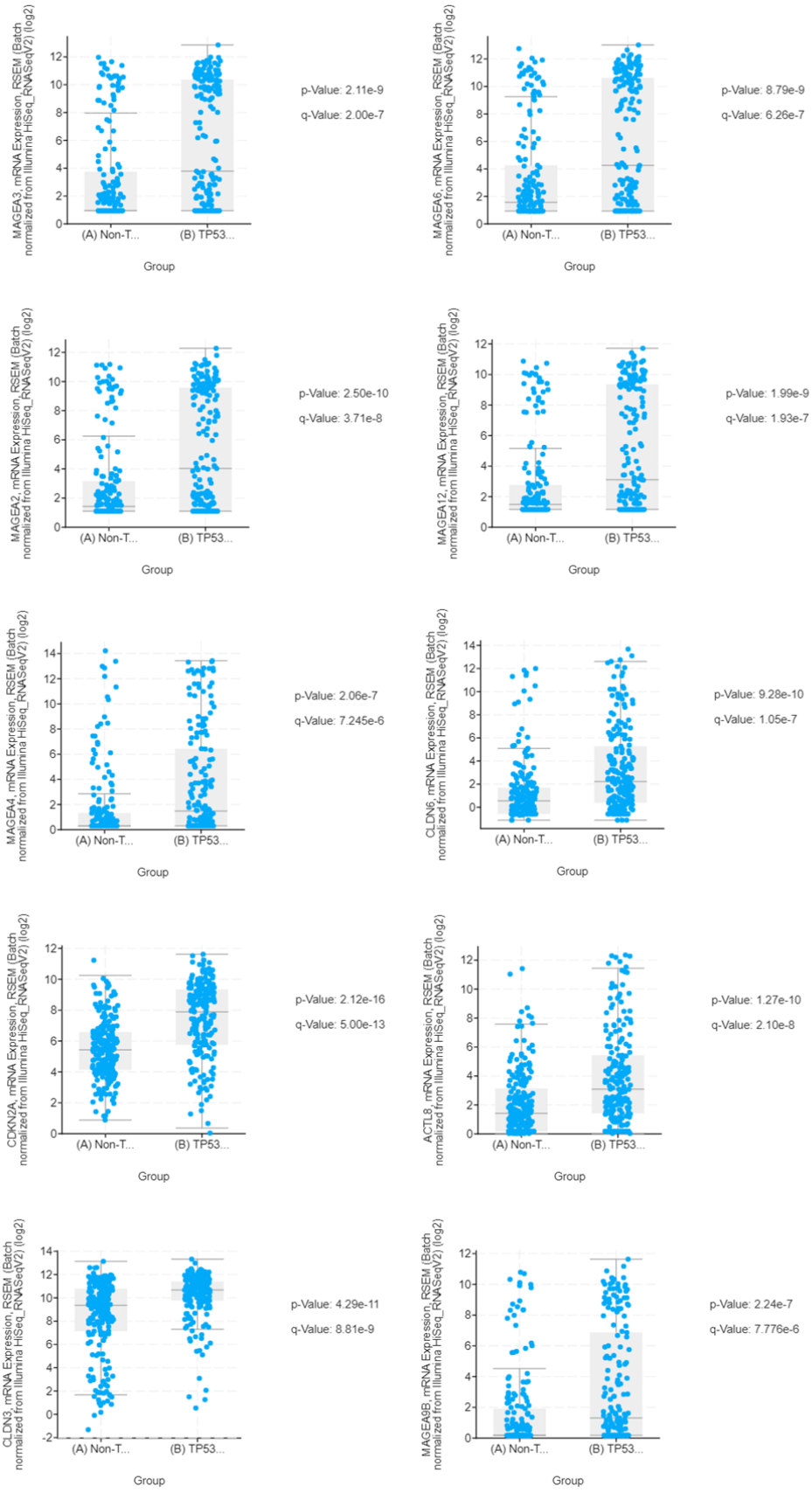

Figure 18 Expression of top 10 DEGs in TP53 group samples over non TP53 group samples (mRNA expression, batch normalized from illumine HiSeq_ RNASeqV2).

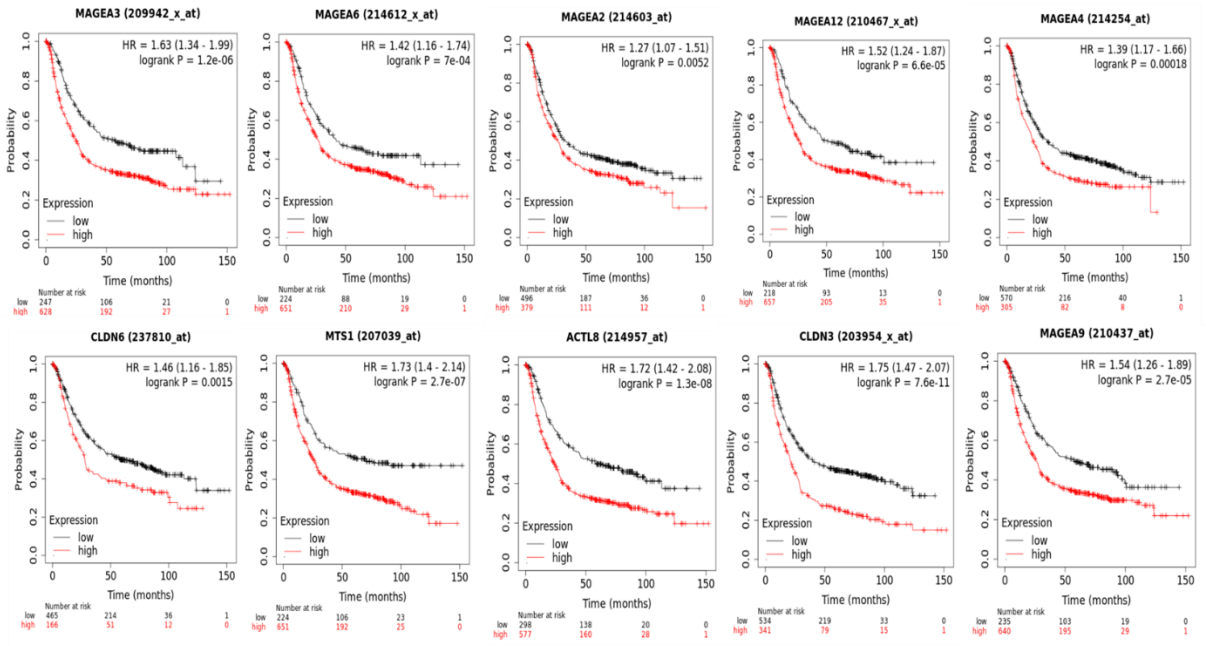

Figure 19 KM plots of overall survival of top 10 DEGs in TP53 group patients in comparison to non TP53 group patients in GC.

10.4.4: Samples with *TP53* mutations have higher mutations in angiogenesis and Notch signaling genes signature

Samples in both groups were further investigated for mutations in cancer related gene signatures provided by CBioPortal. TP53 signaling pathway genes are highly mutated in the TP53 group over non TP53 group. It is rather interesting that there is no substantial difference in most of the gene signatures like cell cycle control, RTK signaling, PI3K-AKT-MTORC1 pathway, and invasion and metastasis but a 12% higher overall mutation in angiogenesis genes and 13% in Notch signaling genes (Figure 20 a). Immune metagene signatures involved in infiltration of immune cells from previous publications (177) were evaluated for overall mutations in both groups using the group-based query gene analysis feature of CBioPortal. Nearly all immune metagene signatures demonstrate higher mutations in the TP53 group with the highest mutations in T cells, activated B cells, TH1 cells, Myeloid-derived suppressor cells (MDSC), neutrophils, and NK cells among others (Figure 20 b).

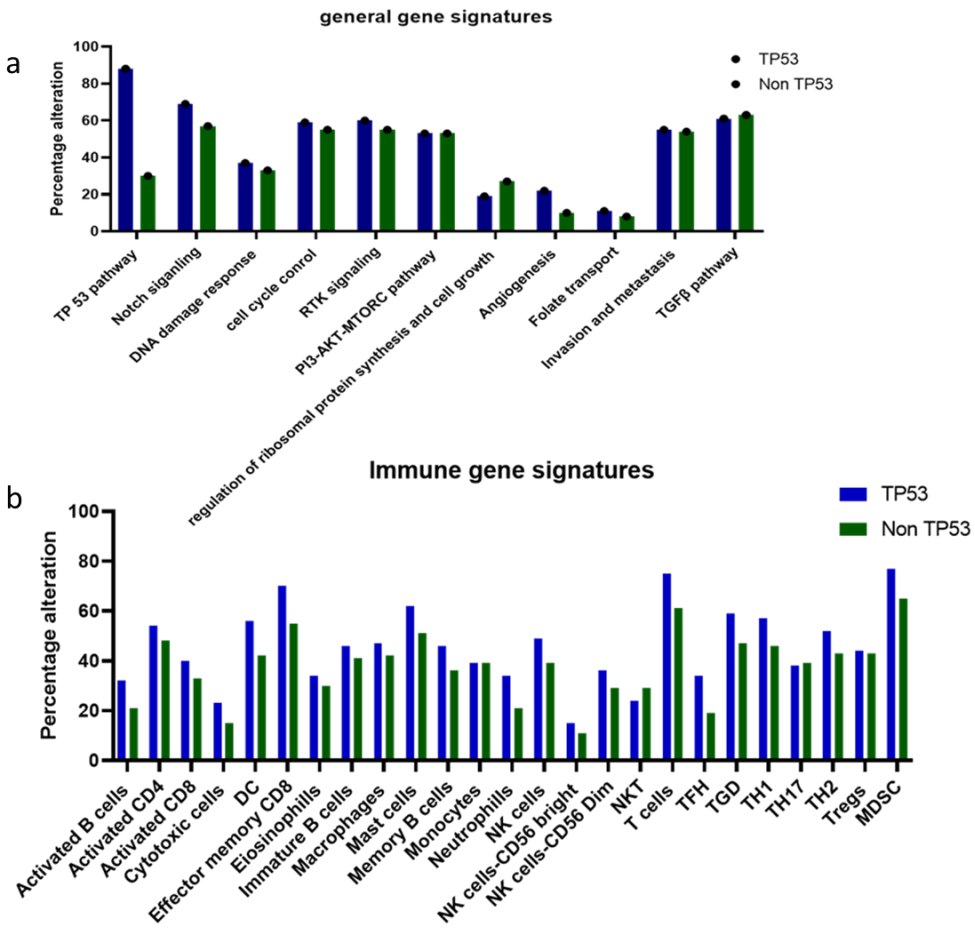

Figure 20 Overall mutations in gene signatures between TP53 and non TP53 groups. a) General pathways associated with cancer b) Immune metagene signatures associated with immune cell infiltration in cancers.

10.5: Correlation between *CLDN6* and *TP53* mutations in GC

10.5.1: *TP53* and *CLDN6* alterations are closely associated in GC

Following the results from the previous analysis where *CLDN6* alteration in samples show a major overlap with *TP53* mutation in samples, we sought further association in sample groups with *CLDN6* and *TP53* alterations. Chromosome wise Copy number alteration (CNA) profile of samples in both groups presents a very similar image with high alterations in chromosomes 1, 3, 6, 7, 8, 13, and 20 (Figure 21). A Venn diagram of DEGs in both groups demonstrates an overlap of 3719 of all genes and 137 genes with log-ratio cutoff ≥1. Functional enrichment of latter common DEGs shows their involvement in epithelium development (20 genes), epithelial cell differentiation (15 genes) in BP, and ER (23 genes), and collagen-containing extracellular matrix (13 genes) in CC categories (Table 9). Notably, beyond DEG overlap both groups have their DEG groups which may provide individuality to each group of samples (Figure 22). As seen before both groups belong to the CIN STAD subtype to confirm that alterations in the

CIN gene signature were checked. Indeed, samples with *TP53* and *CLDN6* alterations attain a very similar mutation pattern of these genes (Figure 23).

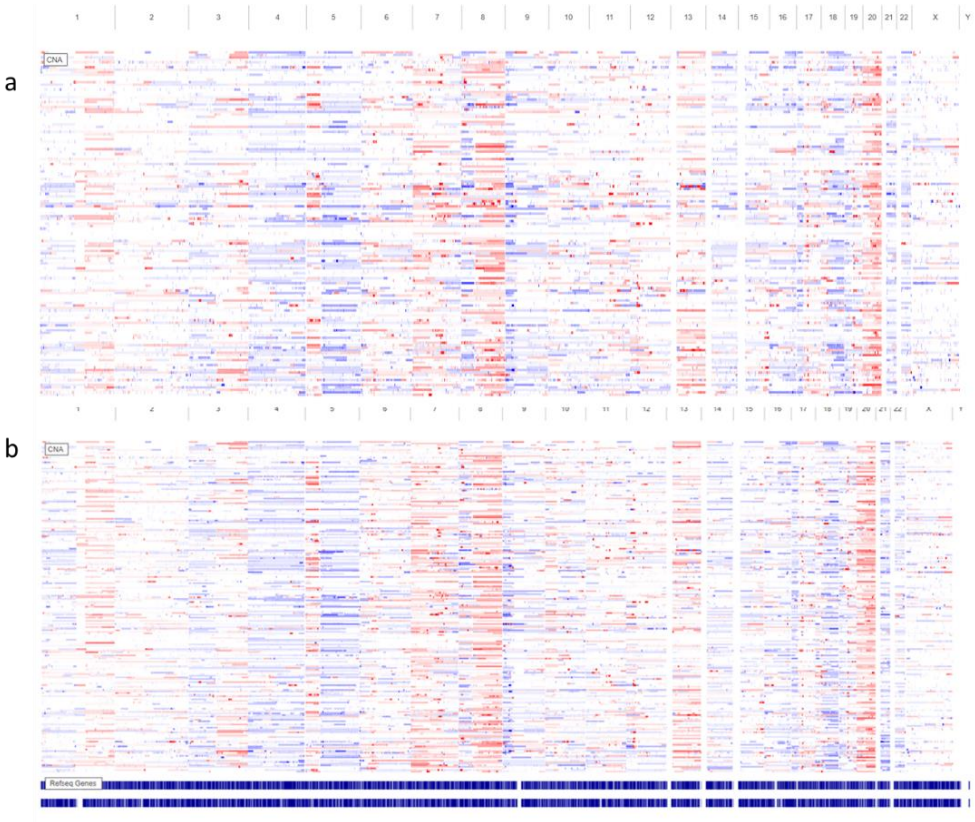

Figure 21 Comparison of Chromosome wise CNAs. a) *CLDN6* alteration samples b) *TP53* mutation samples.

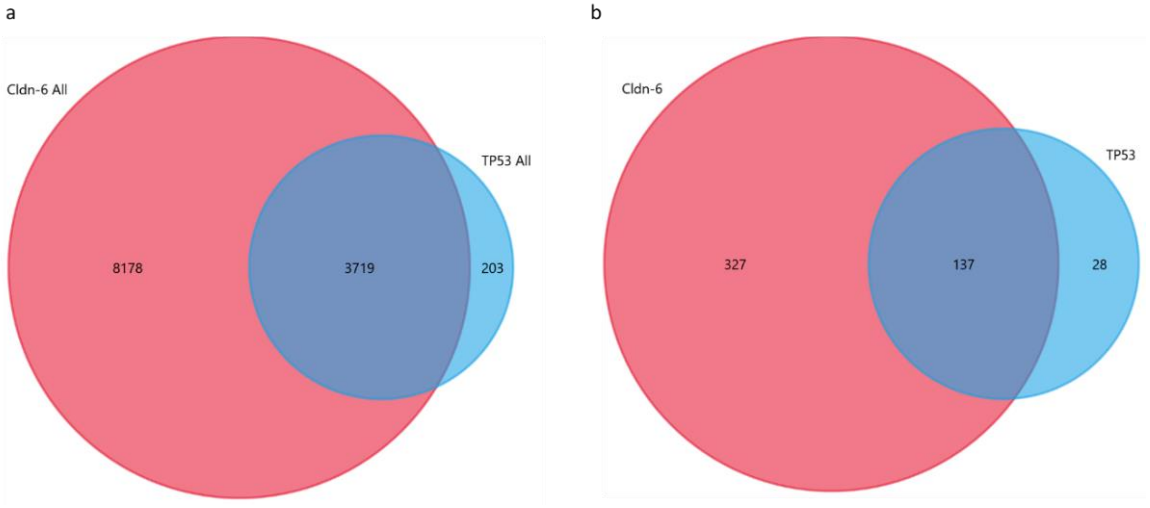

Figure 22 Venn diagram of DEGs in cldn-6 and TP53 group samples. a) all genes b) Genes with log-ratio cutoff≥1.

Table 9 Enrichment of common DEGs (log-ratio cutoff≥1) in GO MSigDB of GSEA.

Gene Set Name [# Genes (K)]	Description	# Genes in Overlap (k)	p-value	FDR q-value
GOCC_COLLAGEN_CONTAINING_EXTRACELLULAR_MATRIX [423]	An extracellular matrix consisting mainly of proteins (especially collagen) and glycosaminoglycans (mostly as proteoglycans) that provides not only essential physical scaffolding for the cellular constituents but can also initiate crucial biochemical and biomechanical cues required for tissue morphogenesis, differentiation and homeostasis. The components are secreted by cells in the vicinity and form a sheet underlying or overlying cells such as endothelial and epithelial cells. [GOC:BHF, GOC:rph, PMID:21123617]	13	2.35 e^{-9}	2.39 e^{-5}
GOCC_EXTERNAL_ENCAPSULATING_STRUCTURE [566]	A structure that lies outside the plasma membrane and surrounds the entire cell or cells. This does not include the periplasmic space. [GOC:go_curators]	14	8.75 e^{-9}	4.02 e^{-5}
GOBP_EPITHELIUM_DEVELOPMENT [1275]	The process whose specific outcome is the progression of an epithelium over time, from its formation to the mature structure. An epithelium is a tissue that covers the internal or external surfaces of an anatomical structure. [GOC:dph, GOC:mtg_lung]	20	1.18 e^{-8}	4.02 e^{-5}
GOBP_EPITHELIAL_CELL_DIFFERENTIATION [775]	The process in which a relatively unspecialized cell acquires specialized features of an epithelial cell, any of the cells making up an epithelium. [GOC:ecd, PMID:11839751]	15	6.37 e^{-8}	1.62 e^{-4}
GOBP_APPENDAGE_DEVELOPMENT [167]	The process whose specific outcome is the progression of an appendage over time, from its formation to the mature structure. An appendage is an organ or part that is attached to the trunk of an organism, such as a limb or a branch. [GOC:jid, GOC:rc]	8	1.1 e^{-7}	2.24 e^{-4}
GOCC_ENDOPLASMIC_RETICULUM [1960]	The irregular network of unit membranes, visible only by electron microscopy, that occurs in the cytoplasm of many eukaryotic cells. The membranes form a complex meshwork of tubular channels, which are often expanded into slitlike cavities called cisternae. The ER takes two forms, rough (or granular), with ribosomes adhering to the outer surface, and smooth (with no ribosomes attached). [ISBN:0198506732]	23	1.74 e^{-7}	2.95 e^{-4}
GOCC_BLOOD_MICROPARTICLE [146]	A phospholipid microvesicle that is derived from any of several cell types, such as platelets, blood cells, endothelial cells, or others, and contains membrane receptors as well as other proteins characteristic of the parental cell. Microparticles are heterogeneous in size, and are characterized as microvesicles free of nucleic acids. [GOC:BHF, GOC:mah, PMID:16373184]	7	6.99 e^{-7}	9.64 e^{-4}
GOBP_NEGATIVE_REGULATION_OF_CATALYTIC_IC_ACTIVITY [816]	Any process that stops or reduces the activity of an enzyme. [GOC:ebc, GOC:jl, GOC:tb, GOC:vw]	14	7.57 e^{-7}	9.64 e^{-4}
GOBP_REGULATION_OF_PROTEOLYSIS [731]	Any process that modulates the frequency, rate or extent of the hydrolysis of a peptide bond or bonds within a protein. [GOC:mah]	13	1.29 e^{-6}	1.43 e^{-3}
GOBP_REGULATION_OF_HORMONE_LEVELS [510]	Any process that modulates the levels of hormone within an organism or a tissue. A hormone is any substance formed in very small amounts in one specialized organ or group of cells and carried (sometimes in the bloodstream) to another organ or group of cells in the same organism, upon which it has a specific regulatory action. [GOC:BHF, GOC:dph, GOC:tb]	11	1.4 e^{-6}	1.43 e^{-3}

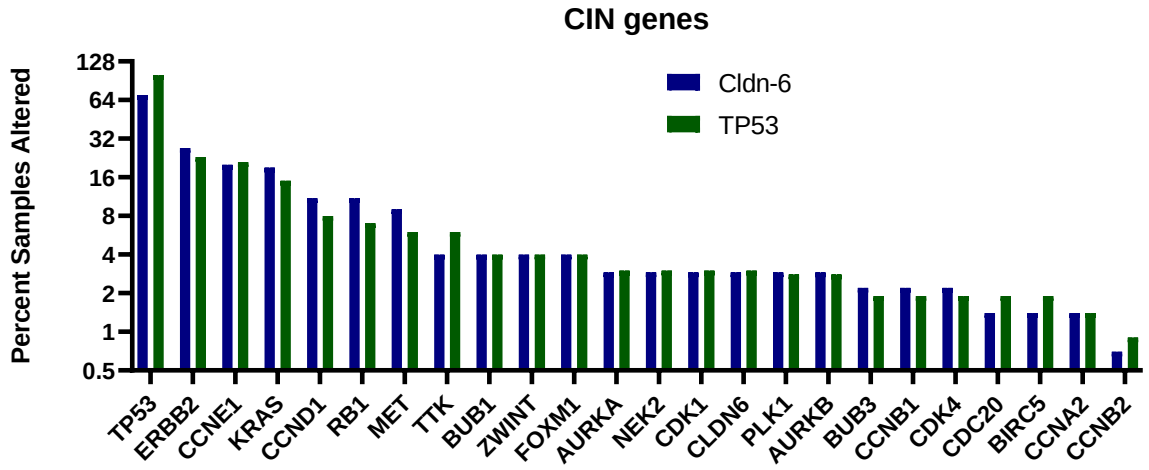

Figure 23 Overall mutation frequency of CIN-related genes between cldn-6 and TP53 group samples

10.5.2: *ORM2* (Orosomucoid 2) and *MAGEA2* as prognostic targets of *TP53* and *CLDN6* alterations GC group

Gene interaction studies explains how a group of genes interact and contribute to a common outcome. To identify such interaction groups, common DEGs (log-ratio cutoff≥1) between cldn-6 and TP53 group samples were analyzed for genetic interactions using GeneMANIA. GeneMANIA finds related gene for a set of input genes based on functional associated data of protein and genetic interactions, pathway and co-expression, co-localization and protein domain similarity. Following network analysis using MCODE (for identification of important

gene clusters), two important clusters- Cluster 1 with a score of 29.46 and cluster 2 with a score of 11.692 were generated (Figure 24 a-c). Cytohubba for identification of hub genes in each cluster, identified *ORM2* and *MAGEA2* as the most important hub genes in clusters (Figure 24 d, e). Overexpression of *ORM2* with a log-ratio of 1.47 and 1.20 and *MAGEA2* with log-ratio of 3.07 and 2.38 in cldn-6 and TP53 group samples (consecutively), indicate their common association with *CLDN6* and *TP53* alterations. A common upregulation of these genes in the cldn-6 and TP53 group samples indicate their prognostic value for both groups.

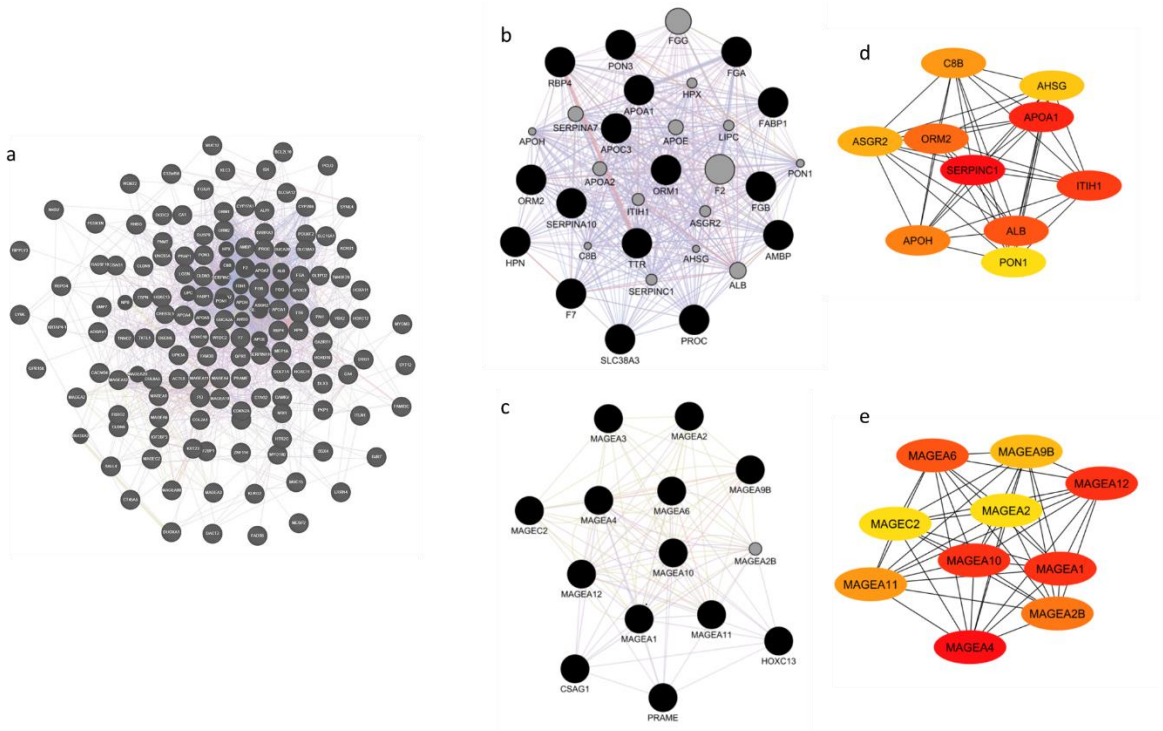

Figure 24 a) Gene interaction network of common DEGs in cldn-6 and TP53 group samples with log-ratio cutoff≥1. b) Cluster 1, c) cluster 2.

11: Discussion

Gastric cancer is one of the most important cancer with a high incident rate and mortality. GC associated mortality highly depends on metastasis, EMT, and tumor immune association. As most of the GC patients are diagnosed in advanced stages with metastasis, more effective diagnostic methods with targeted treatment possibilities are desired. 95% of the cancers are originated from the epithelium. Transformed epithelium share common characteristics like loss of polarized structure which results in loss of cell-to-cell junctional complexes which includes- Tight junctions, Adherent junctions, Desmosomes, and Gap junctions. Claudins which are an integral part of the TJ structure contribute significantly to this process. Upregulation, downregulation, and mis localization of several claudins have been observed in different tumors and their subtypes. In the same manner, CLDN6 and CLDN9 are closely associated with several cancers including GC. CLDN6 interferes with the HIPPO signaling pathway and enhances YAP1 entry to the nucleus and affects its target genes like *CTGF* and *AMOTL2* in GC tumors. In our experimental model, AGS cells transfected with *CLDN6* and *CLDN9* (individually) demonstrate increased proliferation, cell migration, and invasiveness. Moreover, *CLDN6/CLDN9* transfection seems to induce stem cell like properties and promote EMT with higher levels of CD44 and SOX-2 (unpublished results). To further investigate how overexpression of *CLDN6* in AGS cells might affect pathways that support cancer growth and survival, microarray-based gene expression analysis was done. Several differentially expressed genes in AGS-CLDN6 cells were identified over wild type AGS cells. GSEA analysis revealed that these genes are involved in several cancer hallmark processes like unfolded protein response, MTORC1 signaling, cholesterol homeostasis, hypoxia, and TNFα signaling. Collectively this indicates disruption of ER homeostasis with persistent ER stress which contributes to several precancerous attributes (178). Upregulation of MTORC1, cholesterol homeostasis, hypoxia, and TNFα signaling related genes reveal a complex dysregulation of metabolism which promotes vascularization and acquisition of EMT transition phenotype involving HIF, PI3K, MAPK, and NFkB pathways (179). These changes result in enhanced proliferation, cell mobility, and metastasis, which is supported by previous observations of *CLDN6* and *CLDN9* transfected AGS cells.

To investigate further entanglements of *CLDN6* in GC we analyzed TCGA-STAD data using interactive webtool CBioPortal. We found that 34% of GC samples in STAD data have alteration in *CLDN6*. Major alterations of *CLDN6* in these samples were limited to shallow

deletions, diploid, and gain with differentially overexpressed mRNA. Alterations in *CLDN6* were associated with high fraction genome altered, relatively higher aneuploidy scores, and poor overall and progression free survival in most of the patients. GC tumors with *CLDN6* alterations principally belong to CIN type of GC in TCGA-STAD classification. Intriguing that GC samples with *CLDN6* alterations showed 68.79% overlap with *TP53* alterations, indicating they may form a subgroup of CIN GC. Comparison of expression profiles in terms of mRNA z scores between cldn-6 and non-cldn-6 group samples revealed *MAGEA* family genes- *MAGEA6, MAGEA3, MAGEA4, MAGEA9B, MAGEA2, MAGEA12,* and *MAGEA10* are highly overexpressed in these samples along with *IGF2BP1, APOA1, CLDN9,* and several others. These DEGs affect the cell cycle in cldn-6 group samples. Overall higher mutation in *TP53* and cell cycle gene signatures in *CLDN6* alteration samples further validates the inclusion of *CLDN6* in these processes. *CLDN6* overexpression in samples is coupled with low *MDM2* expression and relatively high *CDKN2A* over non-cldn-6 samples. These changes seem directly connected with higher *TP53* mutations in the cldn-6 group.

To further investigate the correlation of *TP53* and *CLDN6* alterations we divided STAD data for *TP53* mutations in TP53 and non TP53 groups. Like cldn-6 group high aneuploidy scores and fractional genome alterations were observed in samples with *TP53* mutations. However, there was no significant difference in overall or progression free survival of the patients between both groups. Validating the TCGA classification of GC tumors with *TP53* mutation grouped in grade 2 and tubular stomach adenocarcinoma with higher frequency but profoundly in CIN STAD, which also justifies the overlap of these patients/samples with the cldn-6 group. Like cldn-6 group DEGs in samples with *TP53* mutations enriched in cell cycle regulation biological process. Moreover, *MAGEA* family genes along with *CLDN6, CLDN3, ACTL8, CDKN2A, CLDN9,* and *APOA1* are among the top altered genes allied with *TP53* mutations. *TP53* mutations were found to be correlated with a higher mutation in Notch signaling and angiogenesis gene signatures along with higher mutations in all most all the gene signatures associated with immune cell infiltration. However, how these mutations affect the actual process is inconclusive but plausible speculation that *TP53* mutations represent early GC tumors with high cell proliferation supported with lower immune infiltration.

Chromosome-wise copy number alterations and mutations in driver genes are other important parameters used in TCGA-STAD classification where CIN GC tumors have high CNA and high mutation in CIN signature genes like *TP53, ERBB2, KRAS, CCND1, BUB1*, etc. GC

samples with *TP53* and *CLDN6* alterations show very similar copy number alterations and pattern of overall mutations in CIN genes comparison to non TP53 and non-cldn-6 alteration group samples. Additionally, we identified a group of common DEGs associated with alterations in *CLDN6* and *TP53*. These genes are involved in epithelium development and differentiation and may serve as common prognostic targets for GC patients belong to these groups. Gene interaction network analysis identified *ORM2* and *MAGEA* gene family clusters and with highest degree scores for *ORM2* and *MAGEA2*, can be used as prognostic targets. ORM2 likely plays important role in anti-inflammation, immunomodulation, drug delivery, and ectopic overexpression of *ORM2* linked with decreased cell migration and invasion of cancer cells (180). This supports the speculation that the TP53 group may represent differentiated low Grade GC with low immune infiltration and angiogenesis. High ORM2 plasma levels as a biomarker, have already been discussed for Colorectal cancer (181,182) and higher expression *ORM2* in CIN GC samples with *TP53* and *CLDN6* alterations may serve the same. The human *MAGE* gene family consists of X-chromosome-linked genes, including *MAGE-A, MAGE-B,* and *MAGE-C* which are silent in normal tissues except in the testis and placenta. Overexpression of these genes is linked with several cancers including Intestinal type GC and is associated with tumor invasiveness, lymph node metastasis, and poor prognosis. In our study, we further conclude the *MAGEA6, MAGEA3, MAGEA2, MAGEA4, MAGEA9b, MAGEA10,* and *MAGEA12* are highly overexpressed along with *CLDN6* and *CLDN9* in CIN GC tumors with *TP53* and *CLDN6* alterations and can be used as therapeutic and prognostic targets.

12: Conclusion

In conclusion, we explored the role of *CLDN6* in GC. Overexpression of *CLDN6* in AGS cells affects several hallmarks of cancer including unfolded protein response, MTORC1 signaling, cholesterol homeostasis, hypoxia, and TNFα signaling. We analyzed TCGA-STAD data and found 34% of total STAD samples have alterations in *CLDN6*. *CLDN6* alterations in GC samples coincide with *TP53* mutations and CIN GC, in terms of DEGs, CIN gene mutations and may represent a subgroup of CIN GC with poor overall and progression free survival. Lastly, *ORM2* and *MAGEA2* can be used as prognostic targets for CIN GC tumors with *TP53* and *CLDN6* alterations.

13: Future prospects

1) Effect of *CLDN6/CLDN9* overexpression in AGS on cytotoxic activity of NK and CTLs.
2) Effect of *CLDN6/CLDN9* overexpression in AGS on infiltration of immune cells
3) Profiling of GC patients in terms of *CLDN6 /TP53* alterations.
4) Validation of prognostic significance of *ORM2* and *MAGEA2* in GC.

14: References

1. Cancer today [Internet]. [cited 2021 Mar 30]. Available from: http://gco.iarc.fr/today/home

2. Siewert JR, Stein HJ. Classification of adenocarcinoma of the oesophagogastric junction. Br J Surg. 1998 Nov;85(11):1457–9.

3. Edge SB, Compton CC. The American Joint Committee on Cancer: the 7th edition of the AJCC cancer staging manual and the future of TNM. Ann Surg Oncol. 2010 Jun;17(6):1471–4.

4. Lauren P. THE TWO HISTOLOGICAL MAIN TYPES OF GASTRIC CARCINOMA: DIFFUSE AND SO-CALLED INTESTINAL-TYPE CARCINOMA. AN ATTEMPT AT A HISTO-CLINICAL CLASSIFICATION. Acta Pathol Microbiol Scand. 1965;64:31–49.

5. Helicobacter pylori infection and the development of gastric cancer - PubMed [Internet]. [cited 2021 Feb 2]. Available from: https://pubmed.ncbi.nlm.nih.gov/11556297/

6. Hu B, El Hajj N, Sittler S, Lammert N, Barnes R, Meloni-Ehrig A. Gastric cancer: Classification, histology and application of molecular pathology. J Gastrointest Oncol. 2012 Sep;3(3):251–61.

7. Cancer Genome Atlas Research Network. Comprehensive molecular characterization of gastric adenocarcinoma. Nature. 2014 Sep 11;513(7517):202–9.

8. Network CGAR. Comprehensive molecular characterization of gastric adenocarcinoma. Nature. 2014;513(7517):202–9.

9. Mocellin S, Pasquali S. Diagnostic accuracy of endoscopic ultrasonography (EUS) for the preoperative locoregional staging of primary gastric cancer. Cochrane Database Syst Rev. 2015 Feb 6;(2):CD009944.

10. Zihni C, Mills C, Matter K, Balda MS. Tight junctions: from simple barriers to multifunctional molecular gates. Nat Rev Mol Cell Biol. 2016 Sep;17(9):564–80.

11. Anderson JM, Van Itallie CM. Physiology and function of the tight junction. Cold Spring Harb Perspect Biol. 2009 Aug;1(2):a002584.

12. Rahimi N. Defenders and Challengers of Endothelial Barrier Function. Front Immunol. 2017;8:1847.

13. Komarova YA, Kruse K, Mehta D, Malik AB. Protein Interactions at Endothelial Junctions and Signaling Mechanisms Regulating Endothelial Permeability. Circ Res. 2017 Jan 6;120(1):179–206.

14. Raleigh DR, Marchiando AM, Zhang Y, Shen L, Sasaki H, Wang Y, et al. Tight junction-associated MARVEL proteins marveld3, tricellulin, and occludin have distinct but overlapping functions. Mol Biol Cell. 2010 Apr 1;21(7):1200–13.

15. Ebnet K. Junctional Adhesion Molecules (JAMs): Cell Adhesion Receptors With Pleiotropic Functions in Cell Physiology and Development. Physiol Rev. 2017 Oct 1;97(4):1529–54.

16. Cichon C, Sabharwal H, Rüter C, Schmidt MA. MicroRNAs regulate tight junction proteins and modulate epithelial/endothelial barrier functions. Tissue Barriers. 2014 Aug 8;2(4):e944446.

17. Robinson K, Deng Z, Hou Y, Zhang G. Regulation of the Intestinal Barrier Function by Host Defense Peptides. Front Vet Sci [Internet]. 2015 [cited 2021 Jul 15];0. Available from: https://www.frontiersin.org/articles/10.3389/fvets.2015.00057/full

18. Mineta K, Yamamoto Y, Yamazaki Y, Tanaka H, Tada Y, Saito K, et al. Predicted expansion of the claudin multigene family. FEBS Lett. 2011 Feb 18;585(4):606–12.

19. Günzel D, Yu ASL. Claudins and the modulation of tight junction permeability. Physiol Rev. 2013 Apr;93(2):525–69.

20. Krause G, Winkler L, Mueller SL, Haseloff RF, Piontek J, Blasig IE. Structure and function of claudins. Biochim Biophys Acta BBA - Biomembr. 2008 Mar 1;1778(3):631–45.

21. Hewitt KJ, Agarwal R, Morin PJ. The claudin gene family: expression in normal and neoplastic tissues. BMC Cancer. 2006 Jul 12;6(1):186.

22. Suzuki H, Nishizawa T, Tani K, Yamazaki Y, Tamura A, Ishitani R, et al. Crystal Structure of a Claudin Provides Insight into the Architecture of Tight Junctions. Science. 2014 Apr 18;344(6181):304–7.

23. Van Itallie CM, Anderson JM. Claudins and epithelial paracellular transport. Annu Rev Physiol. 2006;68:403–29.

24. Krug SM, Günzel D, Conrad MP, Lee I-FM, Amasheh S, Fromm M, et al. Charge-selective claudin channels. Ann N Y Acad Sci. 2012 Jun;1257:20–8.

25. Van Itallie CM, Colegio OR, Anderson JM. The cytoplasmic tails of claudins can influence tight junction barrier properties through effects on protein stability. J Membr Biol. 2004 May 1;199(1):29–38.

26. Fallon RF, Goodenough DA. Five-hour half-life of mouse liver gap-junction protein. J Cell Biol. 1981 Aug 1;90(2):521–6.

27. M F, H C, T K, T S, T W, T Y, et al. Thr203 of claudin-1, a putative phosphorylation site for MAP kinase, is required to promote the barrier function of tight junctions. Exp Cell Res. 2004 Apr 1;295(1):36–47.

28. Nunbhakdi-Craig V, Machleidt T, Ogris E, Bellotto D, White CL III, Sontag E. Protein phosphatase 2A associates with and regulates atypical PKC and the epithelial tight junction complex. J Cell Biol. 2002 Aug 26;158(5):967–78.

29. D'Souza T, Agarwal R, Morin PJ. Phosphorylation of claudin-3 at threonine 192 by cAMP-dependent protein kinase regulates tight junction barrier function in ovarian cancer cells. J Biol Chem. 2005 Jul 15;280(28):26233–40.

30. Soma T, Chiba H, Kato-Mori Y, Wada T, Yamashita T, Kojima T, et al. Thr(207) of claudin-5 is involved in size-selective loosening of the endothelial barrier by cyclic AMP. Exp Cell Res. 2004 Oct 15;300(1):202–12.

31. Yamauchi K, Rai T, Kobayashi K, Sohara E, Suzuki T, Itoh T, et al. Disease-causing mutant WNK4 increases paracellular chloride permeability and phosphorylates claudins. Proc Natl Acad Sci. 2004 Mar 30;101(13):4690–4.

32. Tanaka M, Kamata R, Sakai R. EphA2 phosphorylates the cytoplasmic tail of Claudin-4 and mediates paracellular permeability. J Biol Chem. 2005 Dec 23;280(51):42375–82.

33. Van Itallie CM, Gambling TM, Carson JL, Anderson JM. Palmitoylation of claudins is required for efficient tight-junction localization. J Cell Sci. 2005 Apr 1;118(Pt 7):1427–36.

34. Nitta T, Hata M, Gotoh S, Seo Y, Sasaki H, Hashimoto N, et al. Size-selective loosening of the blood-brain barrier in claudin-5-deficient mice. J Cell Biol. 2003 May 12;161(3):653–60.

35. Gow A, Southwood CM, Li JS, Pariali M, Riordan GP, Brodie SE, et al. CNS myelin and sertoli cell tight junction strands are absent in Osp/claudin-11 null mice. Cell. 1999 Dec 10;99(6):649–59.

36. Ben-Yosef T, Belyantseva IA, Saunders TL, Hughes ED, Kawamoto K, Van Itallie CM, et al. Claudin 14 knockout mice, a model for autosomal recessive deafness DFNB29, are deaf due to cochlear hair cell degeneration. Hum Mol Genet. 2003 Aug 15;12(16):2049–61.

37. Tsukita S, Tanaka H, Tamura A. The Claudins: From Tight Junctions to Biological Systems. Trends Biochem Sci. 2019 Feb;44(2):141–52.

38. Krause G, Winkler L, Mueller SL, Haseloff RF, Piontek J, Blasig IE. Structure and function of claudins. Biochim Biophys Acta BBA - Biomembr. 2008;1778(3):631–45.

39. Litkouhi B, Kwong J, Lo C-M, Smedley JG, McClane BA, Aponte M, et al. Claudin-4 overexpression in epithelial ovarian cancer is associated with hypomethylation and is a

potential target for modulation of tight junction barrier function using a C-terminal fragment of Clostridium perfringens enterotoxin. Neoplasia N Y N. 2007 Apr;9(4):304–14.

40. Amasheh S, Schmidt T, Mahn M, Florian P, Mankertz J, Tavalali S, et al. Contribution of claudin-5 to barrier properties in tight junctions of epithelial cells. Cell Tissue Res. 2005 Jul;321(1):89–96.

41. Angelow S, Kim K-J, Yu ASL. Claudin-8 modulates paracellular permeability to acidic and basic ions in MDCK II cells. J Physiol. 2006 Feb 15;571(Pt 1):15–26.

42. Itallie CV, Rahner C, Anderson JM. Regulated expression of claudin-4 decreases paracellular conductance through a selective decrease in sodium permeability. J Clin Invest. 2001 May 15;107(10):1319–27.

43. Angelow S, El-Husseini R, Kanzawa SA, Yu ASL. Renal localization and function of the tight junction protein, claudin-19. Am J Physiol Renal Physiol. 2007 Jul;293(1):F166-177.

44. Sas D, Hu M, Moe OW, Baum M. Effect of claudins 6 and 9 on paracellular permeability in MDCK II cells. Am J Physiol Regul Integr Comp Physiol. 2008 Nov;295(5):R1713-1719.

45. Turksen K, Troy T-C. Permeability barrier dysfunction in transgenic mice overexpressing claudin 6. Dev Camb Engl. 2002 Apr;129(7):1775–84.

46. Anderson WJ, Zhou Q, Alcalde V, Kaneko OF, Blank LJ, Sherwood RI, et al. Genetic targeting of the endoderm with claudin-6CreER. Dev Dyn Off Publ Am Assoc Anat. 2008 Feb;237(2):504–12.

47. Moriwaki K, Tsukita S, Furuse M. Tight junctions containing claudin 4 and 6 are essential for blastocyst formation in preimplantation mouse embryos. Dev Biol. 2007 Dec 15;312(2):509–22.

48. Hong Y-H, Hishikawa D, Miyahara H, Nishimura Y, Tsuzuki H, Gotoh C, et al. Up-regulation of the claudin-6 gene in adipogenesis. Biosci Biotechnol Biochem. 2005;69(11):2117–21.

49. Nishikiori N, Sawada N, Ohguro H. Prevention of murine experimental corneal trauma by epigenetic events regulating claudin 6 and claudin 9. Jpn J Ophthalmol. 2008 Jun;52(3):195–203.

50. Nakano Y, Kim SH, Kim H-M, Sanneman JD, Zhang Y, Smith RJH, et al. A claudin-9-based ion permeability barrier is essential for hearing. PLoS Genet. 2009 Aug;5(8):e1000610.

51. Clevers H. Wnt breakers in colon cancer. Cancer Cell. 2004 Jan 1;5(1):5–6.

52. Ketola I, Rahman N, Toppari J, Bielinska M, Porter-Tinge SB, Tapanainen JS, et al. Expression and regulation of transcription factors GATA-4 and GATA-6 in developing mouse testis. Endocrinology. 1999 Mar;140(3):1470–80.

53. Xue C, Plieth D, Venkov C, Xu C, Neilson EG. The gatekeeper effect of epithelial-mesenchymal transition regulates the frequency of breast cancer metastasis. Cancer Res. 2003 Jun 15;63(12):3386–94.

54. Peter Y, Comellas A, Levantini E, Ingenito EP, Shapiro SD. Epidermal growth factor receptor and claudin-2 participate in A549 permeability and remodeling: Implications for non-small cell lung cancer tumor colonization. Mol Carcinog. 2009;48(6):488–97.

55. Berx G, Roy FV. The E-cadherin/catenin complex: an important gatekeeper in breast cancer tumorigenesis and malignant progression. Breast Cancer Res BCR. 2001;3(5):289–93.

56. Nakayama F, Semba S, Usami Y, Chiba H, Sawada N, Yokozaki H. Hypermethylation-Modulated Downregulation of Claudin-7 Expression Promotes the Progression of Colorectal Carcinoma. Pathobiology. 2008;75(3):177–85.

57. Li D, Mrsny RJ. Oncogenic Raf-1 Disrupts Epithelial Tight Junctions via Downregulation of Occludin. J Cell Biol. 2000 Feb 21;148(4):791–800.

58. Bartholow TL, Chandran UR, Becich MJ, Parwani AV. Immunohistochemical profiles of claudin-3 in primary and metastatic prostatic adenocarcinoma. Diagn Pathol. 2011 Jan 21;6(1):12.

59. Holczbauer Á, Gyöngyösi B, Lotz G, Szijártó A, Kupcsulik P, Schaff Z, et al. Distinct Claudin Expression Profiles of Hepatocellular Carcinoma and Metastatic Colorectal and Pancreatic Carcinomas. J Histochem Cytochem. 2013 Apr;61(4):294–305.

60. Lin X, Shang X, Manorek G, Howell SB. Regulation of the Epithelial-Mesenchymal Transition by Claudin-3 and Claudin-4. PLOS ONE. 2013 Jun 21;8(6):e67496.

61. Dhawan P, Singh AB, Deane NG, No Y, Shiou S-R, Schmidt C, et al. Claudin-1 regulates cellular transformation and metastatic behavior in colon cancer. J Clin Invest. 2005 Jul 1;115(7):1765–76.

62. Kohmoto T, Masuda K, Shoda K, Takahashi R, Ujiro S, Tange S, et al. Claudin-6 is a single prognostic marker and functions as a tumor-promoting gene in a subgroup of intestinal type gastric cancer. Gastric Cancer. 2020 May 1;23(3):403–17.

63. Rendón-Huerta E, Teresa F, Teresa GM, Xochitl G-S, Georgina A-F, Veronica Z-Z, et al. Distribution and expression pattern of claudins 6, 7, and 9 in diffuse- and intestinal-type gastric adenocarcinomas. J Gastrointest Cancer. 2010 Mar;41(1):52–9.

64. Yu S, Zhang Y, Li Q, Zhang Z, Zhao G, Xu J. CLDN6 promotes tumor progression through the YAP1-snail1 axis in gastric cancer. Cell Death Dis. 2019 Dec 11;10(12):1–14.

65. Zavala-Zendejas VE, Torres-Martinez AC, Salas-Morales B, Fortoul TI, Montaño LF, Rendon-Huerta EP. Claudin-6, 7, or 9 Overexpression in the Human Gastric Adenocarcinoma Cell Line AGS Increases Its Invasiveness, Migration, and Proliferation Rate. Cancer Invest. 2011 Jan 1;29(1):1–11.

66. Torres-Martínez AC, Gallardo-Vera JF, Lara-Holguin AN, Montaño LF, Rendón-Huerta EP. Claudin-6 enhances cell invasiveness through claudin-1 in AGS human adenocarcinoma gastric cancer cells. Exp Cell Res. 2017 Jan 1;350(1):226–35.

67. Kondo M, Weissman IL, Akashi K. Identification of Clonogenic Common Lymphoid Progenitors in Mouse Bone Marrow. Cell. 1997 Nov 28;91(5):661–72.

68. Rosmaraki EE, Douagi I, Roth C, Colucci F, Cumano A, Santo JPD. Identification of committed NK cell progenitors in adult murine bone marrow. Eur J Immunol. 2001;31(6):1900–9.

69. Sojka DK, Tian Z, Yokoyama WM. Tissue-Resident Natural Killer Cells and Their Potential Diversity. Semin Immunol. 2014 Apr;26(2):127–31.

70. Lanier LL, Phillips JH, Hackett J, Tutt M, Kumar V. Natural killer cells: definition of a cell type rather than a function. J Immunol Baltim Md 1950. 1986 Nov 1;137(9):2735–9.

71. Lanier LL. Up on the tightrope: natural killer cell activation and inhibition. Nat Immunol. 2008 May;9(5):495–502.

72. Stebbins CC, Watzl C, Billadeau DD, Leibson PJ, Burshtyn DN, Long EO. Vav1 Dephosphorylation by the Tyrosine Phosphatase SHP-1 as a Mechanism for Inhibition of Cellular Cytotoxicity. Mol Cell Biol. 2003 Sep 1;23(17):6291–9.

73. Vivier E, Nunès JA, Vély F. Natural killer cell signaling pathways. Science. 2004 Nov 26;306(5701):1517–9.

74. Canossi A, Aureli A, Del Beato T, Rossi P, Franceschilli L, De Sanctis F, et al. Role of KIR and CD16A genotypes in colorectal carcinoma genetic risk and clinical stage. J Transl Med [Internet]. 2016;14. Available from: https://www.ncbi.nlm.nih.gov/pmc/articles/PMC4983069/

75. Rajalingam R. Overview of the killer cell immunoglobulin-like receptor system. Methods Mol Biol Clifton NJ. 2012;882:391–414.

76. Braud VM, Allan DS, O'Callaghan CA, Söderström K, D'Andrea A, Ogg GS, et al. HLA-E binds to natural killer cell receptors CD94/NKG2A, B and C. Nature. 1998 Feb 19;391(6669):795–9.

77. Lee N, Llano M, Carretero M, Ishitani A, Navarro F, López-Botet M, et al. HLA-E is a major ligand for the natural killer inhibitory receptor CD94/NKG2A. Proc Natl Acad Sci U S A. 1998 Apr 28;95(9):5199–204.

78. Borrego F, Ulbrecht M, Weiss EH, Coligan JE, Brooks AG. Recognition of Human Histocompatibility Leukocyte Antigen (HLA)-E Complexed with HLA Class I Signal Sequence–derived Peptides by CD94/NKG2 Confers Protection from Natural Killer Cell–mediated Lysis. J Exp Med. 1998 Mar 2;187(5):813–8.

79. Carretero M, Cantoni C, Bellón T, Bottino C, Biassoni R, Rodríguez A, et al. The CD94 and NKG2-A C-type lectins covalently assemble to form a natural killer cell inhibitory receptor for HLA class I molecules. Eur J Immunol. 1997 Feb;27(2):563–7.

80. Martínez-Lostao L, Anel A, Pardo J. How Do Cytotoxic Lymphocytes Kill Cancer Cells? Clin Cancer Res. 2015 Nov 15;21(22):5047–56.

81. Garrity D, Call ME, Feng J, Wucherpfennig KW. The activating NKG2D receptor assembles in the membrane with two signaling dimers into a hexameric structure. Proc Natl Acad Sci U S A. 2005 May 24;102(21):7641–6.

82. Upshaw JL, Arneson LN, Schoon RA, Dick CJ, Billadeau DD, Leibson PJ. NKG2D-mediated signaling requires a DAP10-bound Grb2-Vav1 intermediate and phosphatidylinositol-3-kinase in human natural killer cells. Nat Immunol. 2006 May;7(5):524–32.

83. Horng T, Bezbradica JS, Medzhitov R. NKG2D signaling is coupled to the interleukin 15 receptor signaling pathway. Nat Immunol. 2007 Dec;8(12):1345–52.

84. Sutherland CL, Chalupny NJ, Schooley K, VandenBos T, Kubin M, Cosman D. UL16-binding proteins, novel MHC class I-related proteins, bind to NKG2D and activate multiple signaling pathways in primary NK cells. J Immunol Baltim Md 1950. 2002 Jan 15;168(2):671–9.

85. Billadeau DD. NKG2D recruits two distinct adapters to trigger NK cell activation and costimulation - PubMed. NATURE IMMUNOLOGY; 2003.

86. Diefenbach A, Tomasello E, Lucas M, Jamieson AM, Hsia JK, Vivier E, et al. Selective associations with signaling proteins determine stimulatory versus costimulatory activity of NKG2D. Nat Immunol. 2002 Dec;3(12):1142–9.

87. Kubin M, Cassiano L, Chalupny J, Chin W, Cosman D, Fanslow W, et al. ULBP1, 2, 3: novel MHC class I-related molecules that bind to human cytomegalovirus glycoprotein UL16, activate NK cells. Eur J Immunol. 2001 May;31(5):1428–37.

88. Zhang C, Zhang J, Niu J, Zhou Z, Zhang J, Tian Z. Interleukin-12 improves cytotoxicity of natural killer cells via upregulated expression of NKG2D. Hum Immunol. 2008 Aug;69(8):490–500.

89. Song H, Hur DY, Kim K-E, Park H, Kim T, Kim C-W, et al. IL-2/IL-18 prevent the down-modulation of NKG2D by TGF-beta in NK cells via the c-Jun N-terminal kinase (JNK) pathway. Cell Immunol. 2006 Jul;242(1):39–45.

90. Zhang C, Zhang J, Sun R, Feng J, Wei H, Tian Z. Opposing effect of IFNgamma and IFNalpha on expression of NKG2 receptors: negative regulation of IFNgamma on NK cells. Int Immunopharmacol. 2005 Jun;5(6):1057–67.

91. Cosman D, Müllberg J, Sutherland CL, Chin W, Armitage R, Fanslow W, et al. ULBPs, novel MHC class I-related molecules, bind to CMV glycoprotein UL16 and stimulate NK cytotoxicity through the NKG2D receptor. Immunity. 2001 Feb;14(2):123–33.

92. Takada A, Yoshida S, Kajikawa M, Miyatake Y, Tomaru U, Sakai M, et al. Two Novel NKG2D Ligands of the Mouse H60 Family with Differential Expression Patterns and Binding Affinities to NKG2D. J Immunol. 2008 Feb 1;180(3):1678–85.

93. Groh V, Rhinehart R, Secrist H, Bauer S, Grabstein KH, Spies T. Broad tumor-associated expression and recognition by tumor-derived T cells of MICA and MICB. Proc Natl Acad Sci. 1999 Jun 8;96(12):6879–84.

94. Pende D, Rivera P, Marcenaro S, Chang C-C, Biassoni R, Conte R, et al. Major Histocompatibility Complex Class I-related Chain A and UL16-Binding Protein Expression on Tumor Cell Lines of Different Histotypes: Analysis of Tumor Susceptibility to NKG2D-dependent Natural Killer Cell Cytotoxicity. Cancer Res. 2002 Nov 1;62(21):6178–86.

95. Vetter CS, Groh V, Straten P thor, Spies T, Bröcker E-B, Becker JC. Expression of Stress-induced MHC Class I Related Chain Molecules on Human Melanoma. J Invest Dermatol. 2002 Apr;118(4):600–5.

96. Friese MA, Platten M, Lutz SZ, Naumann U, Aulwurm S, Bischof F, et al. MICA/NKG2D-Mediated Immunogene Therapy of Experimental Gliomas. Cancer Res. 2003 Dec 15;63(24):8996–9006.

97. Cantoni C, Biassoni R, Pende D, Sivori S, Accame L, Pareti L, et al. The activating form of CD94 receptor complex: CD94 covalently associated with the Kp39 protein that represents the product of the NKG2-C gene. Eur J Immunol. 1998;28(1):327–38.

98. Lanier LL, Corliss B, Wu J, Phillips JH. Association of DAP12 with Activating CD94/NKG2C NK Cell Receptors. Immunity. 1998 Jun;8(6):693–701.

99. Vance RE, Jamieson AM, Raulet DH. Recognition of the class Ib molecule Qa-1(b) by putative activating receptors CD94/NKG2C and CD94/NKG2E on mouse natural killer cells. J Exp Med. 1999 Dec 20;190(12):1801–12.

100. Paul S, Lal G. The Molecular Mechanism of Natural Killer Cells Function and Its Importance in Cancer Immunotherapy. Front Immunol. 2017 Sep 13;8:1124.

101. Rah S-Y, Kwak J-Y, Chung Y-J, Kim U-H. ADP-ribose/TRPM2-mediated Ca2+ signaling is essential for cytolytic degranulation and antitumor activity of natural killer cells. Sci Rep. 2015 Mar 25;5:9482.

102. Bryceson YT, Ljunggren H-G, Long EO. Minimal requirement for induction of natural cytotoxicity and intersection of activation signals by inhibitory receptors. Blood. 2009 Sep 24;114(13):2657–66.

103. Bryceson YT, March ME, Ljunggren H-G, Long EO. Synergy among receptors on resting NK cells for the activation of natural cytotoxicity and cytokine secretion. Blood. 2006 Jan 1;107(1):159–66.

104. Topham NJ, Hewitt EW. Natural killer cell cytotoxicity: how do they pull the trigger? Immunology. 2009 Sep;128(1):7–15.

105. Alter G, Malenfant JM, Altfeld M. CD107a as a functional marker for the identification of natural killer cell activity. J Immunol Methods. 2004 Nov;294(1–2):15–22.

106. Hellmich MR, Strumwasser F. Purification and characterization of a molluscan egg-specific NADase, a second-messenger enzyme. Cell Regul. 1991 Mar;2(3):193–202.

107. Itoh M, Ishihara K, Tomizawa H, Tanaka H, Kobune Y, Ishikawa J, et al. Molecular Cloning of Murine BST-1 Having Homology with CD38 and Aplysia ADP-Ribosyl Cyclase. Biochem Biophys Res Commun. 1994 Sep;203(2):1309–17.

108. Goodrich SP, Muller-Steffner H, Osman A, Moutin M-J, Kusser K, Roberts A, et al. Production of calcium-mobilizing metabolites by a novel member of the ADP-ribosyl cyclase family expressed in Schistosoma mansoni. Biochemistry. 2005 Aug 23;44(33):11082–97.

109. Munshi C, Thiel DJ, Mathews II, Aarhus R, Walseth TF, Lee HC. Characterization of the Active Site of ADP-ribosyl Cyclase. J Biol Chem. 1999 Oct 22;274(43):30770–7.

110. Munshi C, Aarhus R, Graeff R, Walseth TF, Levitt D, Lee HC. Identification of the Enzymatic Active Site of CD38 by Site-directed Mutagenesis. J Biol Chem. 2000 Jul 14;275(28):21566–71.

111. Liu Q, Kriksunov IA, Graeff R, Munshi C, Lee HC, Hao Q. Crystal structure of human CD38 extracellular domain. Struct Lond Engl 1993. 2005 Sep;13(9):1331–9.

112. Malavasi F, Deaglio S, Funaro A, Ferrero E, Horenstein AL, Ortolan E, et al. Evolution and function of the ADP ribosyl cyclase/CD38 gene family in physiology and pathology. Physiol Rev. 2008 Jul;88(3):841–86.

113. Malavasi F, Funaro A, Roggero S, Horenstein A, Calosso L, Mehta K. Human CD38: a glycoprotein in search of a function. Immunol Today. 1994 Mar;15(3):95–7.

114. Quarona V, Zaccarello G, Chillemi A, Brunetti E, Singh VK, Ferrero E, et al. CD38 and CD157: a long journey from activation markers to multifunctional molecules. Cytometry B Clin Cytom. 2013 Aug;84(4):207–17.

115. Lee HC. Structure and Enzymatic Functions of Human CD38. Mol Med. 2006;12(11–12):317–23.

116. Reinherz EL, Kung PC, Goldstein G, Levey RH, Schlossman SF. Discrete stages of human intrathymic differentiation: analysis of normal thymocytes and leukemic lymphoblasts of T-cell lineage. Proc Natl Acad Sci U S A. 1980 Mar;77(3):1588–92.

117. Deaglio S, Aydin S, Vaisitti T, Bergui L, Malavasi F. CD38 at the junction between prognostic marker and therapeutic target. Trends Mol Med. 2008 May;14(5):210–8.

118. Lischke T, Heesch K, Schumacher V, Schneider M, Haag F, Koch-Nolte F, et al. CD38 Controls the Innate Immune Response against Listeria monocytogenes. Infect Immun. 2013 Nov;81(11):4091–9.

119. Fujita T, Kantarci A, Warbington ML, Zawawi KH, Hasturk H, Kurihara H, et al. CD38 Expression in Neutrophils From Patients With Localized Aggressive Periodontitis. J Periodontol. 2005 Nov;76(11):1960–5.

120. Alessio M, Roggero S, Funaro A, De Monte LB, Peruzzi L, Geuna M, et al. CD38 molecule: structural and biochemical analysis on human T lymphocytes, thymocytes, and plasma cells. J Immunol Baltim Md 1950. 1990 Aug 1;145(3):878–84.

121. Franco L, Zocchi E, Calder L, Guida L, Benatti U, Deflora A. Self-Aggregation of the Transmembrane Glycoprotein CD38 Purified from Human Erythrocytes. Biochem Biophys Res Commun. 1994 Aug;202(3):1710–5.

122. Ramaschi G, Torti M, Festetics ET, Sinigaglia F, Malavasi F, Balduini C. Expression of cyclic ADP-ribose-synthetizing CD38 molecule on human platelet membrane. Blood. 1996 Mar 15;87(6):2308–13.

123. Gallay N, Anani L, Lopez A, Colombat P, Binet C, Domenech J, et al. The Role of Platelet/Endothelial Cell Adhesion Molecule 1 (CD31) and CD38 Antigens in Marrow Microenvironmental Retention of Acute Myelogenous Leukemia Cells. Cancer Res. 2007 Sep 15;67(18):8624–32.

124. Dianzani U, Funaro A, DiFranco D, Garbarino G, Bragardo M, Redoglia V, et al. Interaction between endothelium and CD4+CD45RA+ lymphocytes. Role of the human CD38 molecule. J Immunol Baltim Md 1950. 1994 Aug 1;153(3):952–9.

125. Deaglio S, Morra M, Mallone R, Ausiello CM, Prager E, Garbarino G, et al. Human CD38 (ADP-ribosyl cyclase) is a counter-receptor of CD31, an Ig superfamily member. J Immunol Baltim Md 1950. 1998 Jan 1;160(1):395–402.

126. Mehta K, Shahid U, Malavasi F. Human CD38, a cell-surface protein with multiple functions. FASEB J Off Publ Fed Am Soc Exp Biol. 1996 Oct;10(12):1408–17.

127. Muñoz P, Navarro M-C, Pavón EJ, Salmerón J, Malavasi F, Sancho J, et al. CD38 signaling in T cells is initiated within a subset of membrane rafts containing Lck and the CD3-zeta subunit of the T cell antigen receptor. J Biol Chem. 2003 Dec 12;278(50):50791–802.

128. Zubiaur M, Fernández O, Ferrero E, Salmerón J, Malissen B, Malavasi F, et al. CD38 is associated with lipid rafts and upon receptor stimulation leads to Akt/protein kinase B and Erk activation in the absence of the CD3-zeta immune receptor tyrosine-based activation motifs. J Biol Chem. 2002 Jan 4;277(1):13–22.

129. Funaro A, Monte LBD, Dianzani U, Forni M, Malavasi F. Human CD38 is associated to distinct molecules which mediate transmembrane signaling in different lineages. Eur J Immunol. 1993;23(10):2407–11.

130. Deaglio S, Zubiaur M, Gregorini A, Bottarel F, Ausiello CM, Dianzani U, et al. Human CD38 and CD16 are functionally dependent and physically associated in natural killer cells. Blood. 2002 Apr 1;99(7):2490–8.

131. Lande R, Urbani F, Di Carlo B, Sconocchia G, Deaglio S, Funaro A, et al. CD38 ligation plays a direct role in the induction of IL-1beta, IL-6, and IL-10 secretion in resting human monocytes. Cell Immunol. 2002 Nov;220(1):30–8.

132. Ausiello CM, Urbani F, la Sala A, Funaro A, Malavasi F. CD38 ligation induces discrete cytokine mRNA expression in human cultured lymphocytes. Eur J Immunol. 1995 May;25(5):1477–80.

133. Aarhus R, Graeff RM, Dickey DM, Walseth TF, Lee HC. ADP-ribosyl cyclase and CD38 catalyze the synthesis of a calcium-mobilizing metabolite from NADP. J Biol Chem. 1995 Dec 22;270(51):30327–33.

134. Gasser A, Bruhn S, Guse AH. Second Messenger Function of Nicotinic Acid Adenine Dinucleotide Phosphate Revealed by an Improved Enzymatic Cycling Assay. J Biol Chem. 2006 Jun 23;281(25):16906–13.

135. Guse AH, da Silva CP, Berg I, Skapenko AL, Weber K, Heyer P, et al. Regulation of calcium signalling in T lymphocytes by the second messenger cyclic ADP-ribose. Nature. 1999 Mar 4;398(6722):70–3.

136. Zocchi E, Podestà M, Pitto A, Usai C, Bruzzone S, Franco L, et al. Stroma-generated cyclic ADP-ribose stimulates the expansion of early human hemopoietic progenitors by a paracrine interaction. FASEB J. 2001;15(9):1610–2.

137. Bruzzone S, De Flora A, Usai C, Graeff R, Lee HC. Cyclic ADP-ribose is a second messenger in the lipopolysaccharide-stimulated proliferation of human peripheral blood mononuclear cells. Biochem J. 2003 Oct 15;375(Pt 2):395–403.

138. Partida-Sánchez S, Cockayne DA, Monard S, Jacobson EL, Oppenheimer N, Garvy B, et al. Cyclic ADP-ribose production by CD38 regulates intracellular calcium release, extracellular calcium influx and chemotaxis in neutrophils and is required for bacterial clearance in vivo. Nat Med. 2001 Nov;7(11):1209–16.

139. Geuze HJ. The role of endosomes and lysosomes in MHC class II functioning. Immunol Today. 1998 Jun;19(6):282–7.

140. Denzer K, Kleijmeer MJ, Heijnen HF, Stoorvogel W, Geuze HJ. Exosome: from internal vesicle of the multivesicular body to intercellular signaling device. J Cell Sci. 2000 Oct;113 Pt 19:3365–74.

141. Zumaquero E, Muñoz P, Cobo M, Lucena G, Pavón EJ, Martín A, et al. Exosomes from human lymphoblastoid B cells express enzymatically active CD38 that is associated with signaling complexes containing CD81, Hsc-70 and Lyn. Exp Cell Res. 2010 Oct;316(16):2692–706.

142. Bahri R, Bollinger A, Bollinger T, Orinska Z, Bulfone-Paus S. Ectonucleotidase CD38 Demarcates Regulatory, Memory-Like CD8+ T Cells with IFN-γ-Mediated Suppressor Activities. Hasenkrug KJ, editor. PLoS ONE. 2012 Sep 17;7(9):e45234.

143. Read S, Mauze S, Asseman C, Bean A, Coffman R, Powrie F. CD38+ CD45RB(low) CD4+ T cells: a population of T cells with immune regulatory activities in vitro. Eur J Immunol. 1998;28(11):3435–47.

144. Hinshaw DC, Shevde LA. The Tumor Microenvironment Innately Modulates Cancer Progression. Cancer Res. 2019 15;79(18):4557–66.

145. Feng X, Zhang L, Acharya C, An G, Wen K, Qiu L, et al. Targeting CD38 Suppresses Induction and Function of T Regulatory Cells to Mitigate Immunosuppression in Multiple Myeloma. Clin Cancer Res Off J Am Assoc Cancer Res. 2017 Aug 1;23(15):4290–300.

146. Mittal S, Marshall NA, Duncan L, Culligan DJ, Barker RN, Vickers MA. Local and systemic induction of CD4+CD25+ regulatory T-cell population by non-Hodgkin lymphoma. Blood. 2008 Jun 1;111(11):5359–70.

147. Yang Y, Li C, Liu T, Dai X, Bazhin AV. Myeloid-Derived Suppressor Cells in Tumors: From Mechanisms to Antigen Specificity and Microenvironmental Regulation. Front Immunol. 2020 Jul 22;11:1371.

148. Wang WW, Yuan XL, Chen H, Xie GH, Ma YH, Zheng YX, et al. CD19+CD24hiCD38hiBregs involved in downregulate helper T cells and upregulate regulatory T cells in gastric cancer. Oncotarget. 2015 Oct 20;6(32):33486–99.

149. Patton DT, Wilson MD, Rowan WC, Soond DR, Okkenhaug K. The PI3K p110δ regulates expression of CD38 on regulatory T cells. PloS One. 2011 Mar 1;6(3):e17359.

150. Flores-Borja F, Bosma A, Ng D, Reddy V, Ehrenstein MR, Isenberg DA, et al. CD19+CD24hiCD38hi B cells maintain regulatory T cells while limiting TH1 and TH17 differentiation. Sci Transl Med. 2013 Feb 20;5(173):173ra23.

151. Domínguez-Pantoja M, López-Herrera G, Romero-Ramírez H, Santos-Argumedo L, Chávez-Rueda AK, Hernández-Cueto Á, et al. CD38 protein deficiency induces autoimmune characteristics and its activation enhances IL-10 production by regulatory B cells. Scand J Immunol. 2018 Jun;87(6):e12664.

152. Karakasheva TA, Waldron TJ, Eruslanov E, Kim S-B, Lee J-S, O'Brien S, et al. CD38-Expressing Myeloid-Derived Suppressor Cells Promote Tumor Growth in a Murine Model of Esophageal Cancer. Cancer Res. 2015 Oct 1;75(19):4074–85.

153. Umansky V, Blattner C, Gebhardt C, Utikal J. The Role of Myeloid-Derived Suppressor Cells (MDSC) in Cancer Progression. Vaccines. 2016 Nov 3;4(4):36.

154. Fredholm BB, Abbracchio MP, Burnstock G, Daly JW, Harden TK, Jacobson KA, et al. Nomenclature and classification of purinoceptors. Pharmacol Rev. 1994 Jun;46(2):143–56.

155. Antonioli L, Blandizzi C, Pacher P, Haskó G. Immunity, inflammation and cancer: a leading role for adenosine. Nat Rev Cancer. 2013 Dec;13(12):842–57.

156. Ferretti E, Horenstein AL, Canzonetta C, Costa F, Morandi F. Canonical and non-canonical adenosinergic pathways. Immunol Lett. 2019 Jan;205:25–30.

157. Petrova V, Annicchiarico-Petruzzelli M, Melino G, Amelio I. The hypoxic tumour microenvironment. Oncogenesis. 2018 Jan;7(1):10.

158. Kim Y, Lin Q, Glazer PM, Yun Z. Hypoxic Tumor Microenvironment and Cancer Cell Differentiation. Curr Mol Med. 2009 May;9(4):425–34.

159. Passarelli A, Tucci M, Mannavola F, Felici C, Silvestris F. The metabolic milieu in melanoma: Role of immune suppression by CD73/adenosine. Tumour Biol J Int Soc Oncodevelopmental Biol Med. 2019 Apr;42(4):1010428319837138.

160. Perrot I, Michaud H-A, Giraudon-Paoli M, Augier S, Docquier A, Gros L, et al. Blocking Antibodies Targeting the CD39/CD73 Immunosuppressive Pathway Unleash Immune Responses in Combination Cancer Therapies. Cell Rep. 2019 21;27(8):2411-2425.e9.

161. Ben Baruch B, Blacher E, Mantsur E, Schwartz H, Vaknine H, Erez N, et al. Stromal CD38 regulates outgrowth of primary melanoma and generation of spontaneous metastasis. Oncotarget. 2018 Aug 7;9(61):31797–811.

162. Favia A, Desideri M, Gambara G, D'Alessio A, Ruas M, Esposito B, et al. VEGF-induced neoangiogenesis is mediated by NAADP and two-pore channel-2-dependent Ca2+ signaling. Proc Natl Acad Sci U S A. 2014 Nov 4;111(44):E4706-4715.

163. Favia A, Pafumi I, Desideri M, Padula F, Montesano C, Passeri D, et al. NAADP-Dependent Ca(2+) Signaling Controls Melanoma Progression, Metastatic Dissemination and Neoangiogenesis. Sci Rep. 2016 Jan 6;6:18925.

164. Chung AS, Ferrara N. Developmental and pathological angiogenesis. Annu Rev Cell Dev Biol. 2011;27:563–84.

165. Berridge MJ, Bootman MD, Roderick HL. Calcium signalling: dynamics, homeostasis and remodelling. Nat Rev Mol Cell Biol. 2003 Jul;4(7):517–29.

166. Schwarz EC, Qu B, Hoth M. Calcium, cancer and killing: The role of calcium in killing cancer cells by cytotoxic T lymphocytes and natural killer cells. Biochim Biophys Acta BBA - Mol Cell Res. 2013 Jul 1;1833(7):1603–11.

167. Streb H, Irvine RF, Berridge MJ, Schulz I. Release of Ca 2+ from a nonmitochondrial intracellular store in pancreatic acinar cells by inositol-1,4,5-trisphosphate. Nature. 1983 Nov;306(5938):67–9.

168. Clapper DL, Walseth TF, Dargie PJ, Lee HC. Pyridine nucleotide metabolites stimulate calcium release from sea urchin egg microsomes desensitized to inositol trisphosphate. J Biol Chem. 1987 Jul;262(20):9561–8.

169. Lee HC, Aarhus R. A derivative of NADP mobilizes calcium stores insensitive to inositol trisphosphate and cyclic ADP-ribose. J Biol Chem. 1995 Feb 3;270(5):2152–7.

170. Kim U-H. Multiple Enzymatic Activities of CD38 for Ca2+ Signaling Messengers. Am Sci Publ. Vol. 3, 6–14, 2014.

171. Lee HC. Structure and Enzymatic Functions of Human CD38. Mol Med. 2006;12(11–12):317–23.

172. Cerami E, Gao J, Dogrusoz U, Gross BE, Sumer SO, Aksoy BA, et al. The cBio cancer genomics portal: an open platform for exploring multidimensional cancer genomics data. Cancer Discov. 2012 May;2(5):401–4.

173. Gao J, Aksoy BA, Dogrusoz U, Dresdner G, Gross B, Sumer SO, et al. Integrative analysis of complex cancer genomics and clinical profiles using the cBioPortal. Sci Signal. 2013 Apr 2;6(269):pl1.

174. Pathan M, Keerthikumar S, Ang C-S, Gangoda L, Quek CYJ, Williamson NA, et al. FunRich: An open access standalone functional enrichment and interaction network analysis tool. PROTEOMICS. 2015;15(15):2597–601.

175. Shannon P, Markiel A, Ozier O, Baliga NS, Wang JT, Ramage D, et al. Cytoscape: a software environment for integrated models of biomolecular interaction networks. Genome Res. 2003 Nov;13(11):2498–504.

176. Bader GD, Hogue CWV. An automated method for finding molecular complexes in large protein interaction networks. BMC Bioinformatics. 2003 Jan 13;4:2.

177. Chae YK, Choi WM, Bae WH, Anker J, Davis AA, Agte S, et al. Overexpression of adhesion molecules and barrier molecules is associated with differential infiltration of immune cells in non-small cell lung cancer. Sci Rep. 2018 Jan 18;8(1):1023.

178. Yadav RK, Chae S-W, Kim H-R, Chae HJ. Endoplasmic Reticulum Stress and Cancer. J Cancer Prev. 2014 Jun;19(2):75–88.

179. Muz B, de la Puente P, Azab F, Azab AK. The role of hypoxia in cancer progression, angiogenesis, metastasis, and resistance to therapy. Hypoxia. 2015 Dec 11;3:83–92.

180. Fang T, Cui M, Sun J, Ge C, Zhao F, Zhang L, et al. Orosomucoid 2 inhibits tumor metastasis and is upregulated by CCAAT/enhancer binding protein β in hepatocellular carcinomas. Oncotarget. 2015 Apr 19;6(18):16106–19.

181. Gao F, Zhang X, Whang S, Zheng C. Prognostic Impact of Plasma ORM2 Levels in Patients with Stage II Colorectal Cancer. Ann Clin Lab Sci. 2014 Sep 21;44(4):388–93.

182. Zhang X, Xiao Z, Liu X, Du L, Wang L, Wang S, et al. The Potential Role of ORM2 in the Development of Colorectal Cancer. PLOS ONE. 2012 Feb 21;7(2):e31868.